PB84-234517

Pilot Scale Evaluation of Photolytic Ozonation for Trihalomethane Precursor Removal

Texas Univ. at Dallas, Richardson

Prepared for

Municipal Environmental Research Lab.
Cincinnati, OH

Aug 84

U.S. Department of Commerce
National Technical Information Service
NTIS

PB84-234517

EPA-600/2-84-136
August 1984

PILOT SCALE EVALUATION OF PHOTOLYTIC OZONATION FOR TRIHALOMETHANE PRECURSOR REMOVAL

by

William H. Glaze, Gary R. Peyton, Brigitte Sohm
The University of Texas at Dallas
Richardson, Texas 75083-0688

and

Dean A. Meldrum
SumX Corporation
Austin, Texas

Cooperative Agreement CR-808825

Project Officer

J. Keith Carswell
Drinking Water Research Division
Municipal Environmental Research Laboratory
Cincinnati, Ohio 45268

MUNICIPAL ENVIRONMENTAL RESEARCH LABORATORY
OFFICE OF RESEARCH AND DEVELOPMENT
U.S. ENVIRONMENTAL PROTECTION AGENCY
CINCINNATI, OHIO 45268

REPRODUCED BY
NATIONAL TECHNICAL
INFORMATION SERVICE
U.S. DEPARTMENT OF COMMERCE
SPRINGFIELD, VA. 22161

TECHNICAL REPORT DATA

(Please read Instructions on the reverse before completing)

1. REPORT NO. EPA-600/2-84-136	2.	3. RECIPIENT'S ACCESSION NO. PB84-234 517
4. TITLE AND SUBTITLE PILOT SCALE EVALUATION OF PHOTOLYTIC OZONATION FOR TRIHALOMETHANE PRECURSOR REMOVAL		5. REPORT DATE August 1984 6. PERFORMING ORGANIZATION CODE
7. AUTHOR(S) W.H. GLAZE, G.R. PEYTON, B.SOHM AND D.A. MELDRUM		8. PERFORMING ORGANIZATION REPORT NO.
9. PERFORMING ORGANIZATION NAME AND ADDRESS The University of Texas at Dallas Box 830688 Richardson, TX 75083		10. PROGRAM ELEMENT NO. BNC1A 11. CONTRACT/GRANT NO. Cooperative Agreement No. CR808825
12. SPONSORING AGENCY NAME AND ADDRESS Muncipal Environmental Research Laboratory--Cin, OH Office of Research and Development U.S. Environmental Protection Agency Cincinnati, OH 45268		13. TYPE OF REPORT AND PERIOD COVERED Final 4/1/81 - 6/30/84 14. SPONSORING AGENCY CODE EPA/600/14

15. SUPPLEMENTARY NOTES

Project Officer: J. Keith Carswell (513) 684-7228

(HO2)(-1)

16. ABSTRACT

The use of ozone combined with ultraviolet radiation has been studied at the pilot-scale for removing trihalomethane (THM) precursors from potable water. The effects of variations in ozone dose rate, UV intensity and other parameters were first studied using a synthetic feedwater. The pilot plant was then operated for 8 months at the Sabine River Water Treatment Plant in Longview, TX. Kinetic analysis was performed on data collected during ozone photolysis experiments in the presence and absence of known hydroxyl radical scavengers. This analysis indicated that ozone photolysis in aqueous solution leads directly to the formation of hydrogen peroxide, which then produces hydroxyl radical by secondary reaction of peroxy anion (HO_2^-) and subsequent species with ozone. The mechanistic results predict a maximum yield of 2/3 hydroxyl radical for each ozone molecule that is consumed by photolysis or subsequent reaction. The mechanistic results also predict a plateau in the hydroxyl radical yield as a function of the fraction of ozone photolyzed. The plateau in the hydroxyl radical yield in turn implies a plateau in treatment efficiency for organic compounds. A simple model was developed for ozone mass transfer with chemical and photochemical reaction. Using pilot plant data, a treatment cost projection for removing THMFP by photolytic ozonation was made. At 1-MGD capacity, projected treatment costs were 55¢, 70¢ & 90¢ per 1000 gal. for 60%, 70% & 80% THMFP removal respectively, assuming an electrical energy cost of 10¢ per kilowatt-hour.

17. KEY WORDS AND DOCUMENT ANALYSIS

a. DESCRIPTORS	b. IDENTIFIERS/OPEN ENDED TERMS	c. COSATI Field/Group

18. DISTRIBUTION STATEMENT RELEASE TO PUBLIC	19. SECURITY CLASS *(This Report)* UNCLASSIFIED	21. NO. OF PAGES 204
	20. SECURITY CLASS *(This page)* UNCLASSIFIED	22. PRICE

EPA Form 2220-1 (9-73)

DISCLAIMER

The information in this document has been funded wholly or in part by the United States Environmental Protection Agency under assistance agreement number CR808825 to The University of Texas at Dallas. It has been subject to the Agency's peer and administrative review, and it has been approved for publication as an EPA document. Mention of trade names or commercial products does not constitute endorsement or recommendation for use.

FOREWORD

The U.S. Environmental Protection Agency was created because of increasing public and government concern about the dangers of pollution to the health and welfare of the American people. Noxious air, foul water, and spoiled land are tragic testimonies to the deterioration of our natural environment. The complexity of that environment and the interplay of its components requires a concentrated and integrated attack on the problem.

Research and development is that necessary first step in problem solution; it involves defining the problem, measuring its impact, and searching for solutions. The Municipal Environmental Research Laboratory develops new and improved technology and systems to prevent, treat, and manage wastewater and solid and hazardous waste pollutant discharges from municipal and community sources, to preserve and treat public drinking water supplies, and to minimize the adverse economic, social, health, and aesthetic effects of pollution. This publication is one of the products of that research and provides a most vital communications link between the researcher and the user community.

Reported here are the results of a pilot scale evaluation of one treatment technique for the removal of trihalomethane precursors from drinking water: photolytic ozonation.

Francis T. Mayo
Director
Municipal Environmental Research
Laboratory

ABSTRACT

The use of ozone combined with ultraviolet radiation has been studied at the pilot scale for removing trihalomethane (THM) precursors from potable water. The effects of variations in ozone dose rate, UV intensity, and other parameters were first studied using a synthetic feedwater that was reconstituted from a humic concentrate. This concentrate was obtained by eluting GAC columns with sodium hydroxide solution. The column had been used for the adsorption of humic material from water in a previous project. The pilot plant was then operated for 8 months at the Sabine River Water Treatment Plant in Longview, Texas.

A laboratory investigation of the mechanism of the ozone/UV process was also conducted. Kinetic analysis was performed on data collected during ozone photolysis experiments in the presence and absence of known hydroxyl radical scavengers. This analysis indicated that ozone photolysis in aqueous solution leads directly to the formation of hydrogen peroxide, which then produces hydroxyl radical by secondary reaction of peroxy anion (HO_2^-) and subsequent species with ozone.

The mechanistic results predict a maximum yield of 2/3 hydroxyl radical for each ozone molecule that is consumed by photolysis and subsequent reactions. The mechanistic results also predict a plateau in the hydroxyl radical yield as a function of the fraction of ozone photolyzed. This plateau in hydroxyl radical yield in turn implies a plateau in treatment efficiency for organic compounds. A simple model was developed for ozone mass transfer with chemical and photochemical reaction. Correlation of this model with mechanistic and pilot plant data is ongoing.

Analysis of the residual trihalomethane formation potential (THMFP) after treatment, coupled with operating data from the pilot plant, provided the basis for a treatment cost projection for removing THMFP by photolytic ozonation. At 1-MGD plant capacity, projected treatment costs were $0.55, $0.70 and $0.91 per thousand gallons for 60%, 70% and 80% THMFP removal, respectively, assuming an electrical cost of $0.10 per kilowatt hour. At this capacity, projected treatment costs

were still decreasing rapidly with increased plant capacity.

This report was submitted in fulfillment of Cooperative Agreement No. CR808825 by the University of Texas at Dallas under the sponsorship of the U.S. Environmental Protection Agency. This report covers the period 4/1/81 to 6/30/84, and the work was completed as of 6/30/84. Portions of the work were performed at SumX Corporation, Austin, Texas, under subcontract to the University of Texas at Dallas.

CONVERSION OF ENGLISH UNITS TO METRIC

To Convert	To	Multiply by
feet	meters	0.3048
gallons	liters	3.785
inches	centimeters	2.540

CONTENTS

Foreword iii
Abstract iv
Conversion vi
Figures viii
Tables xi
Abbreviations and Symbols xiii

1. Introduction 1
2. Conclusions 2
3. Recommendations 3
4. Background 4
5. Laboratory Study 11
    Objectives 11
    Experimental Methods 12
    Results 15
    Conclusions 36
6. Pilot Scale Studies 37
    Introduction 37
    Mass Transfer Characteristics of the Reactors 42
    Parametric Variation Studies on Synthetic Lake Water 51
    Results of Pilot Studies at Longview, Texas. 107
7. Cost Analysis 139
8. Byproducts of Photolytic Ozonation 148
    Experimental Techniques and Equipment . . . 148
    Sample Work-up, Analytical Details and Results 151
9. Quality Assurance Practices 154

References 160

APPENDICES

A. Water Quality Data from Sabine River Water Treatment Plant 165
B. Treatment Cost Information 171
C. Narrative Statement Concerning Q.A. Practices . . 175

FIGURES

Number		Page
1	Two film model of mass transfer	7
2	Laboratory ozonation system	13
3	Construction details of continuous stirred-tank reactor	14
4	Ozone photolysis in acetic acid solution. HBI, Ti(IV) and BKI/M measure ozone, hydrogen peroxide and total oxidant levels respectively	17
5	Effect of pH on hydrogen peroxide accumulation. . .	18
6	Hydrogen peroxide accumulation in the presence of acetic and sulfuric acids	19
7	Ozone photolysis in presence of bicarbonate	20
8	Oxidant concentrations during ozone photolysis in distilled water	21
9	Proposed ozone/UV reaction system	26
10	Flow diagram of the pilot water treatment research facility	39
11	Radiative and mass transfer with chemical and photochemical reaction	50
12	Ozone and ozone/UV reduction of trihalomethane formation potential	59
13	TOC reduction by ozone and ozone/UV	60
14	Ozone/UV reduction of THMFP using two UV lamps . .	61
15	Ozone/UV destruction of THMFP. Four lamps	63
16	Applied ozone dose required for 63% removal of TTHMFP	64

17 THMFP reduction, flow runs. Ozone dose rate = 1.4 mg/L-min. 66

18 THMFP reduction, flow runs. Ozone dose rate = 2.4 mg/L-min. 67

19 THMFP reduction, flow runs. Ozone dose rate = 4.0 mg/L-min. 68

20 Applied ozone dose required for 63% removal of TTHMFP 69

21 Utilized dose required for 63% removal of TTHMFP 73

22 Capture efficiency in CSTR flow experiments . . . 75

23 Utilization efficiencies in TPR experiments 99

24 Formation potential removal in TPR experiments . . 101

25 THMFP removal using simultaneous contacting and photolysis in CSTR 108

26 Change of normalized TTHMFP (C/C_0) with time during lamp well coating experiment 110

27 Effect of ozone dose on TTHMFP removal in DI and CP modes 113

28 TTHMFP removal using TCSTR CP (4L) configuration . 124

29 Formation potential removal in the tubular photochemical reactors 126

30 Comparison of configurations for THMFP removal . . 127

31 Projected treatment costs as a function of TTHMFP removal 142

32 Projected treatment costs for systems up to 5 MGD 143

33 GC/FID chromatogram of derivatized methanol extract from Experiment I 150

34 Total ion chromatogram of derivatized methanol extract from Experiment I 152

35 Day-to-day electron-capture detector response of individual trihalomethanes 156

36 Effect of sample storage on total trihalomethane formation potential 158

A-1 Chloride content of finished water during pilot operation 166

A-2 Correlation of summed water quality parameters with total residue 167

TABLES

Number Page

1 Hydrogen Peroxide Photolysis Rate Constants in the Absence and Presence of Scavengers 23

2 Rate Constants used for Kinetic Analysis of the Ozone/UV System, $M^{-1}s^{-1}$ 27

3 Laboratory Experiments on Effect of Wavelength . . 35

4 Mass Transfer Coefficients for the TCSTR 44

5 Mass Transfer Coefficients for the TCSTR 45

6 Mass Transfer Coefficients from Field Data 46

7 Percent of Influent Ozone Found in TCSTR Off-gas . 72

8 Efficiency Data for Set A 79

9 Efficiency Data for Set B 80

10 Efficiency Data for Set C 85

11 Efficiency Data for Set H 87

12 Efficiency Data for Set I 90

13 Oxidant Data for Data Set I 92

14 Efficiency Data for Set J 93

15 Oxidant Data for Set J 94

16 Efficiency Data for Set K 96

17 Efficiency Data for Set L 97

18 Effect of Second Pair of TPR's on Ozone Utilization Efficiency 105

19 Data from Experiment H 112

20 Ozone Decomposition in Stainless Steel Tubing . . . 119

21 Formation Potential Data for Experiment W 120

22 Formation Potential Data for Experiment X 122

23 Formation Potential Data for Experiment Y 123

24 TOC Removal in the TCSTR System 130

25 TOC Removal in TPR System 131

26 Ozone Dose Requirements of the Configurations Tested 138

27 Capital Cost for THMFP Removal Using Photolytic Ozonation 140

28 Operating and Maintenance Costs 141

29 Projected Treatment Costs 144

30 Projected Treatment Costs as a Function of TTHMFP Removal 147

31 Effect of Storage on TTHMFP Analysis 157

A-1 Alkalinity Data Outside of Normal Range 168

A-2 Hardness Data Outside of Normal Range 170

LIST OF ABBREVIATIONS AND SYMBOLS

A_v	-	surface area per unit volume m_i/m
BKI	-	boric acid buffered iodimetric analytical method for oxidants
BKI/M	-	modification of BKI method by addition of molybdate catalyst
CSTR	-	continuous stirred tank reactor
D	-	ozone dose in mg/L
D	-	ozone dose rate in mg/L-min
D_1	-	applied ozone dose required for removal of substrate to 1/e of its initial value
D_1	-	utilized ozone dose required for removal of substrate to 1/e of its initial value
D_I - II	-	notation for description of experimental configuration. Ozone is added in the reactor signified by the first subscript and removed in the latter
E_c	-	ozone capture efficiency, $E_c = 1 - C_g^{out}/C_g^{in}$
E_u	-	ozone utilization efficiency, $E_u = 100(1-FP/FP_o)D^{-1}$
EC	-	electron capture detector (GC)
FID	-	flame ionization detector (GC)
FP	-	trihalomethane formation potential, when used to describe a substance, rather than the result of an analytical measurement
FP/FP_o	-	fraction of FP remaining after treatment
GC	-	gas chromatograph, gas chromatography

GC/MS - GC/MS/DS

GC/MS/DS - gas chromatograph with mass spectrometer as detector and computer-controlled data acquisition

GPM - gallons per minute

h - Planck's constant

HBI - analytical technique for aqueous ozone, developed by Hoigne and Bader

HM - humic material, undifferentiated with respect to type, molecular weight, etc.

HPLC - high performance liquid chromatography

k_{ij} - second-order reaction rate constant between species i and j, $(\text{mole/L})^{-1}\ \text{sec}^{-1}$

k_l - mass transfer coefficient, $m_l^3/m_i^2\text{sec}$, or ms^{-1}

kwh - kilowatt hours

L - liter

m - meter

m_i^2 - interfacial surface area, square meters

m_l^3 - liquid volume, cubic meters

s - second

t_l - treatment time required for removal of substrate to 1/e of its initial value

t_r, t_c - average hydrualic retention time of reactor or contactor

TCSTR - CSTR with turbine rather than paddle-type impeller

THMFP - trihalomethane formation potential

Ti(IV) - method of peroxide analysis using titanium in the +4 oxidation state

TOC - total organic carbon

TPR - tubular photochemical reactor

TTHMFP - total trihalomethane formation potential

V_r, V_c - liquid volume of reactor or contactor

W - watt

GREEK LETTERS:

θ - photon to ozone ratio

λ - photon wavelength

ν - photon frequency, $\nu = c/\lambda$

ϕ - quantum yield

ϕ_n - hydroxyl radical yield

SECTION 1

INTRODUCTION

The chlorination of natural water for potable use is known to result in the production of trihalomethanes (THM's), which have been shown to be carcinogenic in laboratory animals. A preliminary laboratory study was reported in 1980(1) showing that the potential of natural waters for producing THM's upon chlorination could be essentially eliminated by treatment with ozone combined with ultraviolet (UV) radiation. The present report describes a pilot-scale evaluation of photolytic ozonation for the destruction of THM precursors in water.

The project was conducted in four parts: 1) a laboratory and theoretical investigation of the mechanism of photolytic ozonation, 2) construction and initial testing of the pilot plant using a reconstituted lake water concentrate for feedwater consistency, 3) continuous operation of the pilot plant using feedwater from the Sabine River Water Treatment Plant located in Longview, Texas, and 4) a laboratory study of byproducts formed upon photolytic ozonation of natural waters. The laboratory studies were performed concurrently with the pilot-scale work. The mechanistic results were used in conjunction with a model that was developed for mass transfer with photochemical reaction to interpret the results obtained. The mechanism of photolytic ozonation was shown to be closely related to that of base-catalyzed and peroxide-catalyzed ozonation. Treatment costs were projected for 0.1-, 0.5-, 1.0- and 5.0- MGD plants from the operating data collected during pilot scale operation in Longview, Texas.

SECTION 2

CONCLUSIONS

The laboratory study shows that the primary mechanism of photolytic ozonation with UV irradiation at 254 nm is the photolysis of ozone to produce hydrogen peroxide, which dissociates to some degree to produce peroxy anion. The reaction between peroxy anion (and in a later step, superoxide) and ozone produces hydroxyl radical, which is the primary active species of the ozone/UV process. These conclusions predict that a) the maximum yield of hydroxyl radical per ozone molecule is 2/3, and b) when more than a third of the available ozone is photolysed, little or no increase in hydroxyl radical production should be obtained.

The pilot-scale study showed that an ozone dose of 27 mg/L of water (i.e., transferred from the gas phase to the liquid) was sufficient to reduce the trihalomethane formation potential (THMFP) of clarified and filtered Sabine River water to 1/e (37%) of its original value, using a continuous flow stirred tank reactor with 0.27 watts of UV per liter applied in the reactor. If UV application was delayed until after initial ozone contacting, or if the stirring or UV was omitted, required dosages (still based on that amount of ozone transferred out of the gas) were 34, 41, and 48 mg/L respectively. The experimental data supported the concept of minimal increase in treatment efficiency above a certain UV intensity. The lowest rate of ozone addition that resulted in the desired THMFP removal was the most efficient in terms of ozone utilization.

The projected treatment costs of the process for a 1 mgd plant for 60%, 70% and 80% removal of THMFP from clarified Sabine River water were $0.55, $0.70 and $0.91 per thousand gallons, respectively, at an assumed electrical cost of $0.10 per kilowatt hour. Treatment costs were still strongly dependent on plant capacity at this size. The increase in process efficiency realized by the addition of stirring and UV greatly outweighed the increased cost over ozonation alone in these cost projections. The dominant term (65%) in the projected treatment cost is the amortized capital cost of the ozone generation and feed equipment.

SECTION 3

RECOMMENDATIONS

Further laboratory scale investigations should be made of several points that either were beyond the scope of this study or emerged too late in the study to be systematically investigated. Ozonation of natural organics in water should be studied to determine how or whether it is possible to suppress the formation of new THM precursor material during the destruction of that which is initially present. If that could be accomplished, the possibility would exist for considerably lowering the ozone dose needed for satisfactory THMFP removal. The model developed for mass transfer with simultaneous chemical and photochemical reaction should be verified in the laboratory under conditions where careful oxidant measurements can be made. The use of a simple model substrate rather than natural organic material would increase the probability of success, as would the use of a photolyte (substance to be photolysed) which is less susceptible to side reactions than ozone. Finally, a survey of ozone dose requirements for water samples from different geographical locations would provide information concerning the transferability of projected treatment costs from one water source to another.

Two further studies are necessary before photolytic ozonation could be recommended as a potable water treatment process. Thorough toxicity/mutagenicity testing should be done on concentrates of treated and untreated water from several different water sources to help insure that public health problems do not develop later. The process itself should be tested at the field scale to verify ozone and UV dose requirements in larger systems and to address the problems associated with scale-up of the complicated photochemically initiated reaction.

Finally, the question of catalytic decomposition of ozone in stainless steel tubing and vessels in the presence of water should be addressed because of its implications in existing ozone applications.

SECTION 4

BACKGROUND

INTRODUCTION

The object of this work was to evaluate the ozone/UV process at the pilot scale to assess the feasibility of the process for the destruction of THM precursors in drinking water. This section outlines the most important information gained from the literature survey which was performed at the beginning of the project and continued throughout. Subsections include mechanistic inferences from the literature, radiative and mass transfer considerations, and by-products of photolytic ozonation.

MECHANISTIC INFERENCES FROM THE LITERATURE SURVEY

Photolytic ozonation has been studied by Glaze, et al(1), and the ozone and ozone/UV literature up to 1980 was reviewed in the final report of that study. Since no mechanistic investigations were conducted during that project, the mechanistic conclusions of that report were drawn solely from the literature. A brief discussion of those conclusions follows.

In the gas phase, the photolysis of ozone produces an oxygen molecule and an oxygen atom, the electronic states of which depend on the wavelength of radiation used. Lin and DeMoore(2) have shown that $O(^1D)$ is produced when λ_{ex} is less than about 310 nm, while $O(^3P)$ is the product at longer wavelengths. When water vapor is present $O(^1D)$ and H_2O react to form two hydroxyl radicals whereas $O(^3P)$ is apparently incapable of this reaction.

In the condensed aqueous phase it is possible that similar processes occur yielding hydroxyl radicals in the primary step. However, on the basis of a study of the photolysis of ozone in aqueous acetic acid solution, Taube(3) concluded that hydrogen peroxide, not two hydroxyl radicals are formed initially. It is not clear whether H_2O_2 is the primary product or the result of geminate recombination of two hydroxyl radicals which do not escape the solvent cage. The two cases are experimentally indistinguishable.

Direct evidence of hydroxyl radicals from the photolysis of ozone in aqueous solution has not been presented before the present study, although Taube and Bray(4) postulated that hydroxyl radicals are formed in secondary reactions between ozone and hydrogen peroxide. The only published attempt to identify active species in ozone photolysis, performed by Leitus and coworkers(5) was interpreted as demonstrating the absence of hydroxyl radicals, because of the similarity between products formed from ozonation and ozone/UV experiments.

At the same time that mechanistic work was proceeding on the present project (discussed in Section 5) a paper was published by Staehelin and Hoigne(6) which threw serious doubt on the interpretations of Leitus et al. In this paper Staehelin and Hoigne showed that in most practical cases, the reaction of ozone with HO_2^-, the anion of hydrogen peroxide, results in the production of hydroxyl radicals by the following sequence:

$$H_2O_2 \rightleftharpoons H^+ + HO_2^- \qquad pK_a = 11.6$$

$$HO_2^- + O_3 \xrightarrow{k_{13}} HO\cdot + O_2^- + O_2 \qquad k_{13} = 2.8\times10^6\ M^{-1}s^{-1}$$

$$O_2^- + O_3 + H_2O \longrightarrow HO\cdot + {}^-OH + 2O_2$$

It is now known that hydrogen peroxide is produced in many reactions of ozone with organic compounds(7-10); thus, it seems likely that Leitus et al.(5) found the same products from ozone and ozone/UV systems because hydroxyl radicals were present in both cases. Since k_{13} is considerably faster than most ozonation reactions(11,12), hydroxyl radical reactions may be quite significant in ozonation reactions even at pH values lower than the value of 9 or 10 which Hoigne and Bader(13) have shown as the pH region where hydroxyl radical reactions become dominant.

Several investigators have studied the ozone/hydrogen peroxide system. Taube and Bray(4) found it necessary to assume the participation of perhydroxyl and hydroxyl radicals to explain their data for the chain reactions of ozone and hydrogen peroxide in acidic solution. As mentioned earlier, Staehelin and Hoigne(6) gave evidence for the importance of the corresponding reaction scheme, where HO_2 is replaced by superoxide (O_2^-) in ozonation systems. Vahidi, Wallace, Alladin and Fernandes(14) showed that in the destruction of THM precursors using ozone and peroxide, the efficiency of precursor destruction per amount of ozone used decreased above a certain liquid phase peroxide concentration, probably due to competitive radical scavenging by peroxide. Namba and Nakagama(15), in experiments similar to those of Hoigne and Bader(13) on the relative disappearance rates of competitive substrates, demonstrated that the active species in the ozone/peroxide reaction was hydroxyl radical. In addition, Baxendale and Wilson(16) showed that the reaction of hydroxyl radicals with many organic compounds results in the generation of hydrogen peroxide, so that the involvement of the hydrogen peroxide in the ozone/peroxide system is at least partially "catalytic".

Thus, from the literature prior to 1983 one could infer from the work of Taube(3), Taube and Bray(4) and Staehelin and Hoigne(6) that hydroxyl radicals are active species in the ozone/UV system, but that they are generated indirectly through hydrogen peroxide. The work described in Section 5 provides the first experimental evidence that this conclusion is correct.

MASS TRANSFER, RADIATIVE TRANSFER, AND PHOTOCHEMICAL REACTION

Two models are most commonly used to describe mass transfer in gas-liquid systems. These models, the surface renewal theory as presented by Danckwerts(17) and the two film model of Whitman(18) and Lewis and Whitman(19), are treated in virtually all chemical engineering textbooks(20) and will not be given here. The modification of the two-film model to include simultaneous chemical reaction in the bulk liquid phase is similarly widely treated (e.g. references 20,21) and will be reproduced in part here only to establish a point of departure for the introduction of the photochemical considerations. For reactions with equal diffusivities of product and reactant the enhancement by chemical reaction has been shown to be insensitive to the choice of mass transfer model(20).

In the two film model it is generally assumed for low-solubiligy gases that the gas-side resistance to mass transfer is small, that is, that the concentration of transferred species A at the gas-liquid interface (C_{gi}) is approximately equal to the bulk gas phase concentration Cg (Figure 1). It is further assumed that the liquid phase concentration at the interface, $C_{li} = C^*$ is that which satisfies the Henry's Law relationship with C_{gi}. Net transport of species A results from diffusion of A from the interface to the bulk phase which is of lower (uniform) concentration C_l in A. The film thickness y_l is loosely defined as the region where $C_{li} > C > C_l$.

In the kinetic regime, intermediate between instantaneous reaction ($C_l = 0$) and very slow reaction ($C_l \cong C_{li}$), mass transfer is proportional to the difference between C^* and C_l.

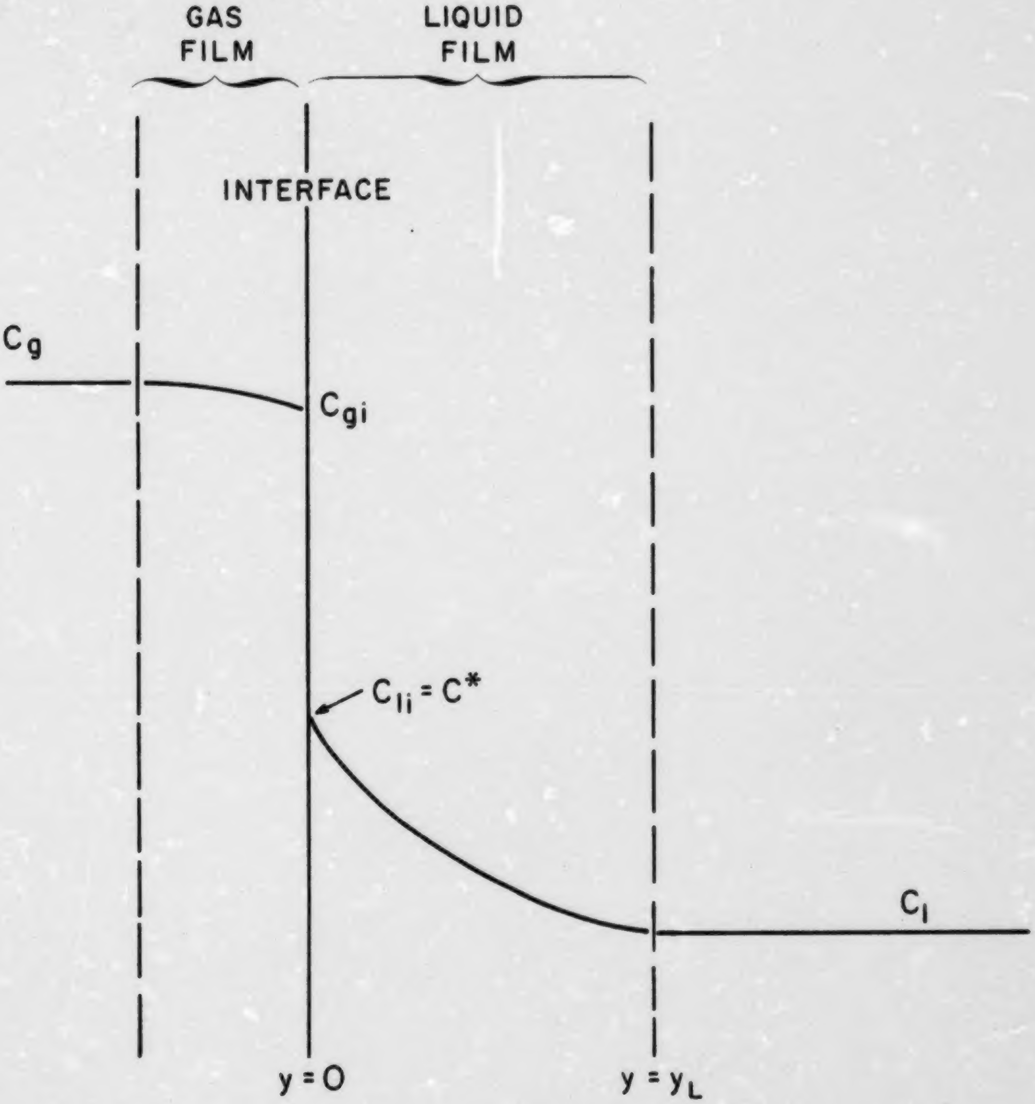
GAS FILM
LIQUID FILM
INTERFACE
C_g
C_{gi}
$C_{li} = C^*$
C_l
y = 0
y = y_L

Figure 1. Two-film model of mass transfer.

The enhancement of mass transfer by the chemical reaction is usually described by a multiplicative factor onto the mass transfer coefficient obtained under similar physical conditions but with no chemical reaction. This factor is sometimes called the Hatta factor(20). Although several cases of interest have been solved in closed form for simpler situations, the present application involves not only pseudo first order reactions of ozone itself such as base and peroxide-catalysed decomposition and direct reactions of ozone, but also an exponential (Beer's Law) dependence of ozone photolysis rate on bulk liquid ozone concentration as well as radial distance from the UV lamp, thus presenting a much more complicated problem.

Most photochemical reactions are either first-order or one-half order depending on whether the reactions are non-chain or chain reactions, respectively. In the former case, the reaction rate can usually be described if the mean rate of photon absorption is known, while in the latter the concentration gradient of highly reactive species may depend on the light absorption profile and transport characteristics(22). Several models have been used to describe the intensity profile emitted by a submerged lamp, among them the simple radial, two dimensional or line source (LS)(23), and the three dimensional, or extended source (ES) model(24).

The radial model assumes all light rays emanate radially (perpendicular) from the lamp, so that a distance r from the axis of the lamp, the flux per unit length of the cylinder is given by(22)

$$I_r = r^{-1} r_o I_{ro} \exp[-u(r-r_o)],$$

where u is the product of the concentration of absorbing species and molar absorption coefficient, and r_o is the radius of the lamp. The line source model assumes that the source (lamp) is a straight line from each point of which light is emitted in all directions. This model results in a more complicated expression for the intensity profile, while the extended source model is more complicated still.

For the present application, it can be seen that a simple model is desirable for use in kinetic and mass transfer relationships. Although Tournier and Deglise(22) found the radial model unsatisfactory as such for their purposes, they were able to show excellent correlation with measured intensity values by applying a multiplicative parametric correction factor, k, to u. Their value, (k = 1.14) is greater than unity because the rays which are emitted at a higher or lower angle than perpendicular to the lamp traverse a longer path length before reaching the wall of the reactor. Furthermore, their results showed that for optical densities less than 0.40 cm^{-1} the results of the simple radial model were satisfactory for the present purposes, since for the highest residual ozone concentration measured in the present work,

$$u = \varepsilon c = 3 \times 10^3\ M^{-1}cm^{-1} \times 10^{-4}\ M = 0.3\ cm^{-1}.$$

Thus, the modified radial model is used in Section 6 to develop a mathematical model of mass transfer with chemical and photochemical reaction.

BYPRODUCTS OF PHOTOLYTIC OZONATION

In an earlier section it has been implied that photolytic ozonation, ozone/hydrogen peroxide, and indirect ozonation (as defined by Hoigne(13,25)) all have common intermediates and active species, and differ mainly in their origin and rate of production. Indeed, by evaluating ozonation rate constants under conditions where free radical reactions are carefully suppressed, Hoigne and Bader(11,12) and Staehelin and Hoigne(25) have shown that many "ozonation" products which have been reported in the past, may actually be products of the indirect, i.e., free radical reaction. This free radical reaction can be initiated even at relatively low pH since the aqueous decomposition of ozonides is known to yield peroxides in some cases(26). One consequence of the above is that by-products of photolytic ozonation can be expected to resemble many of the products reported previously for ozonation in systems where the free radical reactions were not suppressed.

Many such product studies were reviewed in a previous report(1). Typically in these and later studies, rings and chains are oxidatively dismantled until small molecules such as formic and oxalic acids are reached. While reactions of these acids with ozone are relatively slow(12), reaction of oxalic acid with hydroxyl radical is in the $10^6 - 10^7\ M^{-1}\ s^{-1}$ range and formic is 10-100 times faster(27), so that in the free radical systems (O_3/UV, O_3/H_2O_2, $O_3/^{-}OH$) these acids are not as refractory to treatment. Introduction of an oxygen containing functional group into an aromatic ring generally makes the molecule more reactive to both ozone(12) and hydroxyl radical(27), although the latter system is complicated by the apparent reversibility of hydroxyl radical reactions with some aromatic compounds(28). This reversibility leads not only to rearrangement of products, but can actually catalyse other reactions which otherwise would not occur. For example, when a dilute aqueous solution of benzene/nitrobenzene is subjected to persulfate thermolysis at 80°C, phenol, biphenyl, and o- and p-nitrophenol are formed(28). When benzene is replaced by toluene or anisole, no nitrophenols are formed. The above illustrates the difficulty of inferring mechanistic information from organic reaction products in a complex system.

The presence of oxygen in solution has a profound effect on the products of hydroxyl radical reactions, as was seen in the work of Baxendale and Wilson(16) referred to earlier. Also oxygen has been shown to remove a hydrogen atom from the hydroxycyclohexadienyl radicals formed from reaction of hydroxyl radical and benzene(29), to give phenol and HO_2 (O_2^-) which further disproportionates to yield hydrogen peroxide(30,31,32).

The result of ring and chain scission by ozone or hydroxyl radical is generally the formation of aldehydes and acids which undergo further degradation(7,8,9,10,29). With the molecular weight of humic material assumed to be in the range of a few thousand to tens of thousands, little accumulation of any major products would be expected until the very end of the process where products such as the simple one and two carbon acids and aldehydes are the meeting points of various degradative pathways. The appearance of major products larger than one ring would have important implications about the structural regularity of humic material. An active species as unselective as hydroxyl radical, however, is considerably less likely to leave even a highly ordered humic material in the same manner a sufficient number of times to produce large (greater than one ring) major products, than is a more selective species such as ozone.

SECTION 5

LABORATORY STUDY

OBJECTIVES

The original objectives of the laboratory study were to determine the active specie(s) responsible for the effectiveness of the ozone/UV process and, if possible, to outline the mechanism by which the process works. The former would aid correlation of experimental data and perhaps prediction of interferences, while the latter could allow a more complete microscopic description of the relationship between mass transfer, photolysis, active species generation, and substrate destruction.

APPROACH

The ozone/UV-organic compound reaction system is a complicated one. Many of the results from the previous study(1) as well as inferences from the ozone photolysis literature (Section 4) indicated that the process was probably free radical in nature, promising an even more complicated reaction system when secondary reactions of organic radicals are included. Due to that complexity, the approach taken in the present study was to investigate ozone photolysis itself, in order to elucidate the initiation steps as well as the network of reactions which take place in the absence of organic substrate. The substrate could then be added to the reaction system as a perturbation or as a radical scavenger. In order to elucidate the initiation steps, the work of Taube(3) was chosen as the starting point, and it was decided to study the effect of known radical scavengers on hydrogen peroxide accumulation during ozone photolysis. When these studies gave unexpected results, data were analyzed from peroxide photolysis experiments being run simultaneously in this laboratory as part of another project. These results shed light on unexpected participation by radical species thought to be relatively inert. Further literature study stimulated by these results yielded sufficient information from which to construct the reaction network which is now thought to be operative in the ozone/UV system. Knowledge of this reaction network unifies base-catalysed, peroxide-catalysed, and photolytic ozonation into one reaction system which can be entered into from several different points and with differing efficiencies, depending on how the process is carried out.

EXPERIMENTAL METHODS

Laboratory Ozonation System

The apparatus used for ozonation studies is shown in Figure 2. Ozone was generated from oxygen using a plate-type Grace or Union Carbide ozone generator. After passing through stream splitting and flow controlling/measuring equipment the ozone/oxygen gas stream was sent through a six-port valve to the stirred-tank reactor (CSTR) in such a manner that either the feed gas or off-gas ozone concentration could be monitored spectrophotometrically. Rotometers were calibrated against a Hastings-Teledyne mass flowmeter, and the ozone monitor was calibrated iodometrically in the CSTR.

The CSTR was of two liter capacity, with standard relative dimensions(33,34,35), with quartz UV lamp sheathes extending through the four quadrants of the reactor, as recommended by Prengle(1,36). The reactor was constructed of glass pipe with teflon heads and aluminum baffles and impeller (Figure 3). All fittings were teflon and all tubing either glass or teflon. The reactor was stirred by a hand drill motor regulated by a variac. The stirring speed was set to 550 rpm using a phototachometer. This speed was found by Yocum(35) and Prengle(34) to give good reactor performance. Samples were withdrawn through a teflon stopcock on the bottom of the reactor.

Analytical Procedures

Samples were analysed for organic compounds by gas chromatography, using either direct aqueous injection onto Chromosorb 101 where possible, or liquid-liquid extraction where necessary. THM analyses are described in Section 6.

Ozone in the aqueous phase was analysed by the indigo method of Hoigne and Bader(37,38). This method was calibrated against the iodimetric method of Flamm(39) and checked by UV absorbance using the extinction coefficient of Hart et al(40). Hydrogen peroxide was measured by complexation with Ti(IV)(41) or by the method of Masschelein et al(42). Ozone was found to be a negative interference in the Ti(IV) peroxide method and when present was removed by oxygen sparging prior to the peroxide analysis. Total oxidants were measured iodimetrically by the method of Flamm(39) but with the addition of a small quantity of ammonium molybdate to catalyse the reaction with peroxides.

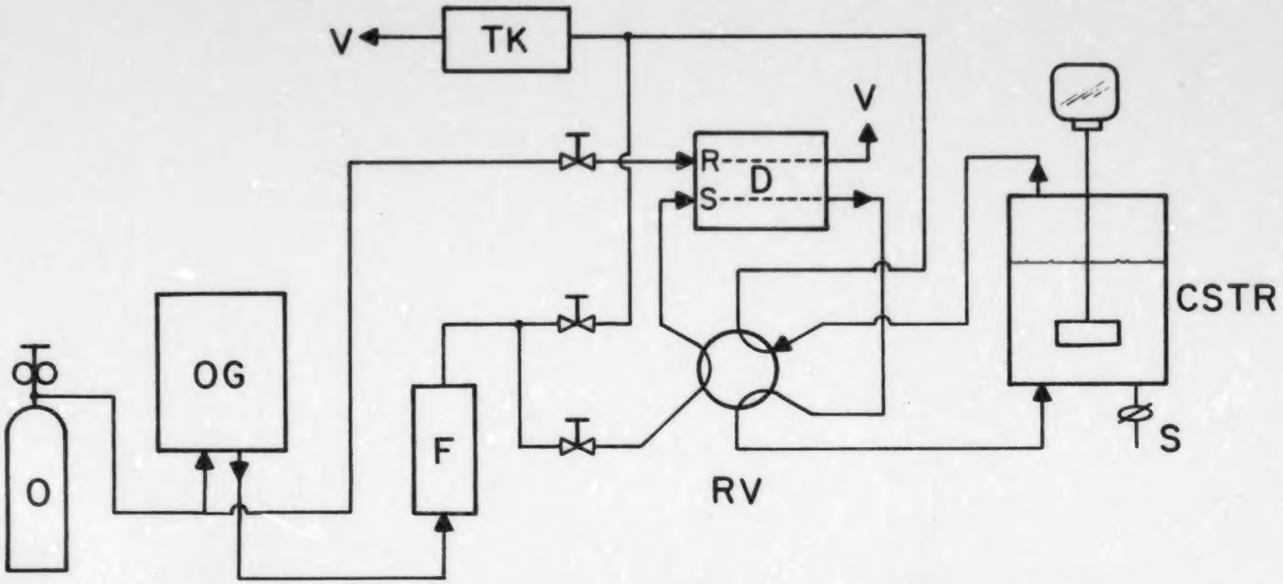

O = OXYGEN
OG = OZONE GENERATOR
V = VENT
TK = THERMAL OZONE KILL UNIT
F = ROTAMETER

D = OZONE DETECTOR
R = REFERENCE SIDE
S = SAMPLE SIDE
RV = ROTARY VALVE
CSTR = STIRRED TANK REACTOR
S = SAMPLE POINT

Figure 2. Laboratory ozonation system.

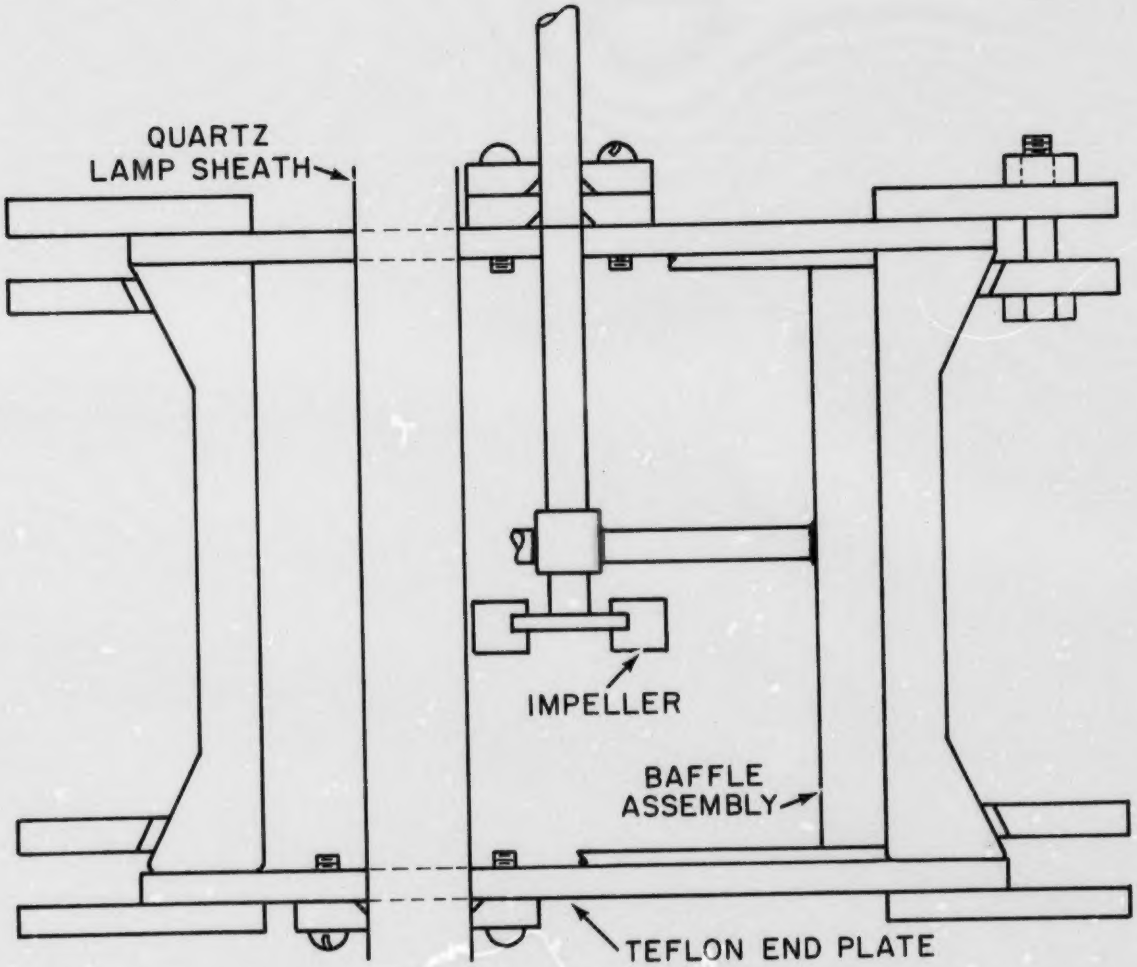
QUARTZ
LAMP SHEATH
IMPELLER
BAFFLE
ASSEMBLY
TEFLON END PLATE

Figure 3. Construction details of continuous stirred-tank reactor.

Water was purified by a Millipore or equivalent ion-exchange/carbon-filtration system, after which it was distilled from alkaline permanganate. Typical TOC levels of the final product water were 60-100 μg/L above the instrument blank, as measured by a Dohrmann DC-54 low-level carbon analyser.

Other chemicals were reagent grade and were used without further purification.

Problems Encountered

Many of the early problems were related to water purity. As in the previous project(1) it was found that transfer of ozone into purified water resulted in a higher steady-state ozone concentration in the water than in subsequent experiments using the same water after a few minutes treatment with ozone/UV ("burning out" the water). Possible explanations are that; 1) substances are formed during ozonation which interfere positively with ozone measurement, 2) a substance (such as peroxide) is formed during the ozone/UV treatment which then reacts with ozone during subsequent experiments, or 3) the ozone is initially protected from hydroxyl radical attack by organic matter which remains despite the purification procedure. The fact that the second, third, etc. experiments yield fairly consistent values compared to the first, seems to favor the third explanation. In addition it was found by continuously monitoring the liquid phase ozone concentration while sparging ozone, that in "unburned" water the ozone concentration reached a maximum then fell asymptotically with time to some steady level. When "burned" water was used, no such maximum occurred, but the steady-state level reached was the same as the asymptote in the previous experiment. Furthermore, if deionized, carbon-filtered water which had not been distilled was used, the initial maximum was even higher. A similar effect could be produced by adding small quantities of various organic compounds to "burned" water, giving further credibility to the first explanation above. The question of water purity will be returned to in the section on Results, below. The above data implied that results from small scale batch (with respect to ozone) experiments would be difficult to interpret, and those experiments were discontinued in favor of the continuously sparged experiments described below.

Results

In order to check the results of Taube(3) 0.015M acetic acid in purified water was placed in the CSTR, UV lamps turned on, stirring started and ozone flow begun. Samples were withdrawn as a function of time and analysed for ozone (HBI), hydrogen peroxide (Ti(IV)) and total oxidants (BKI/M). Results are shown in Figure 4 where it is seen that a linear buildup of hydrogen peroxide occurred while ozone remained at a very low level. It is also seen that the total oxidant level measured is equal to the sum of the hydrogen peroxide and ozone levels measured, within experimental error. These results are in agreement with those reported by Taube.

Similar experiments were performed, varying the pH while maintaining total acetic acid/acetate constant. These results are shown in Figure 5, where a definite pH effect can be seen above pH 5 with a break in behavior between pH 6 and 7. In order to establish whether the above results were in some way merely a pH effect, experiments were run substituting sulfuric acid/sulfate for acetic acid/acetate. As seen in Figure 6, very little peroxide accumulated during these experiments. It appears that the correct interpretation of these results is that acetic acid/acetate acts as a hydroxyl radical scavenger, so that as peroxide is produced by the photolysis of aqueous ozone, it is destroyed by secondary reactions with radicals and ozone unless an efficient scavenger is present. The experiment designed to confirm that hypothesis, however, yielded unexpected results.

Acetic acid was replaced by bicarbonate, known also to be a good hydroxyl radical scavenger. The results of these experiments are shown in Figure 7. Contrary to expectation, the presence of bicarbonate does not allow the accumulation of hydrogen peroxide, even though bicarbonate is a good hydroxyl radical scavenger. At this point two experiments were run in purified water with no scavengers added. These results are shown in Figure 8, and appear to be intermediate between those with added bicarbonate and those with added acetic acid. The possibilities are as follows:

Case I. Hydrogen peroxide is produced by aqueous ozone photolysis and is destroyed by secondary free radicals unless protected by an efficient radical scavenger.

$$O_3 + H_2O \xrightarrow{h\nu} O_2 + H_2O_2$$

In this case, the data of Figure 4 appear reasonable, but in order to explain the data of Figure 7, one must then assume that carbonate radical anion, the product of hydroxyl radical scavenging by bicarbonate, or some resultant species, reacts further with peroxide to prevent its accumulation.

$$\cdot OH + HCO_3^- \longrightarrow H_2O + \cdot CO_3^-$$

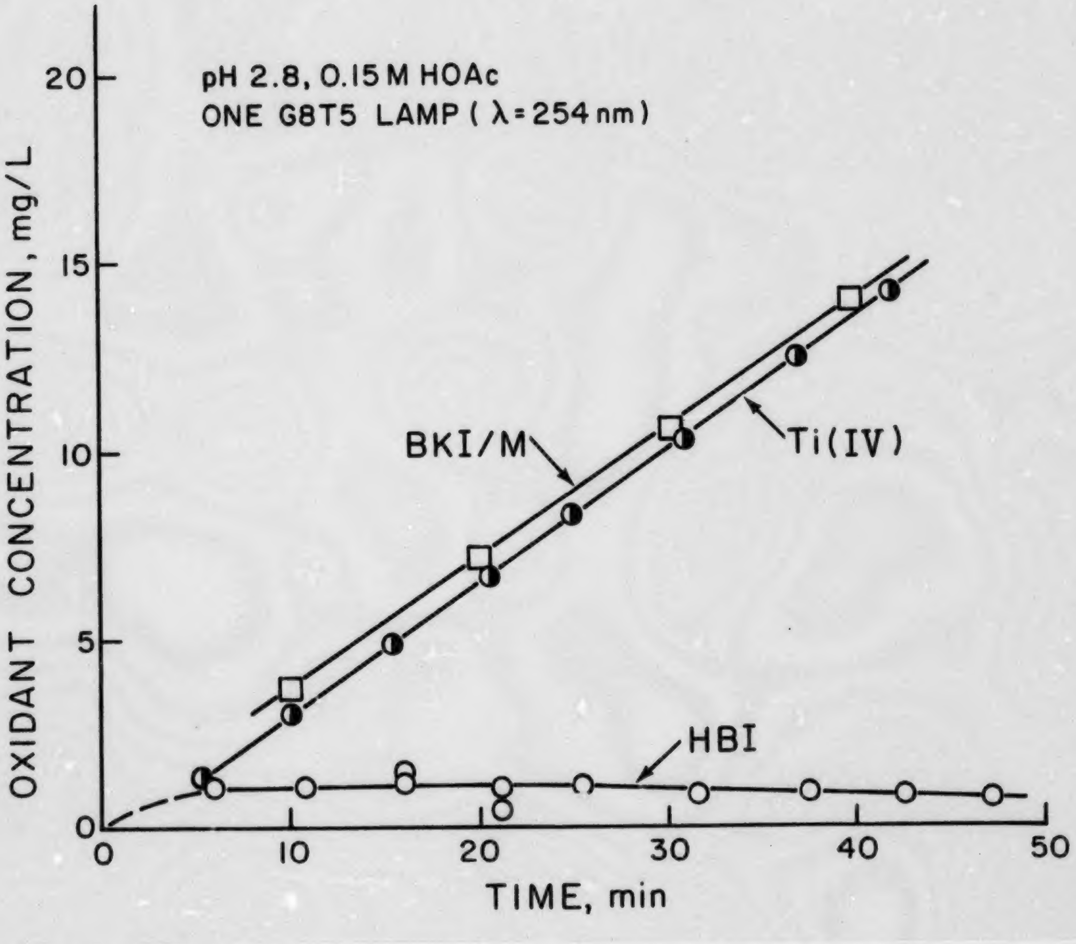

Figure 4. Ozone photolysis of acetic acid solution. HBI, Ti(IV) and BKI/M measure ozone, hydrogen peroxide and total oxidant levels respectively.

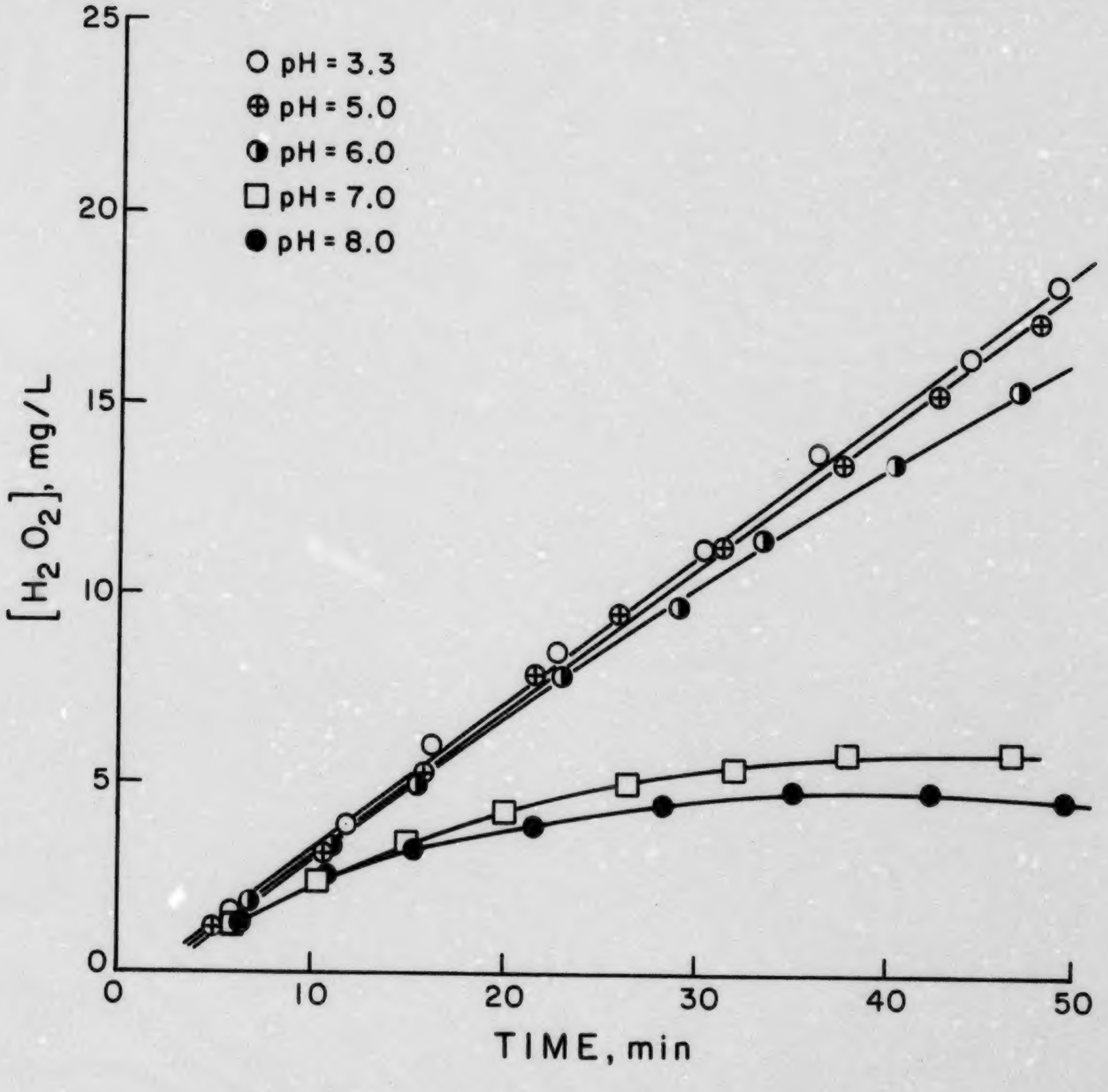

Figure 5. Effect of pH.

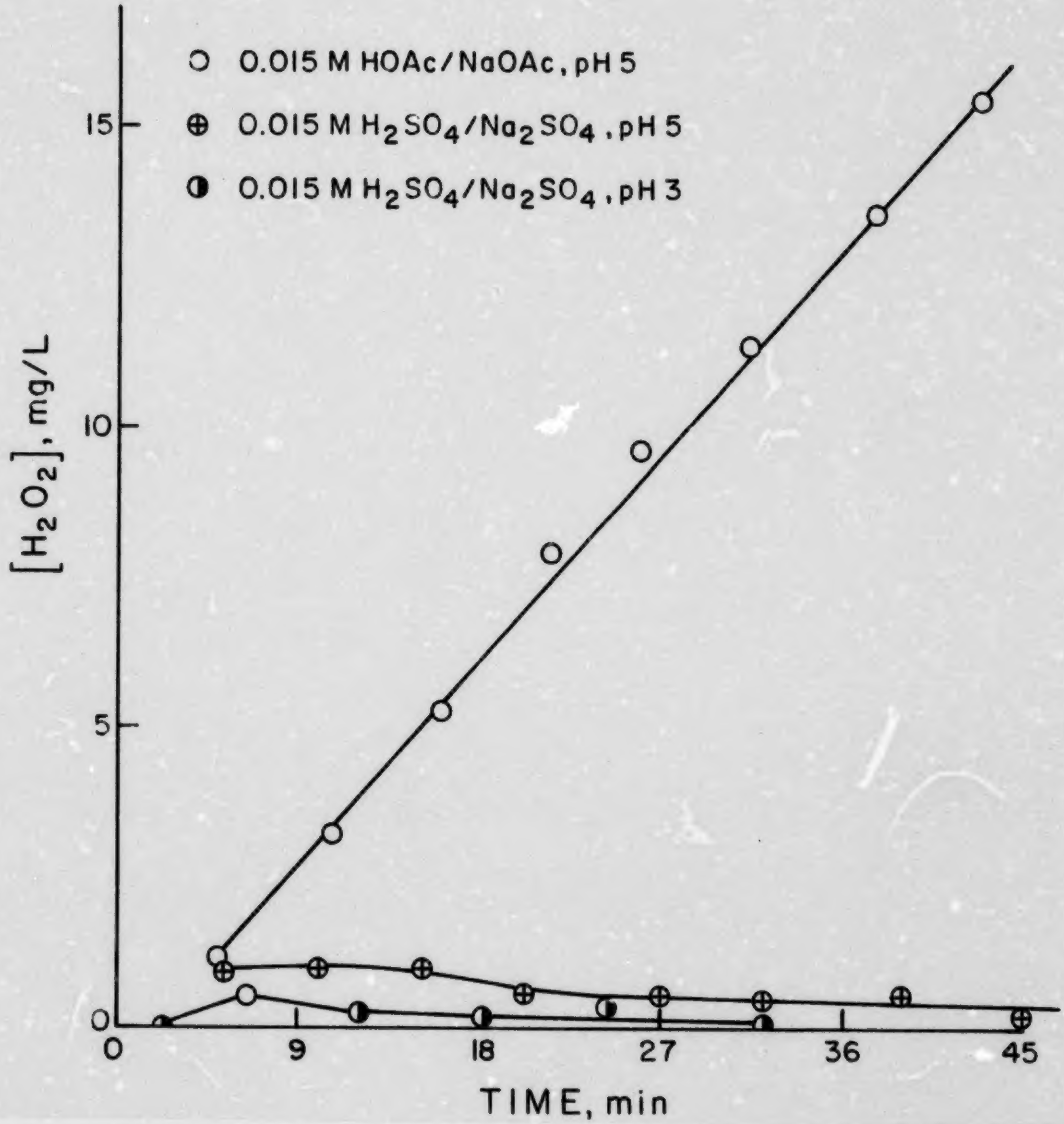

Figure 6. Hydrogen peroxide accumulation in the presence of acetic and sulfuric acids.

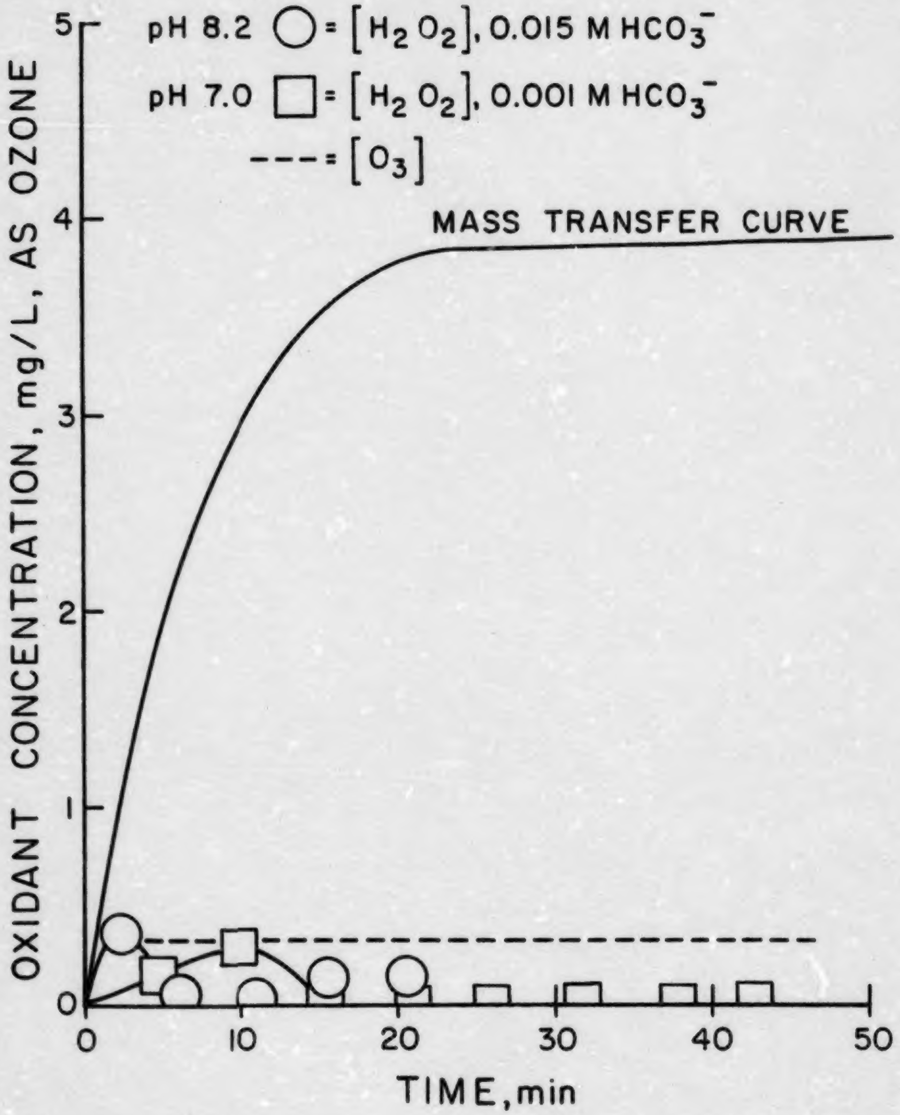

Figure 7. Ozone photolysis in presence of bicarbonate.

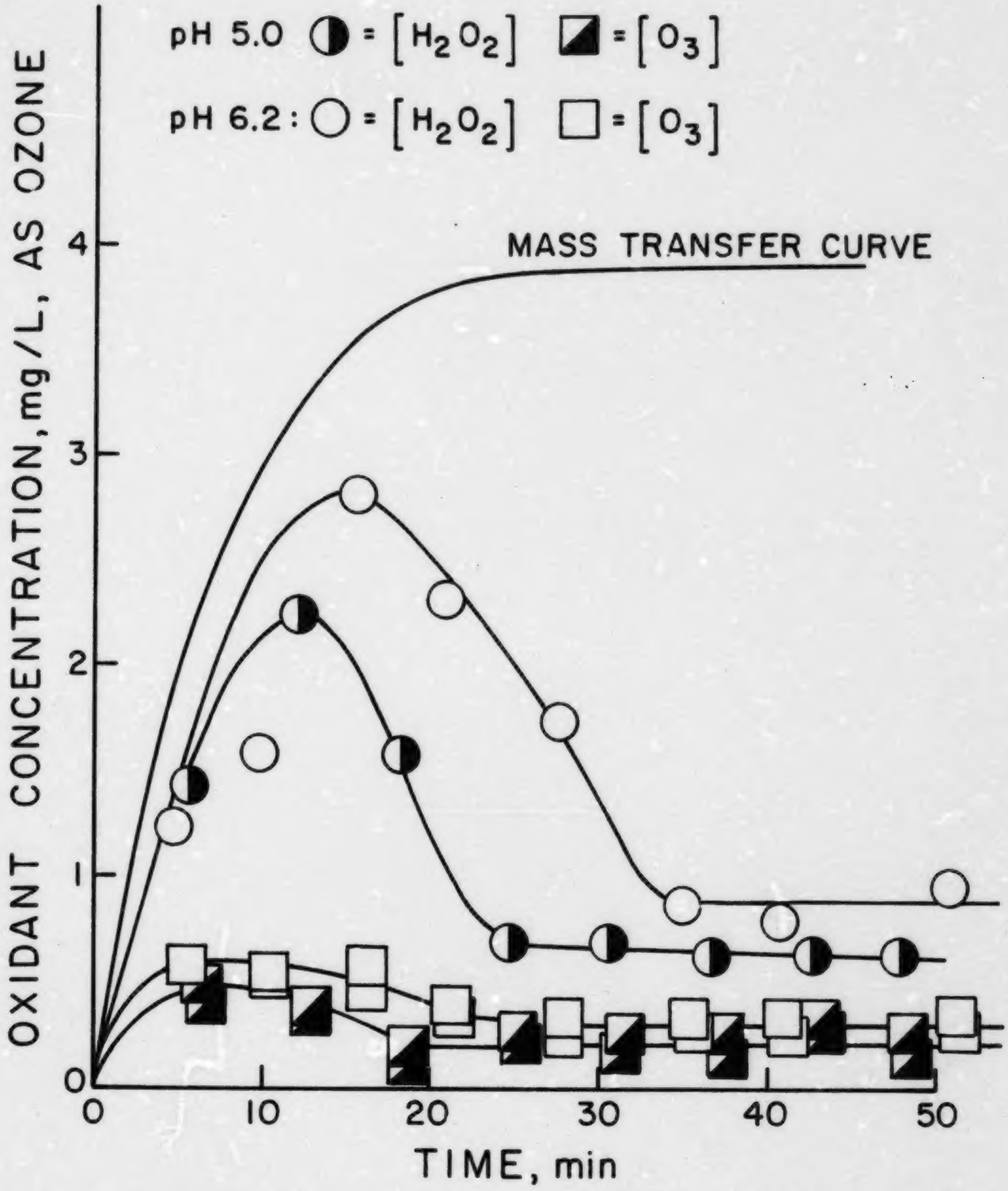

Figure 8. Oxidant concentrations during ozone photolysis in distilled water.

The alternative explanation is

Case II. Hydroxyl radical is produced directly by aqueous ozone photolysis.

$$O_3 + H_2O \xrightarrow{h\nu} O_2 + 2\cdot OH$$

In this case one must assume that the reaction of hydroxyl radical with acetic acid produces hydrogen peroxide indirectly, whereas the bicarbonate data of Figure 7 appear consistent with the assumption of direct hydroxyl radical production followed by scavenging.

Further examination of the literature revealed that Baxendale and Wilson(16) studied the photolysis of hydrogen peroxide in the presence of several organic compounds, one of them acetic acid. Those investigators concluded that the regeneration of hydrogen peroxide in the OH/HOAc system was necessary to explain their data. They found similar behavior of varying degrees with other organic compounds.

In addition, papers by Weeks and Rabani(43) and Behard, Czapski and Duchovny(44) had reported the reaction between $\cdot CO_3^-$ and hydrogen peroxide and had measured the rate constant of that reaction, although unfortunately, they failed to specify the reaction products. Thus, both Case I and Case II appeared possible and hence the identity of the initiation step remained in doubt.

During this time peroxide photolysis experiments were being performed in this laboratory in conjunction with another project. In this study hydrogen peroxide was photolysed in pure water and with bicarbonate or acetic acid added. The relative reaction rates found in these similar experiments are shown in Table 1. The data in the first column indicate that the slight amount of organic matter present in the water was causing a decrease in apparent rate constant as the oxygen content of the water increased (for deaerated to "from bottle" to aerated). This is consistent with the findings of Baxendale and Wilson(16) for many organic compounds, including acetic acid, where it is presumed that dioxygen reacts with intermediate free radicals, ultimately producing hydrogen peroxide. The data in column 3 of Table 1 illustrate that effect clearly. The results of Baxendale and Wilson would predict that the deaerated HOAc + H_2O_2 experiment yield a rate constant equal to 1/2 that of deaerated H_2O_2 only.

TABLE 1. HYDROGEN PEROXIDE PHOTOLYSIS RATE CONSTANTS IN THE ABSENCE AND PRESENCE OF SCAVENGERS.

Solution	Apparent Rate Constants, $\text{min}^{-1} \times 10^{-3}$		
Conditions	H_2O_2 only	$H_2O_2 + HCO_3^-$	H_2O_2 + HOAc
deaerated	10.5	9.8	3.8
aerated	8.2	9.6	1.6
from bottle*(a)	9.8	10.2	2.8

(a) meaning neither aerated nor deaerated

Since our reaction vessel was not air-tight, the tabulated value is probably within experimental error of being half the "H_2O_2 only" value. The apparent decrease in reaction rate constant with aeration is actually due to regeneration of peroxide from OH + HOAc. The bicarbonate data (column 2) is fairly consistent with the "H_2O_2 only" data, and the three values in column 2 are undoubtedly within experimental error of one another.

In order to interpret these results one must consider the corresponding reaction systems, where for simplicity of example, the equilibrium $HO_2\cdot \rightleftharpoons H^+ + O_2^-$ has been ignored, as has the actual quantum yield of the photolysis step.

H_2O_2 only:

$$H_2O_2 \xrightarrow{h\nu} 2 \cdot OH$$

$$2 \times (H_2O_2 + \cdot OH \longrightarrow H_2O + HO_2\cdot)$$

$$2\ HO_2\cdot \longrightarrow H_2O_2 + O_2$$

net reaction $2\ H_2O_2 \longrightarrow 2\ H_2O + O_2$

quantum yield $\phi = 2$

$H_2O_2 + HCO_3^-$:

$$H_2O_2 \xrightarrow{h\nu} 2 \cdot OH$$

$$2\ x\ (\cdot OH + HCO_3^- \rightarrow H_2O + \cdot CO_3^-)$$

$$2\ x\ (H_2O_2 + \cdot CO_3^- \rightarrow \text{Products})$$

net reaction $3\ H_2O_2 + 2\ HCO_3^- \rightarrow \text{Products}$

quantum yield $\phi = 3$

$H_2O_2 + HOAc$:

$$H_2O_2 \xrightarrow{h\nu} 2\ \cdot OH$$

$$2\ x\ (\cdot OH + CH_3CO_2H \rightarrow H_2O + \cdot CH_2CO_2H)$$

$$2\ \cdot CH_2CO_2H \longrightarrow H_2O_2 + \text{Products}$$

No net destruction of H_2O_2

quantum yield $\phi = 0$

In the last case the stoichiometry of two carboxymethyl radicals regenerating only one peroxide has been inferred from the fact no negative apparent rate constants were observed, either in the case of Baxendale and Wilson's findings or in the present work. In both studies the nonzero rate constant for the HOAc case indicates that the regeneration step is not 100% efficient, perhaps competing with other reactions of carboxymethyl radical.

The most instructive feature of the above data, however, is that in the present study, the apparent rate constant for $H_2O_2 + HCO_3^-$ was the same as for H_2O_2 only, rather than 50% larger as would be indicated by the quantum yields above. One must therefore conclude that the products of the reaction between hydrogen peroxide and carbonate radical anion are species that can themselves regenerate one peroxide molecule for every two times the H_2O_2/CO_3 reaction takes place. Such a reaction is:

$$H_2O_2 + \cdot CO_3^- \longrightarrow HO_2\cdot + HCO_3^-$$

$$2\ HO_2\cdot \longrightarrow H_2O_2 + O_2$$

or for the whole sequence,

$$H_2O_2 \xrightarrow{h\nu} 2\ \cdot OH$$

$$2 \times (\cdot OH + HCO_3^- \longrightarrow H_2O + \cdot CO_3^-)$$

$$2 \times (H_2O_2 + \cdot CO_3^- \longrightarrow HO_2\cdot + HCO_3^-)$$

$$2\ HO_2\cdot \longrightarrow H_2O_2 + O_2$$

---

net reaction $2\ H_2O_2 \longrightarrow 2\ H_2O + O_2$

quantum yield $\phi = 2$

Armed with this information and the rate constant measured by Behard, Czapski, and Duchovny(44), it is instructive to calculate the predicted steady-state levels of the various species present for the data shown in Figures 7 and 8. Similar calculations cannot be made for the acetic acid case since neither the pathway nor the rate constants for peroxide regeneration are known. The rate must however be fairly fast compared with the time scale of the experiment shown in Figures 4 and 5.

Kinetic Analysis of the Ozone/UV Reaction System.

The reactions which contribute to the system of rate equations which must be solved are given in Figure 9, where the indices on the rate constants refer to Table 2. The extinction coefficient of ozone is that of Hart et al.(40) and that of H_2O_2 was measured in this laboratory. Values of the rate constants used are given in Table 2. Complete rate equations for the

$$O_3 + H_2O \xrightarrow{h\nu} H_2O_2 + O_2 \qquad \varepsilon_{254} = 3185\ m^{-1}cm^{-1}$$

$$H_2O_2 \xrightarrow{h\nu} 2\cdot OH \qquad \varepsilon_{254} = 17.2\ m^{-1}cm^{-1}$$

$$H_2O_2 \rightleftharpoons HO_2^- + H^+ \qquad p^Ka = 11.6$$

$$HO_2\cdot \rightleftharpoons H^+ + \cdot O_2^- \qquad p^Ka = 4.69$$

$$O_3 + H_2O_2 \xrightarrow{k_{12}} O_2 + HO_2\cdot + \cdot OH$$

$$O_3 + HO_2^- \xrightarrow{k_{13}} 2O_2 + HO\cdot + \cdot O_2^-$$

$$O_3 + HO_2\cdot \xrightarrow{k_{14}} 2O_2 + \cdot OH$$

$$O_3 + \cdot O_2^- \xrightarrow{k_{15}} (\cdot O_3^- + O_2) \xrightarrow{H_2O} \cdot OH + OH^- + 2O_2$$

$$O_3 + \cdot OH \xrightarrow{k_{16}} O_2 + HO_2\cdot$$

$$H_2O_2 + HO_2\cdot \xrightarrow{k_{24}} \cdot OH + H_2O + O_2$$

$$H_2O_2 + \cdot OH \xrightarrow{k_{26}} HO_2\cdot + H_2O$$

$$HO_2^- + \cdot OH \xrightarrow{k_{36}} H_2O + \cdot O_2^-$$

$$HO_2\cdot + HO_2\cdot \xrightarrow{k_{44}} H_2O_2 + O_2$$

$$HO_2\cdot + \cdot O_2^- \xrightarrow{k_{45}} HO_2^- + O_2$$

$$HO_2\cdot + \cdot OH \xrightarrow{k_{46}} O_2 + H_2O$$

$$\cdot O_2^- + \cdot O_2^- \xrightarrow[H_2O]{k_{55}} HO_2^- + OH^- + O_2$$

$$\cdot O_2^- + \cdot OH \xrightarrow{k_{56}} {}^-OH + O_2$$

$$\cdot OH + \cdot OH \xrightarrow{k_{66}} H_2O_2$$

Equations in scavenged systems

$$HCO_3^- + \cdot OH \xrightarrow{k_{67}} HOH + \cdot CO_3^-$$

$$CH_3CO_2H + \cdot OH \xrightarrow{k_{8,10}} HOH + \cdot CH_2CO_2H$$

$$\cdot CO_3^- + H_2O_2 \xrightarrow{k_{28}} HCO_3^- + HO_2\cdot$$

$$\cdot CO_3^- + HO_2^- \xrightarrow{k_{38}} HCO_3^- + \cdot O_2^-$$

$$\cdot CO_3^- + \cdot O_2^- \xrightarrow{k_{58}} \text{Products}$$

$$\cdot CO_3^- + \cdot CO_3^- \xrightarrow{k_{88}} \text{Products}$$

Figure 9. Proposed ozone/UV reaction system.

TABLE 2. RATE CONSTANTS USED FOR KINETIC ANALYSIS OF THE OZONE/UV SYSTEM, $M^{-1}s^{-1}$.

INDEX		1	2	3	4	5	6
	SPECIES	O_3	H_2O_2	HO_2	HO_2	O_2^-	OH
1	O_3	-	0.14(a)	$2.8x10^6$(b)	-	$1x10^9$(c)	$3x10^9$(d)
2	H_2O_2	0.14	-	-	3.0(e)	2-8(f)	$2.7x10^7$(g)
3	HO_2	$2.8x10^6$	-	-	-	-	$7.5x10^9$(h)
4	HO_2	-	3.0	-	$8.6x10^5$(i)	$1.0x10^8$(j)	$4.5x10^9$(k)
5	O_2	$1x10^9$	2-8	-	$1x10^8$	<0.35(l)	$1x10^{10}$(k)
6	OH	$3x10^9$	$2.7x10^7$	$7.5x10^9$	$4.5x10^9$	$1x10^{10}$	$4x10^9$(k)
7	HCO_3	-	-	-	-	-	$1.5x10^7$(b)
8	CO_3	$1x10^5$(n)	$8x10^5$(o)	$5.6x10^7$(o)	-	$4x10^8$(p)	-
9	CO_3^{-2}	-	-	-	-	-	$4.2x10^8$(b)
10	HOAc						$2x10^7$(k)
11	OAc						$8.5x10^7$(k)

(a)	ref.4	(b)	ref.6	(c)	ref.60
(d)	ref.61	(e)	ref.62	(f)	ref.63
(g)	ref.64	(h)	ref.27	(i)	ref.65
(j)	ref.66	(k)	ref.27	(l)	ref.67
(m)	ref.27	(n)	ref.68	(o)	ref.43
(p)	ref.69				

species H_2O_2, HO_2^-, $HO_2\cdot$, O_2^-, $\cdot OH$, and where applicable, $\cdot CO_3^-$ were assembled from the equations shown in Figure 9 for four cases:

No Scavenger Present

Case I: Assume $O_3 + H_2O \xrightarrow{h\nu} H_2O_2$ (Direct Production of Hydrogen Peroxide)

Case II: Assume $O_3 + H_2O \xrightarrow{h\nu} 2\ \cdot OH + O_2$ (Direct Production of Hydroxyl Radicals)

Scavenger Present (0.015 M $NaHCO_3$)

Case III: Direct Production of Hydrogen Peroxide in Presence of Scavenger

Case IV: Direct Production of Hydroxyl Radicals in Presence of Scavenger.

In kinetic analyses of this type, it is usually assumed that the ratio of the concentrations of weak acids and their conjugate bases are fixed by their dissociation constants,

$$\frac{[H^+]\ [HO_2^-]}{[H_2O_2]} = 10^{-11.6}$$

and

$$\frac{[H^+]\ [O_2^-]}{[HO_2\cdot]} = 10^{-4.69}$$

However, since many of the reactions in this system are diffusion controlled, it is conceivable that the slower of the two reactions involved could be outrun and the concentration ratio deviate from that dictated by the equilibrium constant. Accordingly, in the kinetic analysis, these equilibrium constants were considered parameters rather than fixed relationships. The analysis of the sensitivity of the results to these parameters is not completed, however, and all of the work which follows is based on the assumption that the equilibrium relationships are obeyed.

The rate expressions were all equated to zero in order to compare steady-state concentrations of the various species with the values obtained from experiment. In general, the type of expressions which result are

$$C_A = \frac{\sum_{ij} k_{ij} C_i C_j}{\sum_n k_{An} C_n}$$

$$= \frac{\text{(sum of rates of reactions producing species A)}}{\text{(sum of pseudo first order rate constants for the disappearance of A)}}$$

Insignificant contributors are culled from sums of terms in order to give expressions which show the major ways in which species are produced and disappear. The system of equations which results is in general not linear, and solution by direct substitution rarely proves suitable.

The procedure used was to substitute experimental values for the ozone and hydrogen peroxide concentrations into the least sensitive expression to obtain a starting value of some species, then iteratively solve the relationships for [O_2], [OH],and [CO_3^-]. It should be recalled that [HO_2] and [HO_2] are now imbedded in these relationships via the equilibrium constants, so that they no longer appear separately. The resulting concentrations are substituted back into the expression for [H_2O_2] and that value compared with the experimental value from which the concentrations of O_2 , OH, and CO_3 were derived. This consistency along with any other discrepancies, were used as indicators of the correct mechanism. The cases are discussed individually below, with common features being summarized at the end.

Case I: Direct Production of Hydrogen Peroxide

- No Scavenger

This case of course corresponds to the direct production of hydrogen peroxide at rate R_p by ozone photolysis. The rate R_p was taken to be equal to the rate of accumulation in the low pH acetic acid experiments, since even if a small amount of OH is formed from H_2O_2, peroxide is almost quantitatively regenerated from OH and acetic acid. The iteration converged, values obtained were self-consistent and reasonable, and no apparent contradictions were observed.

Case II: Direct Production of Hydroxyl Radical

- No Scavenger

The rate of hydroxyl radical production was taken as $2R_p$ for reasons described above. Although Baxendale and Wilson(16) found the regeneration rate of peroxide to be only 84% of the photolysis rate, their system was aerated only at the beginning of the experiment, while in the present work oxygen was continuously sparged throughout the experiment, so that the water in a continuously-sparged ozone/UV CSTR is always supersaturated in oxygen. Carefully-performed dissolved oxygen measurements in the pilot plant have indicated oxygen concentrations greater than twice the usual solubility of oxygen under those conditions. Thus 100% regeneration is assumed.

When the trial OH concentration was calculated from the H_2O_2 equation, a value of 1.76×10^{-7} M was obtained compared with 2.5×10^{-10} M in Case I. At the experimentally determined ozone concentration, the rate of the ozone-OH reaction would be 3×10^{-3} M s^{-1} but since the OH generation rate is only 3.5×10^{-7} M s^{-1}, the calculated OH level could not be maintained, and thus the model conflicts with the experimental measurement. The equation for [OH] predicts that $[OH] \rightarrow 1.9 \times 10^{-11}$ as $[H_2O_2] \rightarrow 0$, but substituting that value of [OH] into the H_2O_2 equation yields $[H_2O_2] = 2.5 \times 10^{-9}$, a factor of 10^4 too low. Thus the calculations do not converge and unreasonable values are predicted.

Case III: Direct Peroxide Production in the presence of Scavenger.

As in the unscavenged case, this model converges nicely and predicts the experimental H_2O_2 concentration within a factor of 2.3.

Case IV: Direct Hydroxyl Radical Production in Presence of Scavenger.

In this model, the iteration on more reactive species converges to reasonable values but fail to predict experimental peroxide values (1.5×10^{-3} compared to 2.1×10^{-6} experimental).

Thus, the calculations indicate that the mechanism by which the ozone/UV process operates is the direct production of hydrogen peroxide, followed by dissociation of peroxide to HO_2^- which reacts with ozone to produce the most active species, hydroxyl radical. This is in agreement with several observations.

1) Taube(3) also reported the results of isotope experiments which indicated that one-half of the oxygen in the peroxide which was generated came from the solvent and one-half from the ozone. This favors the direct peroxide production, although other explanations are possible.

2) When Fowles and Dainton(45) photolysed N_2O in aqueous solution at λ = 185 nm, the only products were N_2, O_2 and H_2O_2, with

$$\phi(N_2) = \phi(H_2O_2) + 2\phi(O_2),$$

providing strong evidence for $O(^1S)$ or $O(^1D)$ insertion into water. In the gas phase N_2O photolysis at 185 nm yields $O(^1D)$, as does O_3 photolysis at 254 nm. During those experiments the H_2O_2 concentration reached 1.3×10^{-4} M in 60 minutes which, by arguments similar to those above, is unreasonable if OH is formed directly. Dainton later pointed out (46) that in the N_2O photolysis case $O(^1D)$ inserts with 100% efficiency while in H_2O_2 photolysis about 50% of the OH escape the solvent cage, even though the energies of the molecules in question are roughly similar.

3) If ozone photolysis led directly to hydroxyl radical, then a yield of two OH per O_3 would be obtained. Even in systems where organic substrate is present in great excess over other species, evidence of this high yield is never observed.

The resulting equations which describe the production and destruction of the various species present in the reactor at steady stage are as follows, where $F_2 = [HO_2^-]/[H_2O_2]$, evaluated from the dissociation constant.

UNSCAVENGED:

$$[H_2O_2] = \frac{R_p(O_3)}{k_{13}[O_3]F_2 + k_{26}[\cdot OH]}$$

$$[O_2]^- = \frac{\{k_{13}F_2[O_3]+k_{26}[OH]\}[H_2O_2] + k_{16}[O_3][\cdot OH]}{k_{15}\ [O_3]}$$

$$[OH] = \frac{R_p(H_2O_2) + \{k_{13}F_2[H_2O_2] + k_{15}[O_2^-]\}[O_3]}{k_{16}[O_3] + k_{26}[H_2O_2]}$$

SCAVENGED:

$$[H_2O_2] = \frac{R_p(O_3)}{k_{13}F_2[O_3] + k_{26}[\cdot OH] + k_{28}[\cdot CO_3^-]}$$

$$[O_2^-] = \frac{\{k_{13}F_2[O_3] + k_{26}[OH] + k_{28}[\cdot CO_3]\}\ [H_2O_2]}{k_{15}[O_3] + k_{58}[\cdot CO_3^-]}$$

$$[OH] = \frac{R(H_2O_2) + \{k_{13}F_2[H_2O_2] + k_{15}[O_2^-]\}\ [O_3]}{k_{16}[O_3] + k_{67}[HCO_3^-]}$$

$$[CO_3^-] = \frac{k_{67}[HCO_3^-][\cdot OH]}{k_{28}[H_2O_2] + k_{38}[H_2O_2]F_2 + k_{88}[\cdot CO_3^-]}$$

Calculated steady state concentrations for the active species $[O_2]$ and $[\cdot OH]$ are 8×10^{-10} M and 3×10^{-10} M respectively, for the unscavenged case, and are 8×10^{-12}, 3×10^{-13} and 3×10^{-8} M for $[O_2\cdot]$, $[\cdot OH]$, and $[\cdot CO_3\ ]$, respectively, with bicarbonate scavenger present. It should be noted that in this model, the concentration of carbonate radical anion approaches that of the stable molecules O_3 and H_2O_2.

It is instructive to compare the relative efficiency of hydroxyl radical generation by the three processes (a) base-catalysed, (b) peroxide-catalysed, and (c) UV-catalysed ozone decomposition, and to calculate a hydroxyl radical yield, ϕ_n = (number of hydroxyl radicals produced/number of ozone or peroxide molecules consumed) for each process:

(a) Base-catalyzed:

$$O_3 + {}^-OH \longrightarrow O_2 + HO_2^-$$

$$O_3 + HO_2\cdot \longrightarrow HO\cdot + O_{2-} + O_2^-$$

$$H_2O + O_3 + O_2^- \longrightarrow HO\cdot + HO^- + 2O_2$$

net reaction $30_2 + H_2O \longrightarrow 2\ {}^\cdot OH + 4O_2 \quad \phi_n = 2/3$

(b) Peroxide-catalyzed:

$$H_2O_2 \rightleftharpoons H^+ + HO_2^-$$

$$O_3 + HO_2 \longrightarrow HO^\cdot + O_2^- + O_2$$

$$H_2O + O_3 + O_2^- \longrightarrow HO^\cdot + HO^- + 2O_2$$

net reaction $2O_3 + H_2O_2 \longrightarrow 2^\cdot\ OH + 3O_2 \quad \phi_n = 2/3$

(c) Ozone/UV:

$$O_3 + H_2O \xrightarrow{h\nu} O_2 + H_2O_2$$

followed by (b)

net reaction $3O_3 + H_2O \longrightarrow 2{}^\cdot OH + 4O_2 \quad \phi_n = 2/3$

Thus, the three processes produce equivalent ·OH yields. The disadvantage of the base-catalysed process is the necessity of pH adjustment of a large stream and the slowness of the reaction. The latter not only necessitates a long contact time, but mass transfer is considerably worse for a given reactor, making more expensive equipment necessary to accomplish a given goal. Between ozone/H_2O_2 and ozone/UV, it appears that one trade-off is between storage and handling of a hazardous substance like hydrogen peroxide and the cost of ozone generation. Concentrated hydrogen peroxide is a dangerous substance to transport and store. If dilute peroxide is used, transportation costs could be quite significant. For example, a 10 mg/L dose in a 1 MGD facility would require approximately 2500 gallons of 3% hydrogen peroxide per day. In addition, the work of Vahidi et al.(49) has shown that it is possible to retard the destruction of THMFP by the addition of too much peroxide, presumably because peroxide competes effectively for hydroxyl radical. The situation is further complicated by the regeneration of peroxide from the reaction of hydroxyl radical with humic material, so that the optimum amount of hydrogen peroxide would change with the quantity and nature of the humic material.

It should be mentioned at this point that although there is some slight photolysis of hydrogen peroxide which takes place in the ozone/UV system, the absorption coefficient of H_2O_2 is about 175 times lower at 254 nm than that of ozone, making the contribution of hydrogen peroxide to the total hydroxyl radical yield negligible.

Finally, before leaving this section, it should be pointed out that in the presence of organic compounds which regenerate peroxide stoichiometrically upon reaction with hydroxyl radical, the hydroxyl radical yield of all three processes could increase to 1.0 after initiation. In actual practice this yield is probably never realized due to a peroxide regeneration efficiency less than 100 percent. Furthermore, in a flow system, some peroxide or peroxide precursors are swept from the reactor in the effluent.

Effect of Wavelength on THMFP Removal

Laboratory studies were carried out on the effect of wavelength on the removal of THMFP by photolytic ozonation, using the reconstituted Cross Lake water described in Section 6. The lamps used and experiments performed are shown in Table 3.

TABLE 3. LABORATORY EXPERIMENTS ON EFFECT OF WAVELENGTH[a]

Run#	# of lamps	lamp type	wavelength, nm	approximate UV output
L38	4	G8T5	254	1.74 w
L39	2	G8T5	254	0.87 w
L40	2	OZ8T5	254 + 185	1.12 w
L41	2	F8T5/350BL	350	0.63 w
L42	0	none	-	-

(a) ozone dose rate = 2.4 mg/L-min in each case

Lamp output was measured radiometrically and thus may include some visible light as well. After twenty minutes the amount of THMFP removal was roughly zero for the ozone-only and 350 nm lamp experiments, with a total ozone dose of 10-12 mg/L being removed from the gas phase. The four-lamp and two-lamp 254 nm experiments gave removals of 44% and 38%, respectively, while 63% removal was obtained using the 185 + 254 nm lamp. The four-lamp experiment generated considerably more THMFP at the beginning of the experiment than did the two-lamp experiment, so that at the point mentioned above, the 4-lamp disappearance curve
was just catching up to that of two lamps.

In comparing the 254 nm lamp with those emitting 185 + 254 nm, 28% more intensity in the latter produced 43% more removal. However, the path length of the radiation in this laboratory scale reactor is 2.5 to 10 cm while that in the pilot scale stirred-tank was 10 to 32 cm. Since 84% of 185 nm radiation is lost to absorption by water in the first cm of reaction zone, it was decided to proceed with the investigation using 254 nm lamps and avoiding the problem of ozone production inside the lamp wells, which would also lead to absorption losses of the 254 nm line as well as present deterioration problems within the pilot plant. The use of short-wavelength lamps is worthy of further investigation.

Conclusions from the Laboratory Study

1) The mechanism of the ozone/UV process appears to be direct production of hydrogen peroxide by ozone photolysis, followed by secondary reactions which produce hydroxyl radical.

2) The data is best explained by assuming that the product of the reaction between carbonate radical anion and hydrogen peroxide is HO_2.

3) A result of the proposed mechanism is that the efficiency of hydroxyl radical production would be lowered if greater than one third of the transferred ozone was photolysed. Whether this situation can occur depends on the rate of the secondary ozone reactions relative to the rate of photon absorption by ozone. More will be said about this point in a later section.

4) The maximum yield of hydroxyl radical is two OH for every three ozone molecules photolysed when no peroxide regeneration occurs. When an organic substance which promotes peroxide regeneration is present the yield may approach one hydroxyl radical per ozone molecule.

5) UV lamps emitting primarily 254 nm radiation are the most efficient for ozone photolysis because of their coincidence with the center of the ozone absorption band. Although a 185 nm photon is more energetic than one at 254 nm, the intensity of the higher energy line is only a fraction of that at 254 nm. In addition, it is absorbed only one-third as well by ozone, but considerably better by water.

SECTION 6

PILOT-SCALE STUDIES

INTRODUCTION

Studies were carried out at the pilot scale in order to determine optimum operating configurations, gather operational data, and learn what operational problems might arise, in order to aid full scale design, anticipate operator time and maintenance requirements in a full scale operation, and make reasonable treatment cost estimates. Pilot scale operation was divided into two phases: 1) parametric variation studies carried out on reconstituted lake water, performed at SumX Corporation in Austin, Texas, and 2) continuous pilot scale operation at the Sabine River Water Treatment Plant in Longview, Texas, using feedwater from within the plant. These phases are discussed in separate sections after a description of the pilot plant.

DESCRIPTION OF THE PILOT PLANT

The basic pilot plant was constructed for another EPA project, the study of biological activated carbon (BAC) for the removal of trihalomethane (THM) precursors from a surface water source(33), conducted at the Amiss water treatment plant at Shreveport, Louisiana. When transferred to this project the pilot plant already included a preoxidation basin, Neptune Microfloc Waterboy^R water treatment package, 600 gallon storage reservoir, 20 gallon continuous stirred tank reactor with 3600 rpm turbine impeller (Howe-Baker Engineers), variable time detention basin, eight 6' x 1' stainless steel columns for granular activated carbon or sand, two backwash basins for the columns, refrigerators for sample storage, numerous pumps and valves, etc. This equipment was housed in a forty foot long drop-frame trailer with its own electrical control circuitry.

At the conclusion of the Shreveport project the trailer was moved to SumX Corporation in Austin, Texas, for refurbishing and initial testing. The trailer was plumbed so that the water first entered the Waterboy^R, where common water treatment unit processes such as chemical addition, flocculation, tube settling and mixed media filtration could be simulated, at a rate of up to 10 GPM. The flow diagram is shown in Figure 10, where sampling points are indicated by S followed by a number. No chemicals were added at the Waterboy during the course of the project, since settled or clarified water was used throughout, so that the Waterboy was only used for additional clarification and filtration. The filter bed was backwashed periodically on the basis of headloss through the filter, as specified by the manufacturer.

Feedwater for the pilot plant was from two sources. In the parametric studies at Austin, Texas, a reconstituted lake water was made up from a "humic/fulvic" concentrate produced by the elution of granular activated carbon columns used in a previous project. Preparation of that reconstituted lake water is described in a later section. During pilot operation in Longview, Texas, feedwater was from one of two points in the Sabine River Water Treatment Plant. Water which had been treated with alum and a small amount of permanganate then settled in a presedimentation basin ("presed" water) was characteristically around pH 4.7 - 5.0 and still contained a great deal of floc, most of which was removed by filtration in the Waterboy. After lime addition and further clarification, the water had a pH of around 9 and was called "clarifier water". This water lacked only final filtration and chlorination or chloramination of being finished water, and was filtered in the Waterboy before use in the pilot plant.

From the Waterboy the water passed to the 600 gallon reservoir which was also used to backwash the Waterboy filter. From there the water passed to the continuous stirred-tank reactor with turbine contactor (TCSTR), an 80-liter stainless steel cylindrical tank 18" in diameter, whose water level is maintained by the exiting water overflowing a weir. Although little rotational motion of the water can be detected during operation, the tank is fitted with six internal baffles to counteract any tendency of the liquid to vortex. The reactor is fitted with two quartz lamp wells (2" diameter) which extend far enough into the liquid that the 17" G10T5-1/2L "slimline" lamps (American Ultraviolet, Chatham, N.J.) used in the experiments are entirely below liquid level. From one to four lamps may be installed in each well. Each lamp is rated at 5.3 watts at 254 nm after 100 hours life and the stated power consumption is 16 watts each. This corresponds to a UV intensity of 0.07 watts/L of reactor volume per lamp used. The turbine contactor used in the TCSTR is of the Kerag design (Howe Baker Engineers, Tyler, Texas). It rotates at 3600 rpm and by its action generates a suction which causes the pressure

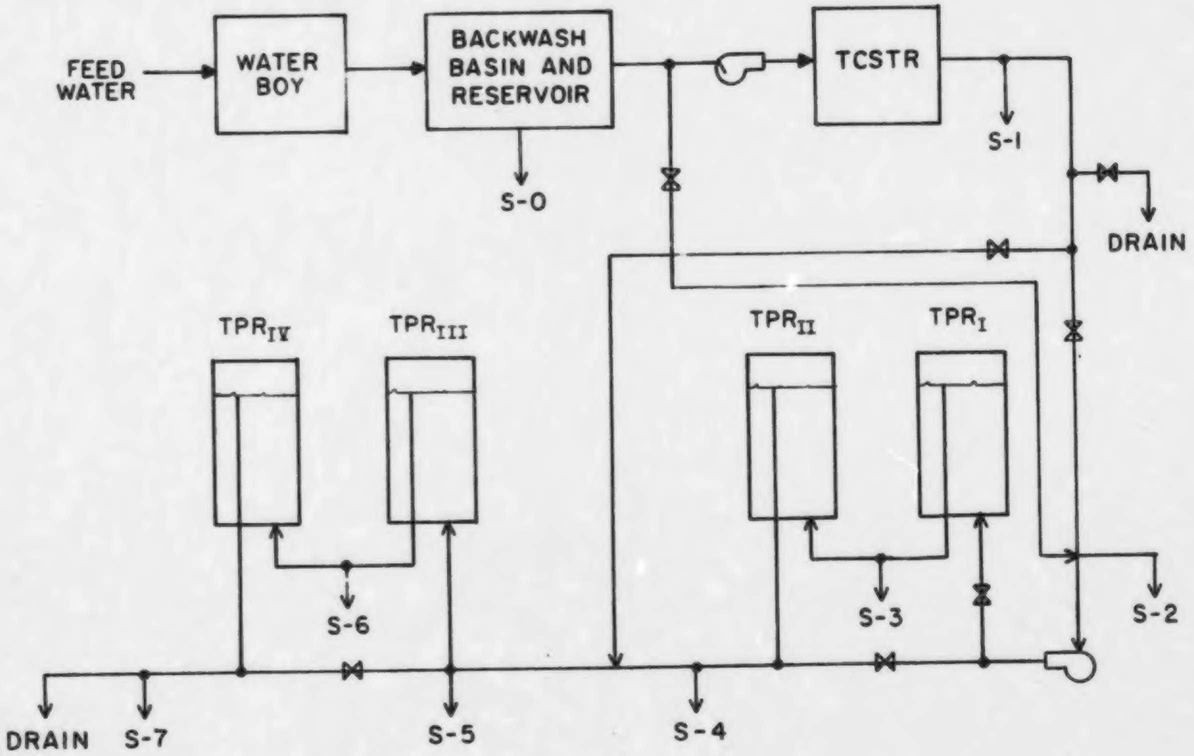
FEED WATER
WATER BOY
BACKWASH BASIN AND RESERVOIR
S-0
TCSTR
S-1
DRAIN
S-2
TPR_{IV}
TPR_{III}
TPR_{II}
TPR_{I}
S-6
S-3
DRAIN
S-7
S-5
S-4

Figure 10. Flow diagram of pilot water treatment research facility.

in the inlet line (between ozone generator and turbine) to be below atmospheric.

From the TCSTR the water passes either to the drain or to the tubular photochemical reactor (TPR) area, a new area of the plant which was constructed during the refurbishing. In this area the water may pass through one or two pairs of tubular photochemical reactors, each made of 6' x 6" diameter pyrex pipe. The stainless steel heads each have two 1" holes for quartz lamp wells which are sealed in with viton o-rings, and two 1" NPT threaded holes for water and gas connections. Water enters these reactors from the bottom and must overflow a standpipe to exit the reactor. The liquid volume of these reactors is 27.7 liters (7.32 gallons) with two lamp wells and the standpipe installed. Lamps for these reactors are G36T6L "slimline" (American Ultraviolet), rated at 13.8 watts of 254 nm radiation after 100 hours, with a power consumption of 39 watts apiece. The entire arc length (30 inches) is adjacent to liquid in this configuration, and either one or two lamps may be used. Only the first 30 inches of each TPR is irradiated, giving an intensity of 1.2 watts/L of reactor volume per lamp used. In the TPR's, as in the TCSTR, electrical connections from the transformers to the lamps were terminated in alligator clips. Although less safe and less reliable than the sockets supplied by the manufacturer, the configurational flexibility outweighed those considerations for this phase of the project. This type of connection is not recommended for normal operation in a water plant installation.

Several methods of ozone contacting were tried in the TPR's. The first, used throughout the parameter variation studies in Austin, used a circle of 3/8" O.D. 304 stainless steel tubing with 1/16" holes drilled every inch around the perimeter. This ring tube contactor was connected to the ozone source and located just above the floor of the TPR. While 1/16" holes may be used in a pilot or large scale TCSTR with paddle-type impeller, there is not adequate turbulence in a bubble column (TPR) to create sufficient shear force to keep bubble size small, so that the mass transfer characteristics of this contactor were not particularly good. In order to further increase gas/liquid contacting, the gas was not vented from TPR_I, and gas and liquid were both forced through an ejector consisting of five 1/8" holes drilled in a pipe cap, when entering TPR_{II}, and similarly for III to IV. This arrangement created somewhat of a backpressure problem, and in actual practice would constitute a separate contacting step, requiring pressurization of the gas, pumping of the liquid, or both, as well as higher pressure requirements on the reactors. This combined method was intended to simulate sampling at various points along a single column, but was deemed unsatisfactory and was later replaced by a different type of arrangement.

In the meantime a section of stainless steel porous fritted material was obtained from Mott Metallurgical Corporation (Farmington, Conn.) and the ring tube spargers replaced with 3" sections of the 1/2" diameter frit, which had a 2 μm pore size. This arrangement worked noticeably better and was used throughout the balance of the Austin studies in conjunction with the pipe cap ejector arrangement. When the plant was moved to Longview, Texas for continuous operation, these spargers and the ejectors were replaced with fritted stainless steel spargers in every reactor, mounted in the mouths of the 3/4" pipes entering each of the reactors. The spargers were placed in the pipes so that the shear force of the flowing liquid would shear bubbles off at a smaller size than that at which they would normally leave the sparger in a still liquid. Sparger and pore size (0.5 μm) were chosen according to engineering data supplied by Mott Metallurgical Corporation, the manufacturer. This arrangement gave very small bubbles, but in the field on partially treated river water these frits were totally unsatisfactory due to clogging within a 1-3 day period. In many cases there was no visual indication of any change in a frit which had become clogged and no effort was made to identify the clogging material.

The porous stainless steel spargers were replaced by two-inch segments of 3/8" diameter PTFE tubing, sealed on one end and located concentrically in the 3/4" pipe, again at the entrance to the reactor. The segment of PTFE tubing had approximately forty 1/64" holes drilled randomly in it, spaced as far apart as possible. With PTFE tubing mounted inside the 3/4" pipe and the open end of the PTFE tubing connected to the atmosphere, a liquid flow rate of 3.3 gpm (through the 3/4" pipe) was sufficient to aspirate air from the atmosphere into the reactor which was also open to the atmosphere. This arrangement was used throughout the balance of the studies.

Ozone was generated from oxygen using either a TII tube-and-shell water-cooled ozone generator or W.R. Grace or Union Carbide air-cooled plate-type generators. All three types had a 15 psig upper pressure limit which in some TPR configurations limited the gas flow which could be sent to the first TPR because of the resistance of piping, valves, and other reactors downstream. The generators supplying the TPR's had to be operated so close to their maximum pressure that once when the oxygen pressure dropped, water backed up past an apparently faulty check valve into the plate-type ozone generator, damaging it.

Ozone concentration in the gas was measured by a PCI ozone monitor, high concentration model HC-NEMA 12, designed for high concentrations. For pilot scale studies this monitor has the disadvantage that it alternates between 1 liter/min. taken from the sample stream (ozone) and the reference stream (oxygen). Thus, if 1 liter/minute is a significant portion of the total ozone/oxygen flow, ozone dose calculations must be corrected for its part-time removal. Other than extensive problems with the solenoid valve in this monitor (discussed in a later section), its operation was stable and reliable.

Piping, valves, tubing, and fittings throughout the trailer were 316 stainless steel except for the tubing leading to and into the tubular reactors for ozone sparging. This tubing was replaced with PTFE and aluminum because of ozone decomposition problems which are described later. Ozone off gas lines all contained 1 psi relief valves to create sufficient pressure to send the gas through the ozone monitor if desired. The TCSTR off-gas line incorporated an adjustable relief valve to maintain an internal pressure of 4-5 psi in the TCSTR as per the manufacturer's specifications.

MASS TRANSFER CHARACTERISTICS OF THE REACTORS

TCSTR Characterization

It was desirable to characterize the reactors used in this study in order to insure their adequacy and to help model the difference in performance between ozonation and photolytic ozonation. The TCSTR was characterized from data collected during flow runs on reconstituted lake water at neutral pH. Although some direct reaction of ozone is taking place, in most cases the ozone dose is far above the ozone demand of the feedwater. Since the kinetics of the direct reaction have not been clearly defined, the direct reaction is neglected in the mass transfer calculations. This is especially justified in the case of photolytic ozonation.

The rate of transfer of ozone into the liquid is given by

$$NA_v = k_l A_v (C_i - C_l) \quad ,$$

where N = transfer flux across phase boundary in kmol/m^2 interface per minute

A_v = gas/liquid interfacial area in m^2 interface/m^3 liquid

k_1 = liquid side mass transfer coefficient in m^3 liquid/m^2 interface per minute

c_i = ozone concentration in the liquid at the interface, kmol/m^3 liquid

c_1 = bulk liquid ozone concentration in kmol/m^3 liquid

This NA_v is the rate R (in kmol/m^3 min) of ozone transfer from gas to liquid. The liquid concentration at the interface, C_i, is assumed to be given by a Henry's law relationship with the bulk gas since gas side resistance in the film is usually small. Thus

$$k_1 A_v = R(Cg/Z - C_1)^{-1}$$

where instead of the Henry's law constant, the dimensionless partition coefficient Z as defined by Kosak-Channing and Helz(47) has been used.

The assumption which is usually made when dealing with a CSTR is that the value of Cg to be used in the mass transfer equation above is that of the off gas, due to intimate and repeated gas/liquid mixing, while the logarithmic mean concentration is usually used with bubble columns. The turbine contactor functions by drawing water into the bottom of the turbine and ejecting it centrifugally through vanes, and thus does not achieve the same degree of overall mixing in the reactor as would the six-bladed paddle impeller of a standard CSTR. Thus the average gas concentration in the TCSTR is probably somewhere between the off-gas and log mean concentrations, where

$$\text{log mean concentration} = Cg = \frac{Cg_{in} - Cg_{out}}{\ln(Cg_{in}/Cg_{out})}$$

Calculated values of the mass transfer coefficient using the log mean concentration for the TCSTR are shown in Table 4

TABLE 4. MASS TRANSFER COEFFICIENTS FOR THE TCSTR(a) ASSUMING C_g = log mean C_g.

Run #	Ozone Concentration in feed gas, wt %	Liquid Flow rate, GPM	Mass Transfer Coefficient, k_1A_v, min^{-1}				
			number of UV lamps				
			0	2	4	6	8
21-B	0.8	2.0	(b)	0.78	0.73	0.73	0.90
23-B	1.4	1.3	0.89	0.61	0.77	0.74	0.69
22-B	1.4	4.0	0.56	0.65	0.72	0.82	0.79
25-B	2.3	1.3	0.51	0.83	(c)	(c)	(b)
24-B	2.3	2.0	0.54	0.73	(c)	(c)	(c)
25-A	2.3	4.0	0.87	0.96	(c)	(c)	(b)
26-A	2.8	4.0	0.36	0.48	0.58	0.56	0.57

a) All gas flows 9.9 SLM except experiment 26-A, where Fg = 11.4 SLM. T = 20°C
b) Data not available.
c) Data for C_1 do not appear reliable.

TABLE 5. MASS TRANSFER COEFFICIENTS FOR THE TCSTR ASSUMING $C_g = C_g^{out}$ (a)

Run #	Ozone Concentration in feed gas, wt %	Liquid Flow rate, GPM	Mass Transfer Coefficient k_1A_v, min^{-1}				
			number of UV lamps				
			0	2	4	6	8
21-B	0.8	2	(b)	(c)	2.10	2.14	2.56
23-B	1.4	1.3	2.39	1.52	1.51	1.71	1.71
22-B	1.4	4.0	1.39	1.74	2.18	3.16	2.64
25-B	2.3	1.3	1.15	(5.22)d	(d)	(d)	(b)
24-B	2.3	2.0	1.29	2.73	(d)	(d)	(d)
25-A	2.3	4.0	1.41	2.06	(d)	(d)	(b)
26-A(a)	2.8	4.0	0.57	0.87	1.20	1.12	1.15

a) Gas flow 9.9 SLM except experiment 26-A where Fg = 11.4 SLM. T = 20°C.
b) Data not available.
c) Calculated $k_1A_v < 0$, due to inaccurate C_1 data.
d) Data for C_1 not reliable.

TABLE 6. MASS TRANSFER COEFFICIENTS FROM FIELD DATA[a]

Experiment						k_1A_v, min^{-1}	
Type	Nbr.	Cg^{in}, mg/Lg	Cg^{out}, mg/Lg	log mean Cg, mg/Lg	Transfer Rate, mg/L-min	using Cg	using Cg^{out}
ozone only, TCSTR	W_1	14.0	7.92	10.7	0.63	0.16	0.22
	W_2	21.7	8.83	14.3	1.31	0.25	0.40
	W_3	30.9	9.85	18.4	2.16	0.32	0.60
O_3/UV 4 lamps, TCSTR	X_1	14.5	2.09	6.4	1.29	0.55	1.68
	X_2	22.9	3.79	10.6	1.99	0.51	1.43
	X_3	25.9	5.08	12.8	2.16	0.46	1.16
O_3/UV TPR, 2 lamps each	Y_1	13.2	4.23	7.88	0.57	0.20	-
	Y_2	26.3	7.81	15.2	1.10	0.20	-
	Y_3	38.7	10.7	21.8	1.77	0.22	-
	Y_4	47.5	12.6	26.3	2.27	0.23	-

a) Gas flow rate for TCSTR: 17.6 SCFH, TPR: 1.65 - 1.80 SLM per reactor.

as a function of feed gas concentration and the number of lamps present in the reactor. For the experiments run at 2.3% ozone, the ozone residual data do not seem reliable, increasing with greater number of lamps above two, and giving considerably higher calculated values of $k_l A_v$. These values have been omitted from the table.

The gas holdup volume for the TCSTR was measured to be 2.1 liters (2.6%) at a gas flow rate of 9 SLM, so that the mean gas residence time in the liquid was about 14 seconds. Average bubble diameter was estimated visually at 3-4 mm, giving (for d = 4 mm) a value for A_v of 39 m^2/m^3. No vortexing of the liquid occurs, as in a paddle-stirred CSTR, and the holdup volume is considerably less than a well-sparged CSTR, but the fact that the bubble averages 14 seconds to rise 18-1/2 inches indicates that operation is still considerably closer to that of a CSTR than a bubble column with respect to average gas concentration. Values of the $k_l A_v$ calculated using the assumption $Cg = Cg^{out}$ are given in Table 5, and are seen to be 2-4 times larger than the previous values. Since the assumed values of C_g are lower, however, $C_g/Z - C_l$ is a considerably smaller number, making it more sensitive to error in the experimental measurement of C_l. Values of $k_l A_v$ given in Tables 4 and 5 should be considered lower and upper bounds to the true values. Taking experiment 22-B, 2 lamps, as an example,

$$k_l A_v = 1/2\ (0.65 + 1.74) = 1.20\ \text{min}^{-1},$$

Using the previously determined value of A_v and converting to seconds yields

$$k_l = 5.1 \times 10^{-4}\ \text{ms}^{-1}\ .$$

Mass Transfer Characteristics of the TPR's.

During pilot operation at Longview, Texas ozone residuals were not measured in the field since the very low residuals encountered in ozone/UV systems are not significant compared to the ozone doses used in this study. Thus an approximation must be used in the determination of the mass transfer coefficient. If in the equation

$$\text{Rate of transfer} = R = k_l A_v\ (C_i - C_l)$$

C_l is ignored, then the mass transfer coefficient calculated from experimental data will be underestimated. Table 6 lists values of $k_l A_v$ calculated in this manner for the TCSTR for ozonation-only and with four UV lamps, and for the TPR's with 2 lamps each. Data in Table 6 may be used for comparison between reactor types, while comparison with Tables 4 and 5 will give a better idea of the true magnitude of the values.

MASS TRANSFER WITH PHOTOCHEMICAL REACTION

In order to describe the combination of mass transfer, chemical reaction, and photochemical reaction, a model must be developed which takes into consideration the interaction of those processes and allows, for example, the prediction of the optimum photolysis rate and the amount of UV power which must be applied to achieve that rate. Successful application of that model depends among other things, on an understanding of the mechanism of the process, since quite different optimum conditions are predicted by different mechanisms. As was seen earlier, the production of too much hydrogen peroxide relative to that which most efficiently catalyzes hydroxyl radical production could result in lowered efficiency in at least two ways. One occurs when the photolysis rate exceeds 1/3 of the maximum transfer rate, due to the stoichiometry of the reaction as described in Section 5. The other is a competition for hydroxyl radical between peroxide and substrate as described in Section 4 with reference to the work of Vahidi et al(14). The limits which these effects place on the desirable extent of ozone photolysis are counterbalanced against the enhancement of ozone mass transfer not only by the lowered bulk liquid phase ozone concentration due to photolysis but also by that enhancement produced by the elevated concentration of species undergoing fast reactions with ozone. (see discussion of the Hatta factor, Section 4). The following is offered as a preliminary model to be used in conjunction with mechanistic conclusions concerning the results of the photochemical reaction.

In a continuously sparged flow system in steady-state operation, the steady-state system may be represented by the mass-balance equation

$$\frac{dc_l}{dt} = 0 = K(C^{*}-C_l) - \sum_j k_j C_\ell - \phi P_o F$$

where K has units of reciprocal time and is related to the mass transfer coefficient by $K = k_\ell A_v$, the k_j are pseudo first order reaction rate constants, P_o is the incident UV power in

Einsteins/unit time, F is the fraction of photons absorbed, and ϕ is the average quantum yield of ozone photolysis upon photon absorption. The factor F has the form

$$F = 1 - e^{-ku(r-r_o)} ,$$

when the reactor contains one axially-located UV lamp. This expression was discussed in Section 4.

Clearly for real reactors the above equations are oversimplifications since poor axial and radial mixing will create concentration gradients which affect both mass transfer and chemical/photochemical reaction rates. Therefore K is identified as some average mass transfer coefficient (in the sense of the two-film theory), and the k_j will be lumped together in k_t, the total pseudo first order reaction rate constant.

In many real reactors, particularly bubble columns, K may be a sensitive function of operating conditions in the operating regime, and should be experimentally determined under the same conditions as the reactor is operated. In some cases this means that the concentration of the gas leaving the reactor will be significantly different from that entering and some suitably averaged value must be found from which to calculate C*. One such approximation, useful for bubble columns, is to assume that C_g drops exponentially throughout the length of the column, the transfer rate slowing as the driving force C^*-C_l diminishes. At height Z in the column

$$C_g(Z) = C_g^{in} e^{-az}$$

The average gas concentration is then

$$\frac{1}{h}\int_o^h C(Z)dZ = \frac{C_g^{in} - C_g^{out}}{\ln(C_g^{in}/C_g^{out})} = \overline{C}_g$$

since $ah = \ln(Cg^{in}/Cg^{out})$. For the CSTR, it is usually assumed that $C_g = C_g^{out}$ describes the system adequately.

Since the steady-state mass balance equation is a transcendental equation it may be solved graphically to give a

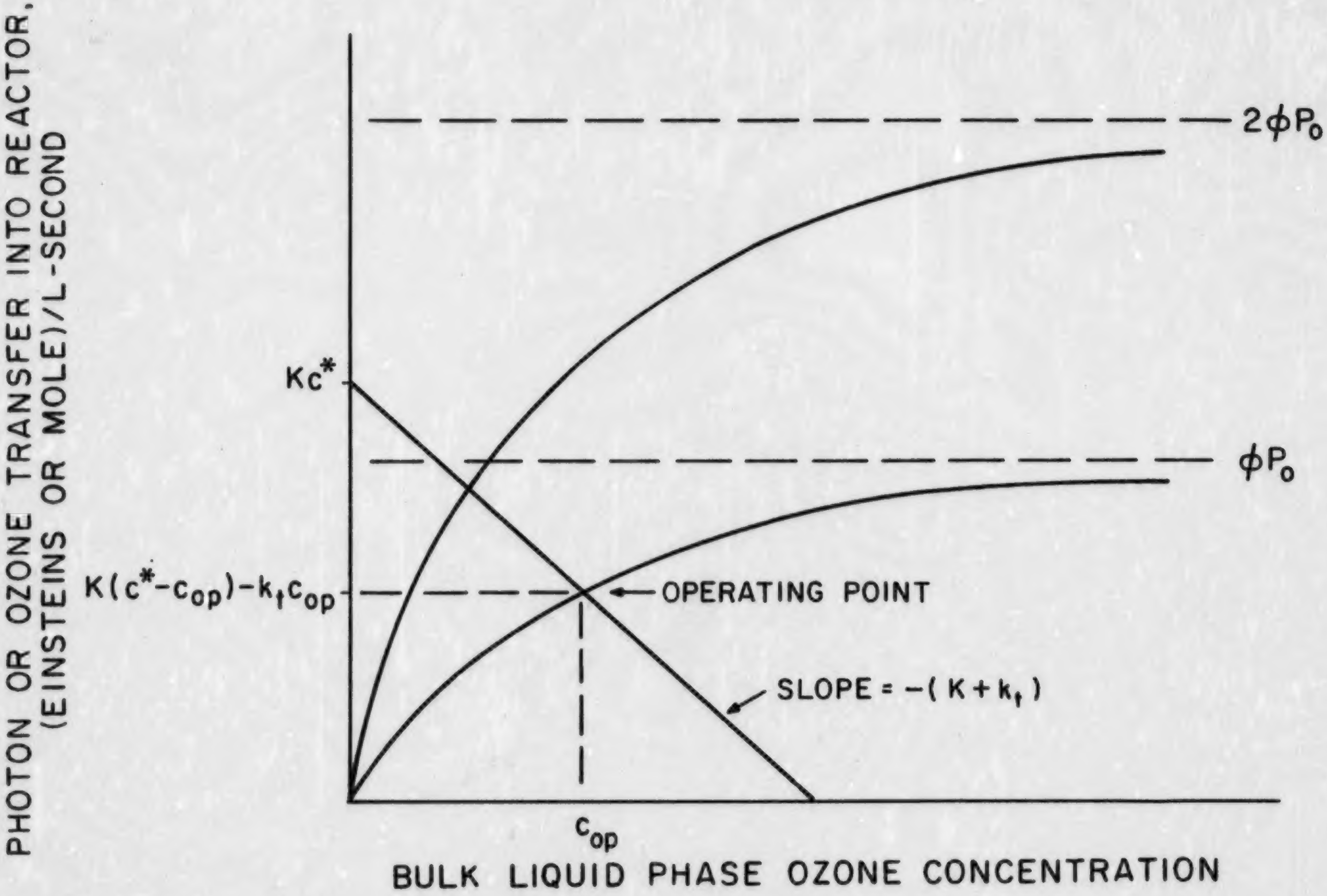

Figure 11. Radiative and mass transfer with chemical and photochemical reaction.

plot similar to Figure 11 by substituting values of C_1 and plotting $KC^* - C_1(K + k_t)$ and ϕP_oF on the same graph. In Figure 11, $K\ C_{op}$ is the resistance to mass transfer generated by concentration C_{op} in the liquid, k_tC_{op} is the portion of ozone consumed in direct reactions, and ϕP_oF_{op} is the portion photolysed. Within the framework of the mechanism proposed in Section 5, it is desirable to photolyse 1/3 of the transferred ozone, minus the amount of hydrogen peroxide which is regenerated by reaction of hydroxyl radical with organic material in an oxygenated system. Indeed, it will be seen that above a certain UV power input, no increase in ozone utilization efficiency and very little increase in mass transfer efficiency is seen. That this occurs under conditions where the number of photons absorbed is considerably less than 1/3 of the ozone which is transferred, indicates that substantial hydrogen peroxide regeneration is taking place. These results are totally incompatible with a mechanism in which hydroxyl radical is directly produced by ozone photolysis, except in systems where the UV intensity is so high that all transferred ozone is photolysed before anything else can happen to it. Because of the incompleteness of photon absorption and a quantum yield considerably less than unity(3), a photon to ozone ratio of 10 to 20 would be required before the plateau in utilization efficiency would occur. Photon to ozone ratios are considerably less than that in the experiments which are described. Work is continuing to verify the photochemical model in a quantitative manner.

A comment about H_2O_2/UV is also in order at this point. Although the preceding comments concerning H_2O_2 regeneration make hydrogen peroxide photolysis itself seem attractive as a treatment process, it must be recalled that the absorption coefficient of H_2O_2 at 254 nm is approximately 175 times lower than that of ozone. It will be shown in Section 7 below that less than 10% of the total treatment cost is due to the use of ultraviolet radiation, while the treatment efficiency is increased 78% over ozonation alone. Clearly, a loss of UV utilization by a factor of 175 has disastrous effects on treatment costs, even before the competitive absorption of photons by the solutes to be treated is considered.

PARAMETRIC VARIATION STUDIES ON SYNTHETIC LAKE WATER

After initial refurbishing of the pilot plant trailer a parametric study was conducted at SumX Corporation to determine the effect of ozone dose rate, UV intensity, and type of contactor (i.e., TCSTR or bubble column) on the efficiency of trihalomethane formation potential (THMFP) removal. In order to keep conditions as constant as possible throughout the study, a synthetic lake water was produced using a humic/fulvic concentrate obtained by eluting the organic material from several GAC columns used in the Shreveport BAC study using sodium hydroxide solution. During that study some of these columns received water which had undergone preozonation. The columns were eluted several weeks after the Shreveport study was concluded. Despite the obvious objections to the use of such a concentrate, it was felt that the constancy obtained would be absolutely essential to any attempt to find optimum operating conditions. This assumption was borne out later by the wide variability of results obtained during continuous pilot operation in Longview, Texas, where the characteristics of the water being treated were constantly changing. The use of the concentrate requires some justification as well as some later indication of validity from the data. Throughout the following section the general term humic material, abbreviated HM, will be used for the natural organic material present in water, without regard for the somewhat more specific distinctions intended by the terms humic acid, fulvic acid, etc.

The underlying idea was not that ozone dose information, determined using the concentrate could be quantitatively transferred to another system, but that the combination of parameters found most favorable for THMFP destruction in the reconstituted system would also be most favorable in other systems. This thesis assumes a sort of continuity of the characteristics of formation potential sites from one humic material to another, rather than of the total humic material itself. There is to our knowledge no method currently available for relating amount and type of formation potential sites to other measurable characteristics of aquatic organic material, and it was well beyond the scope of this project to attempt to develop such a relationship. By the same reasoning, the pilot results obtained using Sabine River water, described in a later section, can only be taken as indicative of what might be obtained using feedwater from a different water source.

As stated earlier, it was unknown whether this material could still be considered representative of the humic material present in the lake water, due to microbial action while on the carbon column, storage of the carbon in the columns between projects, and elution with strong alkali. It was, however, assumed that the types of organic functionalities which contribute to the THMFP of a natural organic material are probably of a limited number of chemical varieties and on the whole, the formation potential of the water may or may not be greatly affected by the hydrolysis or oxidative coupling of a few sites, particularly since additional THMFP sites are generated upon ozone or ozone/UV treatment anyway. The material was used to compare the relative effectiveness of different configurations, dose rates, etc. Sabine river water can fluctuate between 100 and 400 μg/L of TTHMFP in just a few days, making relative comparison of configurations much more difficult. No amount of analytical characterization of the humic material would prevent the results from being site-specific or even somewhat day-specific on a river like the Sabine. Similarly no amount of characterization will allow precise extrapolation of the information to a different humic material with today's embryonic understanding of humic material makeup and the haloform formation process in natural systems. Thus, the use of a standardized, well-characterized humic material would have allowed no better extrapolation to other humic materials nor comparison to the river where the actual pilot plant was to operate than was obtained with the concentrate.

While a functional group analysis of this material would have been interesting, it too was beyond the scope of this project, and would not relate directly to formation potential, either that which is initially present or that which is formed upon ozonation. One would have to know in detail how all of the functional groups, rings, and chains are put together in order to predict behavior in this complex reaction system. Many man-years have been spent on that problem in other research groups with very little real progress in the understanding of the structure of humic material. It is not even known whether this material shows definable structural regularity such as repeating units, or is just a potpourri of cellular debris. One "humic molecule" of molecular weight 10^4 D might just be a random jumble of a few thousand functional groups, so that it is hard to see how some average composition over a random distribution of these molecules could yield any direct information about the effect on THMFP of ozonation or ozone/UV. Thus, the assumption discussed above was intuitively reasonable and was dictated by the necessity of maintaining a constant feedwater during the parametric studies. It will be seen below that the data indicate the validity of the use of reconstituted lake water, by the similarity of the required ozone doses between Sabine River water and reconstituted lake water.

The following sections will deal with the experimental procedures used, results obtained, and the interpretation of these results in terms of continuous pilot-scale operation. Operational difficulties will be described in a separate section after pilot scale operation has been dealt with.

Experimental Procedures

Analytical procedures for oxidant analysis were described in Section 5.

Trihalomethanes--

Trihalomethanes are analyzed by the LLE method using 25 mL screw-capped septum vials. Extraction is into pentane and samples are always analyzed the same day as extraction. Because of interferences with more common internal standards by compounds formed upon chlorination of Sabine River water, tetrachloroethylene is routinely used as the internal standard. Internal standard peak areas are compared between blanks, standards, and samples to insure the absence of TCE in the samples, and check samples are extracted with pentane containing a different internal standard as a further precaution. Samples are prepared in triplicate and the first two samples analyzed. If the two samples differ by more than 4%, the third sample is analyzed. Results are averaged and the standard deviation (defined below) calculated. THM concentrations are calculated automatically by the HP 5840 gas chromatograph, and are checked periodically by hand for correctness. The instrument is calibrated against a mid-range standard.

Trihalomethane Formation Potential (TTHMFP)--

Samples are prepared in triplicate, buffered (phosphate) to pH 7, and chlorinated with sodium hypochlorite solution at an applied chlorine dose of 30 mg/L (as chlorine) in excess of any ozone quench which was previously added. Samples are stored in the dark in a laboratory cabinet for seven days, then quenched with sulfite and analyzed by LLE as described above. An unquenched sample is used to verify the presence of a chlorine residual at the end of seven days, and an unchlorinated sample is used to determine any instantaneous THMs present at the time of chlorination.

Chlorine Residual--

Aqueous chlorine is measured in two instances:

a) To determine the concentration of the stock solution of sodium hypochlorite used for chlorination.

b) To confirm the presence of a chlorine residual after the seven-day chlorination in the measurement of formation potential.

In both cases, chlorine is analyzed by the colorimetric determination of iodine liberated from boric acid buffered potassium iodide solution by the chlorine. See Total Oxidants BKI method below for calibration.

Total Organic Carbon (TOC)--

Total Organic Carbon is measured using a Dohrmann DC-54 low-level TOC analyzer. The instrument is standardized against potassium hydrogen phthalate solution which is made up as a primary standard by weighing oven dried KHP. An instrument blank is run and taken into account in the calibration of the instrument (see QA/QC procedures, below).

Flow Measurement--

Water was pumped by gear-type positive displacement metering pumps. Borosilicate glass tubular reactors were graduated for volume using large laboratory graduated cylinders so that liquid flow rates could be measured by stopwatch timing of the water level rise. In later pilot studies at Longview, flow was also measured by the filling of a graduated bucket. This became necessary because as the PTFE side thrust plates in the metering pumps became worn, there was some leakage past the pump gears, resulting in a dependence of the flow rate obtained (for a given pump setting) on the downstream resistance. Gas flow was measured with a Hastings-Teledyne mass flowmeter which was calibrated against other mass flowmeters in the air monitoring lab at SumX Corporation. Output from the flowmeter was recorded on a Perkin-Elmer model 56 strip chart recorder, to be manually integrated in order to correct for the change in flow as the ozone monitor switched between sample and reference mode. It was found that the integral of a sawtooth function between the highest and lowest values indicated digitally by the mass flowmeter gave an excellent approximation to the actual integral and thus the average of the two could be used as the flow rate.

During operation at the Longview site, where the mass flowmeter was not available, Brooks rotameters were used in-line as were the rotameters supplied with the ozone generators. These rotameters were calibrated later using a wet test meter, and found to read within about 10% of the true values under the conditions used. The same saw-tooth approximation was used.

Measurements of pH were made using a pH meter and commercial calibration buffers.

Preparation and Use of the Humic Material Concentrate--

After the pilot-plant trailer arrived in Austin from the previous ozone/GAC project, the carbon columns from that project were eluted with 5% sodium hydroxide solution in order to recover the organic material which had been collected during previous pilot-scale operation using water from Cross Lake, Louisiana. The lake is located in a wooded portion of northwest Louisiana, and the water contains a high concentration of natural organics.

The resulting concentrate had a TOC value of 1.5×10^3 mg/L and a carbonate alkalinity of 7.4×10^3 mg/L (as calcium carbonate), indicating that a 1:500 dilution and pH adjustment to 7 would yield a water with a TOC of 3 mg/L and a bicarbonate content of 1.5×10^{-4} M. Typical clarified water in the Longview, Texas Sabine River Water Treatment Plant has a TOC of 2 - 3 mg/L and a total alkalinity range of $2\text{-}4 \times 10^{-4}$ M.

Dilution water for preparation of the synthetic lake water was Austin, Texas tap water which was run through a 4'deep x 1' diameter GAC column before being pumped into the Waterboy^R reservoir for addition of the HM concentrate and pH adjustment with sulfuric acid. Water was made up batchwise at the beginning of a day's experiments, the unused portion being drained if it was not to be used the next day.

Pilot Scale Experiments--

A typical pilot scale experiment was performed as follows. Liquid flow rate was established at the desired value, followed by gas flow rate through the ozone generator and reactors. After flow stability was confirmed, the UV lamps were turned on and checked. Finally, power was applied to the ozone generator and the potentiometer adjusted until the ozone monitor gave a stable reading at the desired concentration for the feed gas to the reactor. The experiment was allowed to run until at least four times the total volume of the configuration had passed through the entire configuration. The time required for this is $4V_cF^{-1} = 4t_c$, where V_c is the contactor volume, F the liquid flow rate, and t_c the average hydraulic retention time. For a perfectly mixed (TCSTR) one-reactor system, this corresponds to

98% sweeping of the system under the new conditions. In the four TPR configuration, the system would of course be in equilibrium if each reactor were perfectly plug flow. If each reactor were perfectly mixed, an element of fluid entering the first reactor would be 99.8% eluted from the fourth reactor in four configuration volumes(48). Since the actual situation is neither perfectly mixed nor perfect plug flow, the equilibrium of the system is expected to be much slower. Equilibration with respect to THMFP reduction was checked as a function of configuration volumes of flow for a four TPR configuration. Samples were taken at four, eight, twelve, and sixteen configuration volumes after establishing fairly drastic operating conditions, and analysed for TOC, THMFP, aqueous hydrogen peroxide, and aqueous ozone. Almost all parameters were found to be equilibrated, within experimental error, after passage of four configuration volumes through the system, and all subsequent experiments were run using an equilibration time of 4 t_c. These experiments are discussed in more detail in the next Section.

During the experiment, samples were withdrawn as carefully as possible and analyzed for ozone, hydrogen peroxide, and total oxidants by the HBI, TI(IV) and BKI/M methods, respectively. Samples withdrawn for TOC, THMFP, pH, and Ti(IV) were immediately purged vigorously with oxygen to remove unreacted ozone. THMFP samples were buffered at pH 7, chlorinated with sodium hypochlorite solution (checked daily for concentration) at an applied dose of 30 mg/L, and allowed to stand in a dark laboratory cabinet for 3-1/2 days. Previous studies showed three days to be adequate reaction time for THM production to plateau in reconstituted lake water. Approximately 30 percent of the chlorine remained as a residual after that time for a feedwater with TOC in the range of 2-3 mg/L. THM's were analyzed by LLE with internal standard, as described earlier. TOC measurements proved relatively uninteresting and were eventually discontinued except for occasional spot checks, in the interest of more useful data.

Results of Parametric Studies

The results of the parametric studies will be presented in three parts: 1) TCSTR batch results, 2) TCSTR flow results, 3) TPR flow results. No TPR batch experiments were run since the results would not be representative of the actual system due to lack of mixing, effect of liquid flow on sparged bubble size, etc. For all experiments on reconstituted lake water, $[TTHMFP]_o$ typically ranges from 120 to 190 μg/L and $[TOC]_o$ from 2.2 to 3.0 mg/L.

Results of TCSTR Batch Studies--

The first series of batch experiments was run using 5.7 standard liters per minute (SLM) of 1.4% ozone in oxygen, in combination with 0, 2 and 4 UV lamps. A stream of 4.2 SLM of air was added to bring the gas flow up to the manufacturer's specification. An oxygen-ozone mixture containing 1% ozone by weight corresponds to 14.3 mg ozone per standard liter at 20°C and one atmosphere of pressure. The lamp manufacturer's literature states a UV output at 254 nm of 5.3 W per lamp, giving power/volume ratios of 0.133 and 0.267 Watts/liter (W/L) for 2 and 4 lamps respectively. The ozone dose rate is 1.43 mg/L min. The UV to ozone ratio, θ, is defined as the number of Einsteins (moles of 254 nm photons) applied per unit time divided by the number of moles of ozone applied per unit time, and is given by

$$\theta = \frac{I(W/L)*(2.12\text{x}10^{-6}E\ sec^{-1}W^{-1})*(60\ sec\ min^{-1})}{D(mg/L\text{-}min)*\ 1\ mole\ (48\text{x}10^{3}\ mg)^{-1}}$$

$$= 6.11\ \frac{I\ (W/L)}{D(mg/L\text{-}min)}$$

For this experiment, then, the ratio is 0.57 and 1.14 for the two and four lamp runs, respectively. The results of these runs are shown in Figure 12 where it is seen that there is not much difference between the two ozone/UV experiments, which are both considerably different from the ozone-only run. As in earlier work(1), TTHMFP is seen to increase before it starts decreasing in the ozone/UV runs. In the ozonation run, TTHMFP is seen to decrease first then increase followed by a gradual decrease at higher dose rates. The treatment time, t_1, and ozone dose, D_1, required to reduce the substrate (in this case, the TTHMFP) to 1/e (37%) of its original value are convenient parameters for rough comparison of different treatment processes (1) even when the disappearance curve is not exponential. In this experiment, t_1 is found to be 23 and 25 minutes for 2 and 4 lamps respectively, and by extrapolation, about 90 minutes for ozone only. The dose D_1, used in time t_1 is 34 and 35 mg/L respectively for the 2 and 4 lamp experiments compared to 130 mg/L (estimated) for the ozonation.

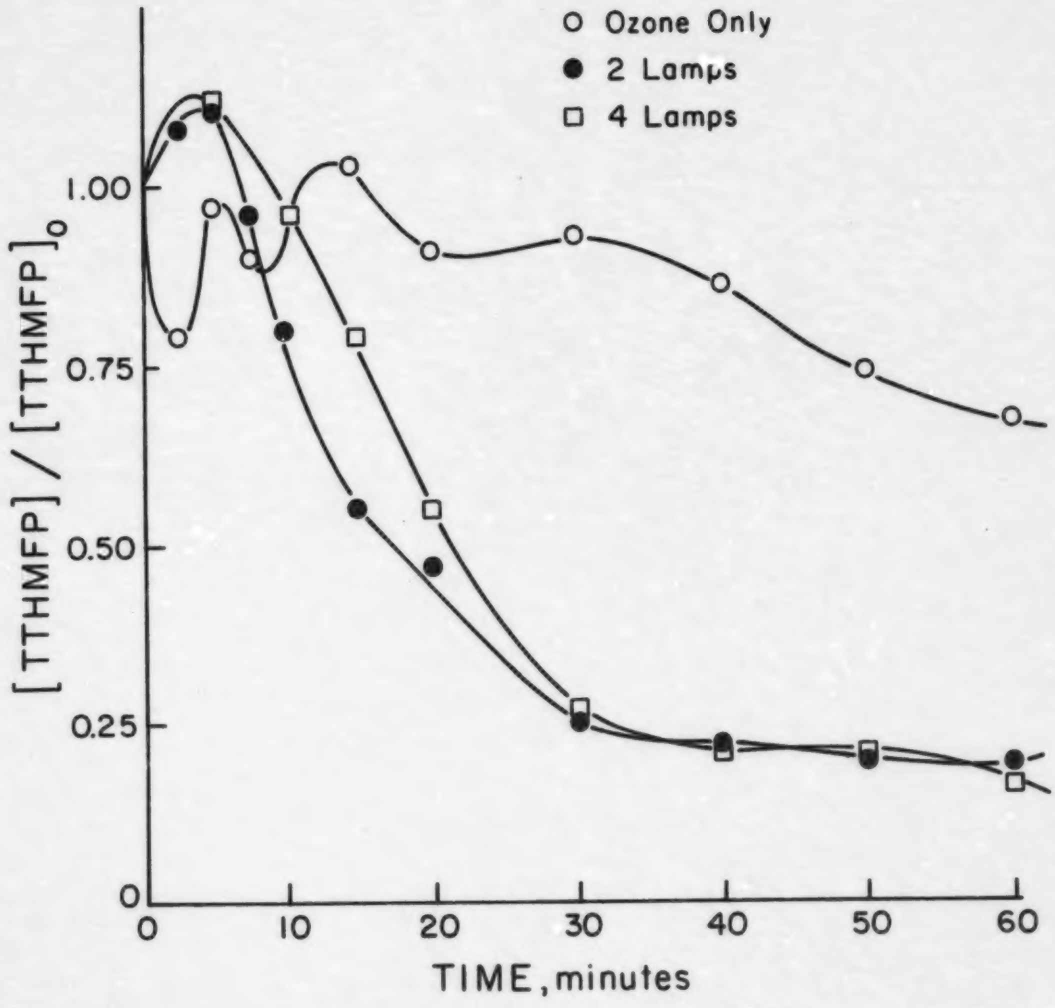

Figure 12. Ozone and ozone/UV reduction of trihalomethane formation potential. Ozone Dose = 1.4 mg/L - mins.

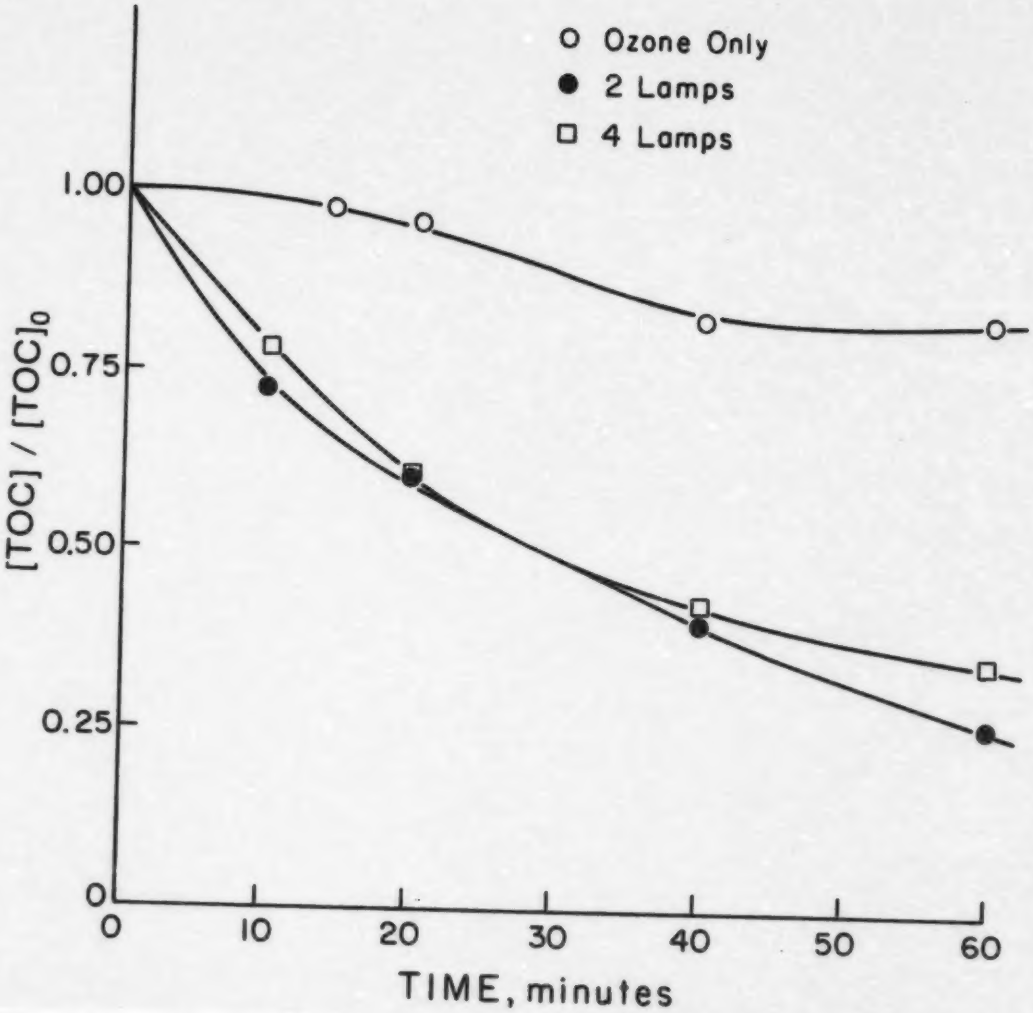

Figure 13. TOC reduction by ozone and ozone/UV. Ozone dose = 1.4 mg/L - mins.

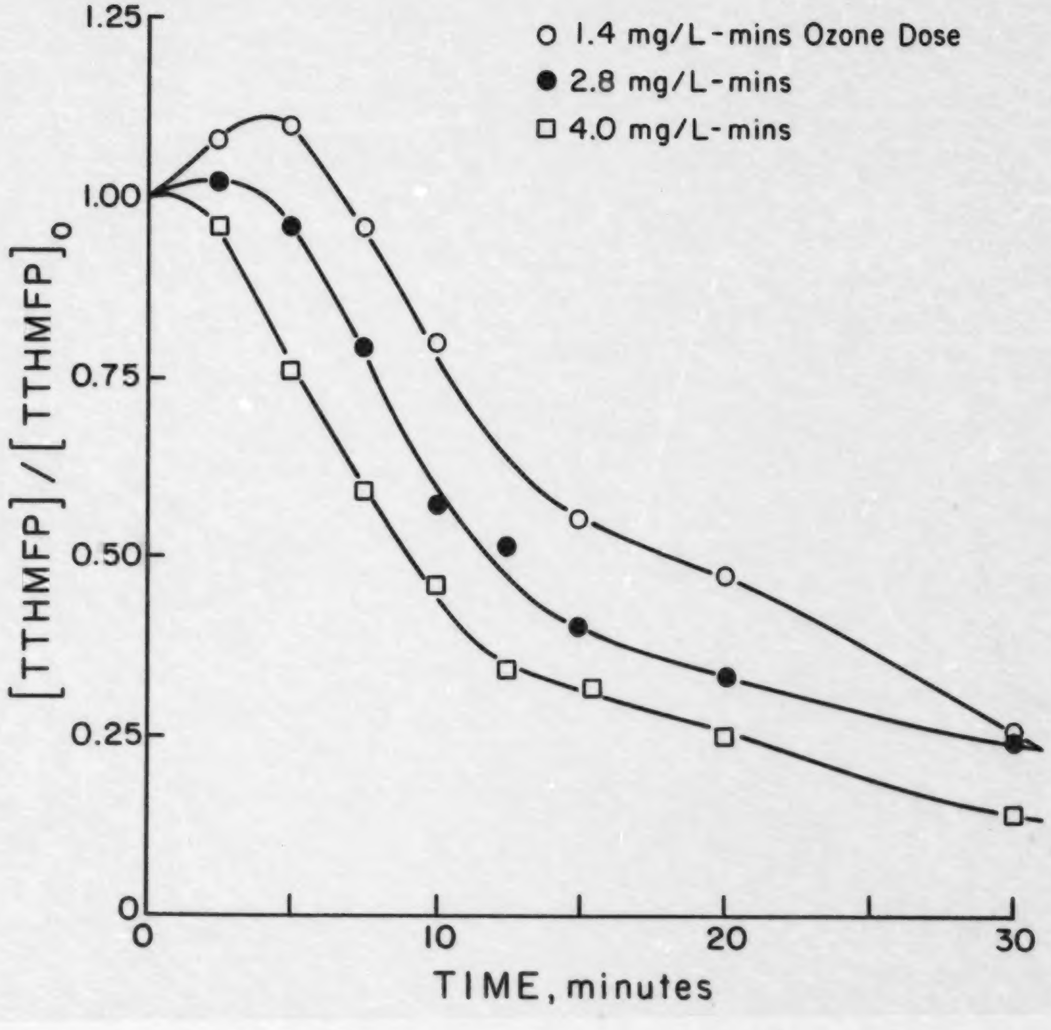

Figure 14. Ozone/UV reduction of THMFP using two UV lamps.

The general shape of the curves is thought to be due to the fact that ozone may react preferentially with THMFP sites while hydroxyl radical, being very reactive and nonspecific, at first generates sites faster than it destroys them. The later rise in the ozonation curve represents generation of new sites by (a) ring rupture and/or (b) the onset of free radical reactions, now known (6,25) to be present in ozonation systems under most conditions. Obviously, if ozone could be made to react specifically with THMFP sites while suppressing the generation of new sites, good removal of THMFP might be realized at an economically feasible ozone dose. As a simple example 300 µg/L of chloroform formation potential (bromide-free system assumed for simplicity of argument) corresponds to 2.5×10^{-6} M sites. At one ozone molecule per site, a little over 0.1 mg/L of ozone would be required. As will be described later, all attempts to selectively destroy THMFP sites during this project have failed. Figure 13 shows TOC removal for the same three experiments and it is seen to follow the same trend although disappearing more slowly than TTHMFP. It is interesting to note that after about 35 minutes TTHMFP decreases only very slowly while TOC still disappears approximately exponentially. This probably represents the point after which the average composition of the remaining organic material may be approximately constant (fully oxidized) after which chain rupture and decarboxylation are the primary reactions.

Shown in Figure 14 is a series of three runs in which the ozone dose rate was varied while the UV intensity was held constant at 0.133 W/L (two lamps). The ozone concentration was 1.4, 2.8 and 4.0% giving dose rates of 1.4, 2.8 and 4.0 mg/L-min and θ = 0.57, 0.29, and 0.20, respectively. The corresponding values of t_1 are 24, 16, and 12 minutes. It is seen that doubling the dose rate does not double the removal rate. That is due in part to the effect of θ on the mass transfer rate, as will be seen when the flow experiments are discussed, but also on other factors. TOC removal shows very little variation between these three runs and is again approximately exponential and about half as fast as TTHMFP removal.

Figure 15 shows two different ozone dose rates using four lamps, and considerable difference is seen between the initial rates of destruction of THMFP. Values of t_1 are 25 and 18 minutes at 1.4 and 2.4 mg/L-min. dose rates, giving D_1 = 35 and 43, respectively. For those runs θ = 1.14 and 0.68 respectively.

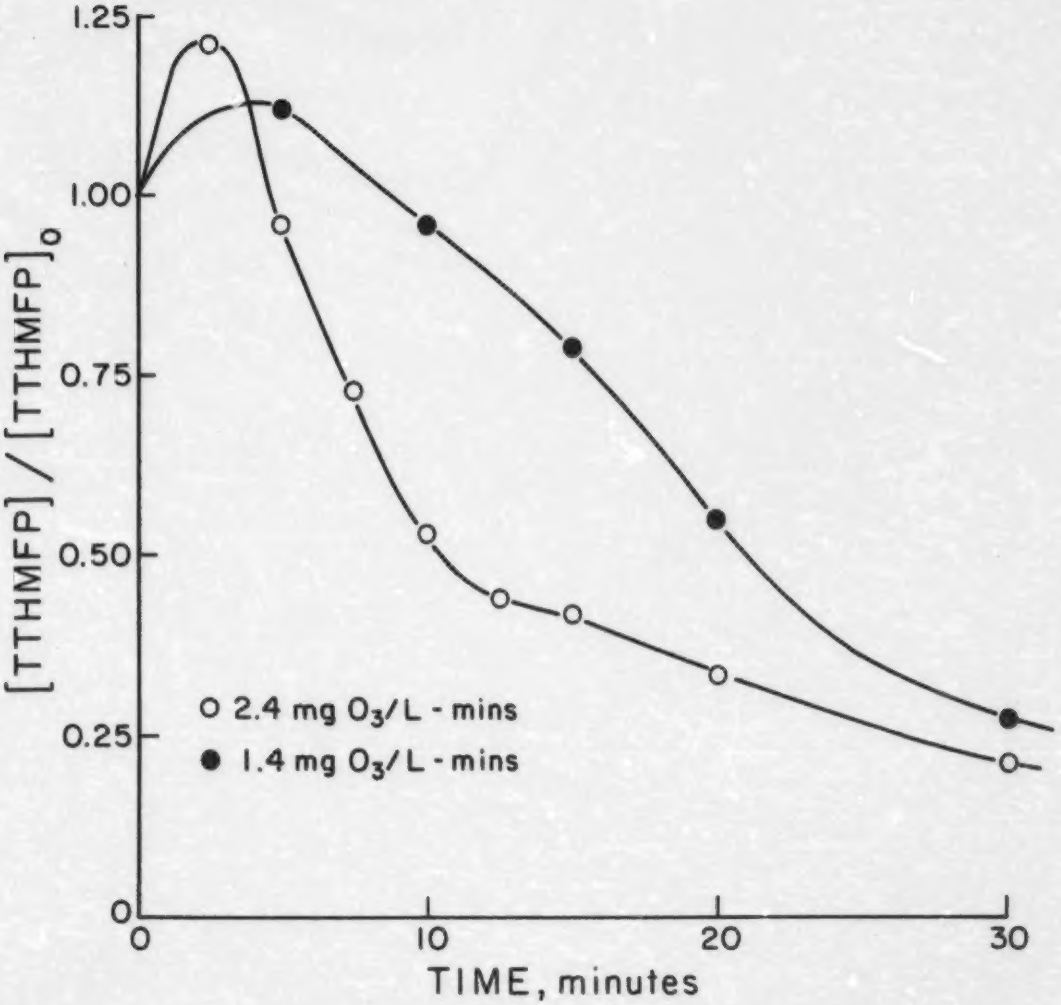

Figure 15. Ozone/UV destruction of THMFP. Four lamps.

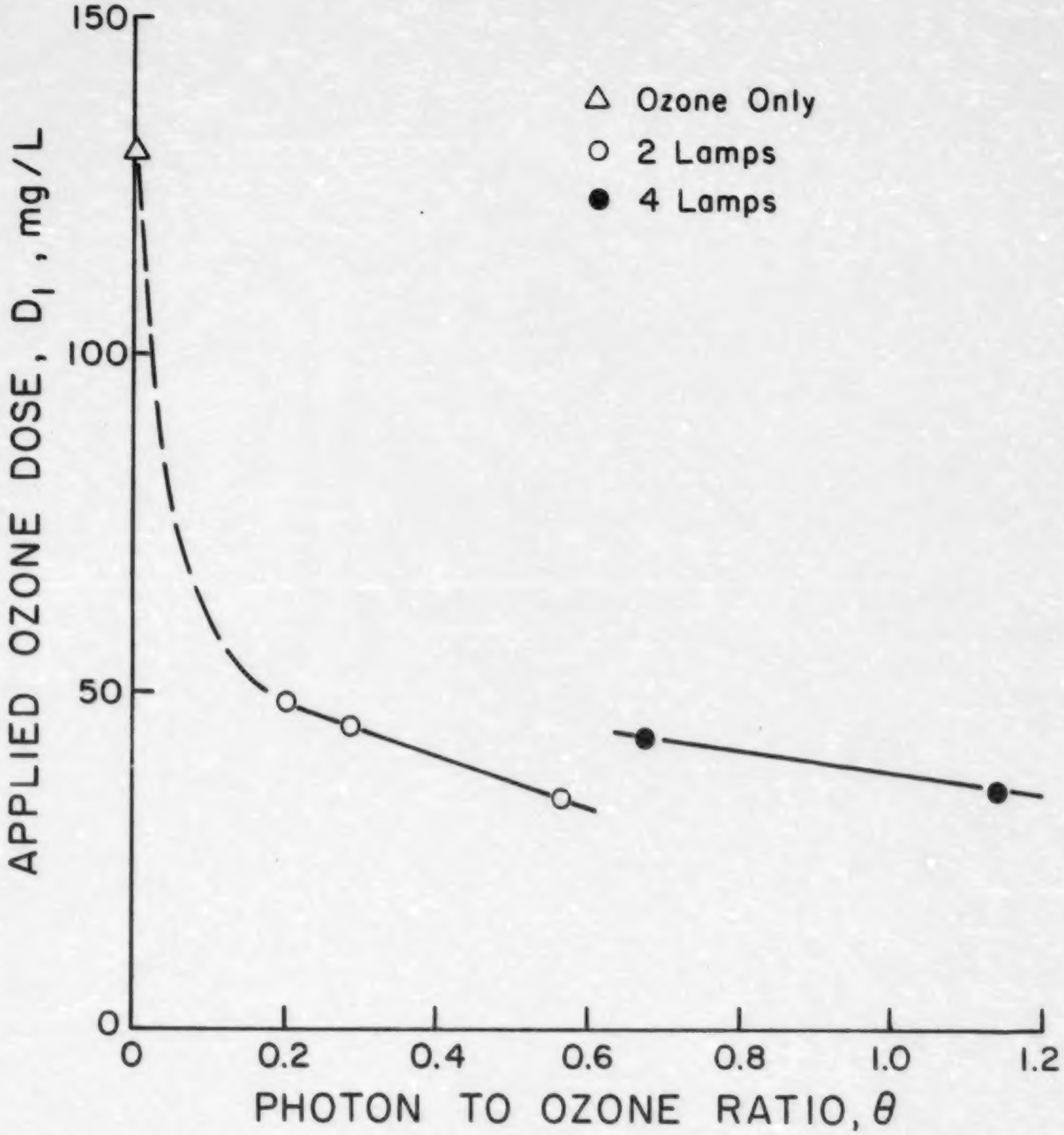

Figure 16. Applied ozone dose required for 63% removal of TTHMFP (TCSTR batch runs).

Shown in Figure 16 is D_1, the dose required to remove 63% of the TTHMFP, versus θ, the photon to ozone ratio. As was seen in previous plots, the increase from two to four lamps has little effect on the amount of FP removed per milligram of ozone applied, and a lower dose rate favors ozone utilization. This is emphasized in Figure 16 by the lines connecting experiments of similar UV intensity but different ozone dose rates. This behavior in the batch system will be compared with that of the flow system in the next section, where it will be shown that an appreciable difference between two and four lamps may be realized only at higher ozone concentrations.

Results of TCSTR Flow Studies--

It is well known that results obtained from experiments run in the batch mode are not always easily extrapolated to the flow mode. This is particularly true if the reactor feed contains a complex mixture of reactants and products with varying reactivities. The batch experiments described above were performed for comparison with the flow mode to enable more efficient data accumulation, should the results prove comparable. Some characteristic features may be obscured in a flow situation which are more discernable when a more "stepwise" progression from more reactive to less reactive substrates is taken. The latter situation is the one frequently seen in product studies where substrate is seen disappearing while the first product appears. Later the first product may decline while a second product forms, etc. In a flow system, material in various stages of reaction is constantly flushed out of the reactor and replaced with untreated substrate.

Experiments were run with ozone dose rates of 1.4, 2.4 and 4.0% and 0, 2, 4, 6 and 8 lamps in the TCSTR. Water flow rate was adjusted so that the average retention times in the TCSTR was 5, 10, and 15 minutes. These conditions spanned an applied ozone dose range of 7-60 mg/L and θ values 0.20 to 2.3.

Figures 17 through 19 show the FP removal curves as a function of retention time and number of lamps for 1.4, 2.4, and 4.0% ozone, respectively. To avoid confusion, only the data points for ozonation have been joined with a line in Figures 17 and 18. The time scale on the abscissa is the average hydraulic retention time in the reactor and thus the points at 5, 10 and 15 minutes represent separate experiments. It is seen in the first of these plots that under these conditions a dose rate of 1.4 mg/L min. was insufficient to remove more than 25% of the FP. In Figure 19, the ten-minute

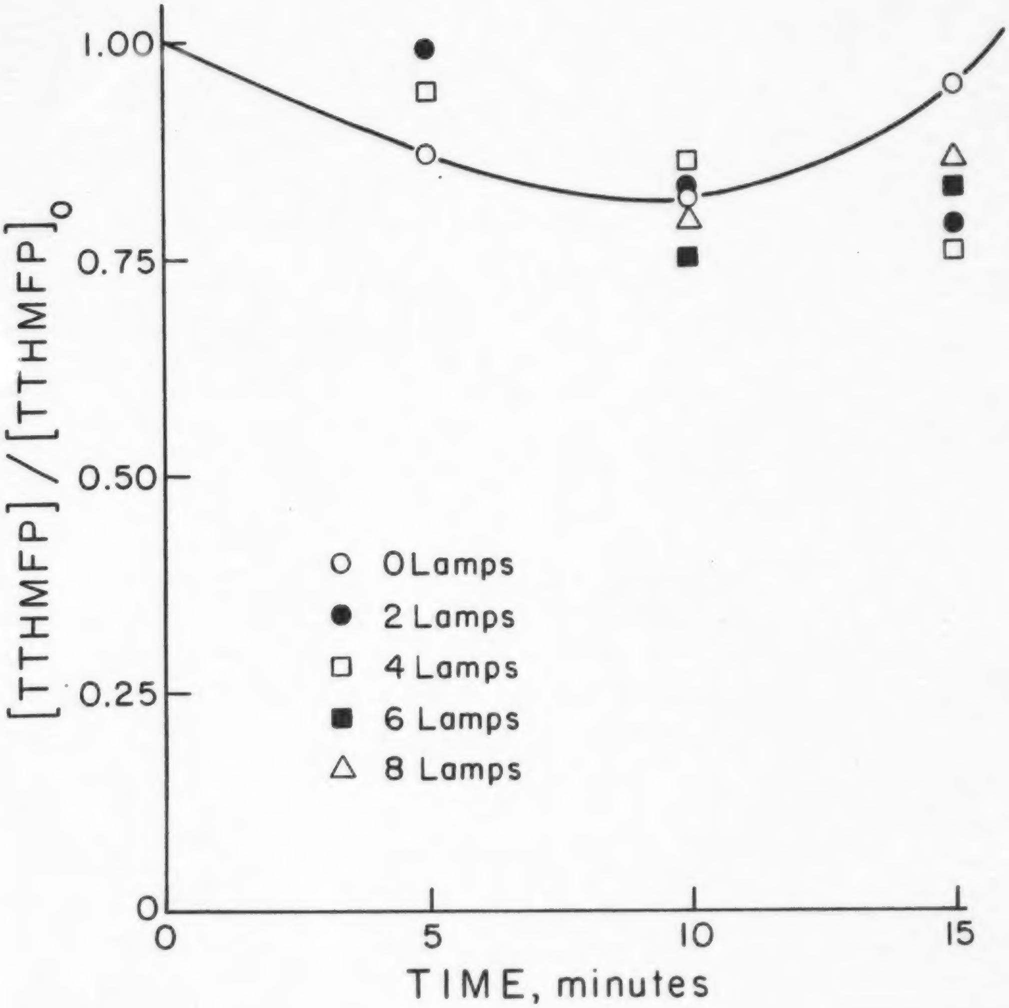

Figure 17. THMFP reduction, flow runs. Ozone dose rate = 1.4 mg/L-min.

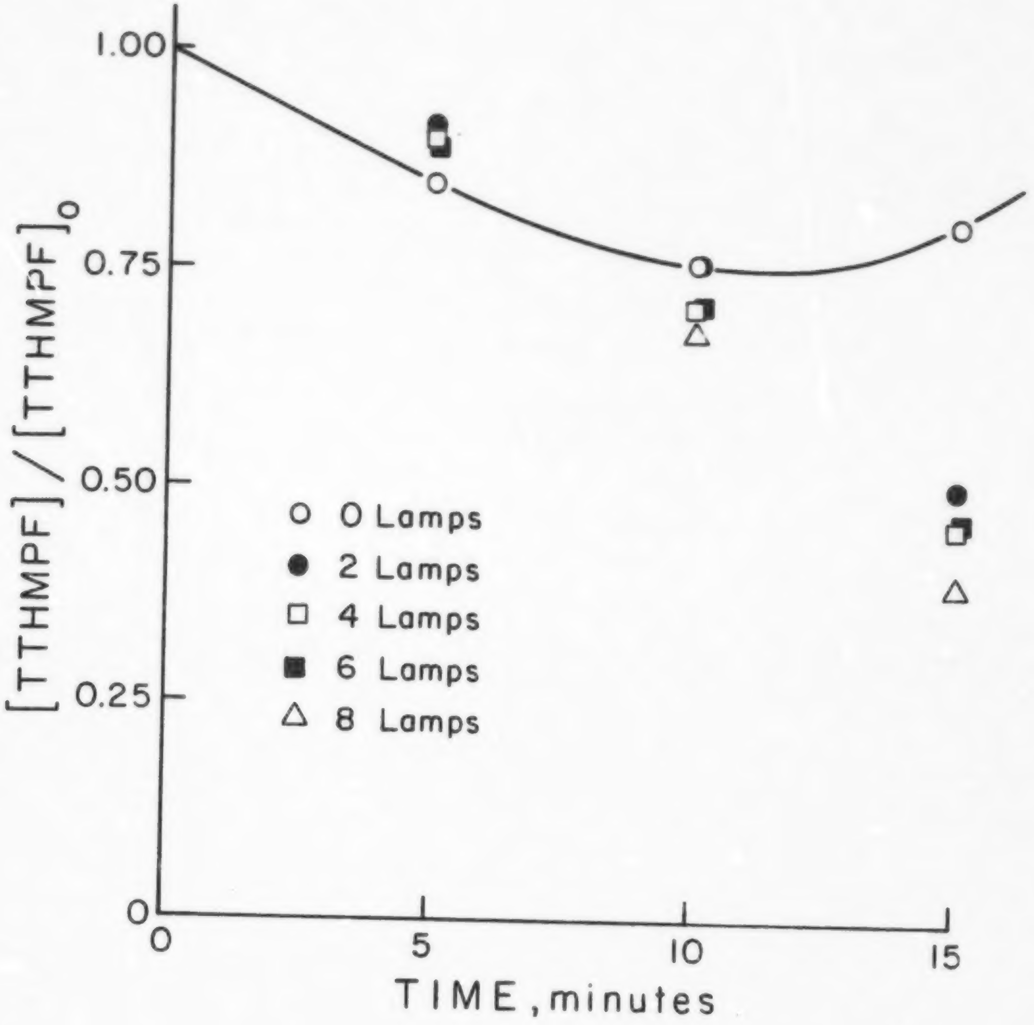

Figure 18. THMFP reduction, flow runs. Ozone dose rate = 2.4 mg/L-min.

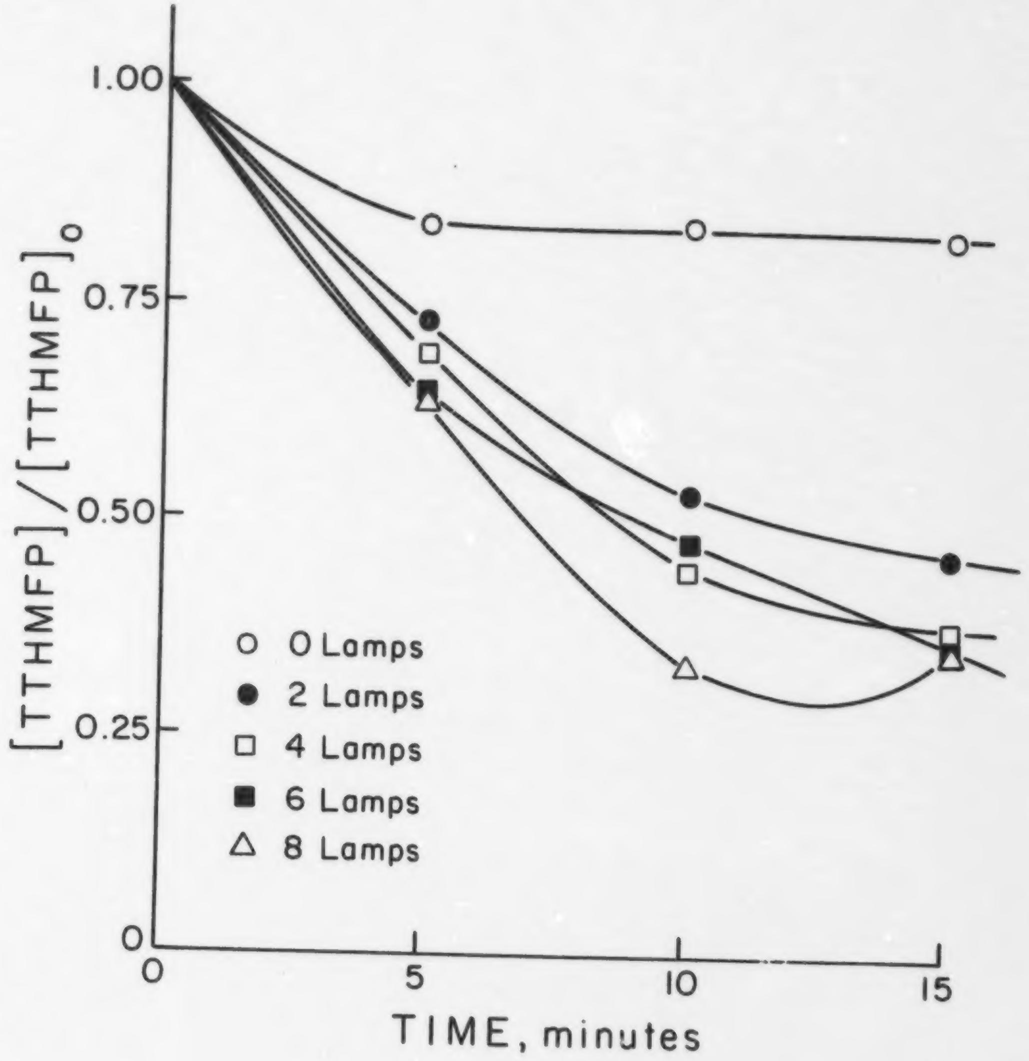

Figure 19. THMFP reduction, flow runs. Ozone dose rate = 4.0 mg/L-min.

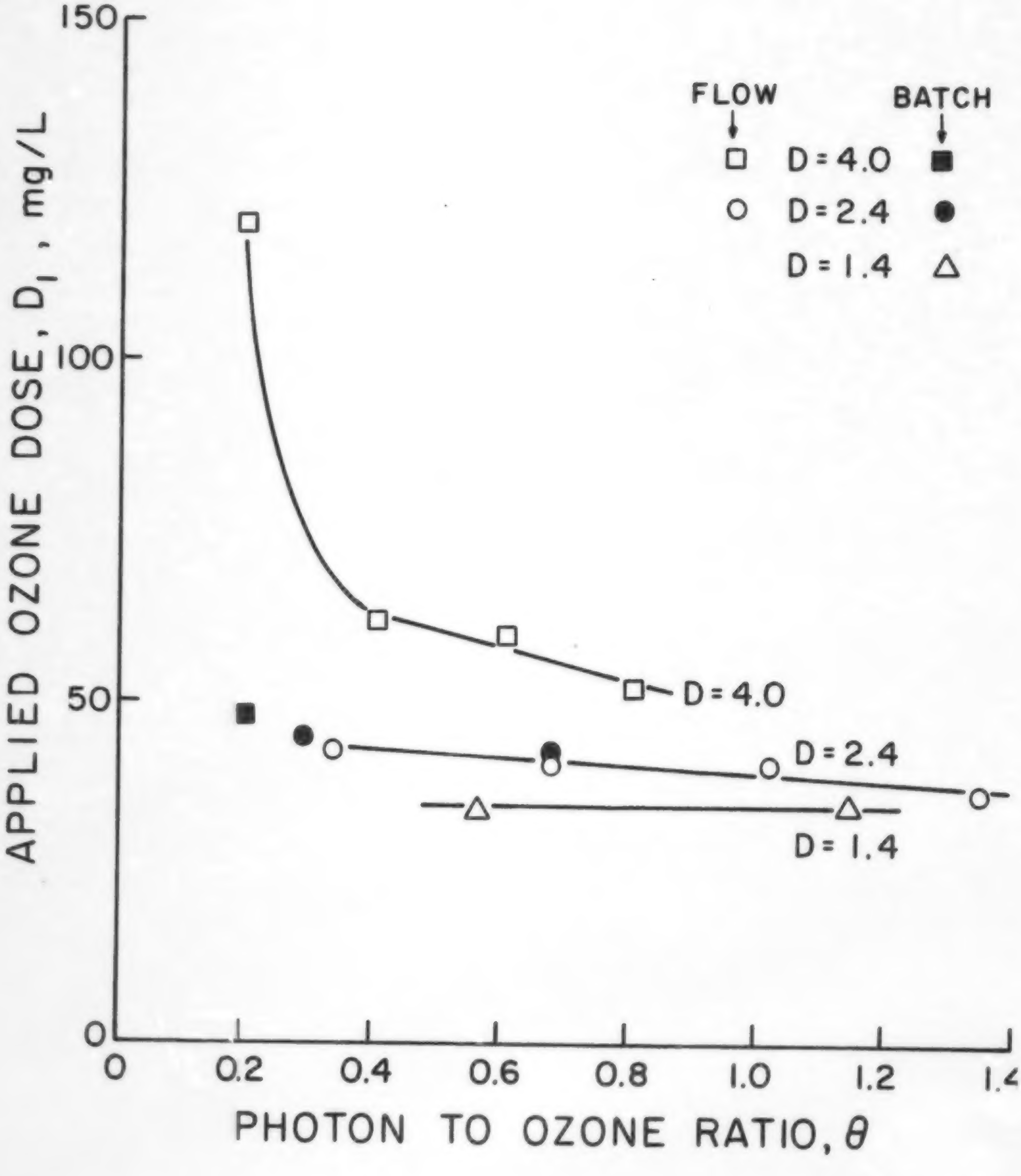

Figure 20. Applied ozone dose required for 63% removal of TTHMFP (TCSTR - batch and flow data).

eight-lamp point is probably too low, so that only the five- and fifteen-minute points were used in the data analysis.

One manner of displaying the data is to plot D_1, versus θ, as was done with the batch data. This plot is shown in Figure 20, where it is seen that ozone is utilized considerably less efficiently when dosed at 4 mg/L-minute than at 2.4. In particular, the 2 lamp point ($\theta = 0.20$) on the 4 mg/L-min. curve shows very poor removal efficiency, requiring a dose of 120 mg/L for 63% FP removal. Shown for comparison are the points from the batch runs described above. It should be noted that in Figure 20 points of equal dose rate and varying UV intensity are connected by lines, whereas the reverse was true in Figure 16. While D_1 is similar for flow and batch runs at 2.4 mg/L-min., utilization appears to be considerably worse for the flow experiments at a dose rate of 4.0 mg/L min. No points corresponding to flow runs at 1.4 mg/L are included since in no case was removal greater than 25%, making the results of extrapolation to 63% removal very questionable. The maximum ozone dose for those experiments was 21 mg/L, whereas the most optimistic extrapolation which can be made from Figure 17 yields a D_1 value of about 53 mg/L.

Regarding the general shape of the THMFP removal curves, it is observed that their shape is irregular, seeming to turn up in Figure 17, down in Figure 18, and to have a somewhat exponential appearance in Figure 19. This is attributable to the fact that the early portions (<50% removal) of THMFP removal curves can vary considerably with operating conditions. In no case do they exhibit the immediate increase in formation potential seen at low ozone doses in the batch runs.

The behavior of the TOC data is relatively uninteresting and somewhat irregular except for three features.

1) ozone alone removes very little TOC (<10%); ozone/UV removes considerably more.

2) TOC removal is less than TTHMFP removal (by percent).

3) TOC removal curves often rise slightly after an initial decrease, then decline again.

This latter behavior has been seen before in this and other research groups and is probably related to the fact that a persulfate/UV photooxidation step is used in the Dohrmann DC-54 carbon analyzer. Presumably, organic materials which are initially refractory to the persulfate/UV treatment as used in the analyzer, become susceptible after ozone/UV treatment for a few minutes. For this reason, comparison of runs using TOC data, and in particular between different water sources, is highly suspect.

Close to the beginning of the TCSTR flow experiment phase, the off-gas plumbing was rearranged so that the amount of ozone leaving the reactor could be measured. Since the manufacturer's specifications stated that a gas flow rate of at least 9 SLM should be maintained through the turbine to avoid cavitation, 4.2 SLM of make-up air was added to the 5.7 SLM from the ozone generator before contacting. Table 7 lists the percent of feed gas ozone which was found in the off-gas for the TCSTR flow experiments. Although the figures for the ozone-only experiments appear high, it must be recalled that the applied ozone doses are tens of milligrams per liter while the solubility of ozone under these conditions is considerably less. For example, at 20°C, t_r = 10 min., influent ozone = 1.0%, the ozone dose = 24 mg/L. Since the average ozone concentration in the gas for a paddle-stirred CSTR is that of the off gas, (see previous section on mass transfer), C_g = 0.46 x 1% x 14.3 mg/L.% = 6.6 mg/L. This gives an equilibrium liquid concentration of 2.0 mg/L using the data of Kosak-Channing and Helz(47). Since this turbine reactor is not paddle stirred and does not have the gas holdup of a paddle-stirred reactor, the average concentration of the gas may be somewhat higher. Thus, the amazing feature is that 54% of the ozone does not appear in the off-gas. When the utilization factors given in Table 7 are taken into consideration, the required ozone doses are reduced by 18-34% in all but one case.

Figure 21 shows the actual ozone dose (ozone utilized rather than applied) required to reduce TTHMFP to 1/e of its original value. The deviation from linearity by the four lower and three of the four upper points is within experimental error. This means that in all but the most extreme point (2 lamps, 4% ozone; the uppermost point), for a given ozone dose rate the number of UV lamps used does not seem to make a difference in FP removal efficiency when based on ozone which is removed from the gas stream. These results suggest that the main effect of added UV is to increase mass transfer to the liquid by a) photolysing ozone in the liquid and perhaps the film, thereby lowering the resistance to mass transfer, rather than to shift from one type of reaction to another, and b) increasing the concentration of species which react with ozone. This idea is given further support by the ozone residual data. It should be noted that even though the slope of the D_1 vs θ curve went to zero in going from Figure 20 to Figure 21, the

TABLE 7. PERCENT OF INFLUENT OZONE FOUND IN TCSTR OFF-GAS

Number of lamps	Influent Ozone Concentration[1]						
	0.8%	1.4%			2.3%		
	t_r = 10 min	t_r = 5 min	10 min	15 min	5 min	10 min	15 min
0	32%	46%	46%	56%	50%	54%	54%
2	26%	28%	28%	30%	32%	34%	34%
4	20%	24%	24%	24%	26%	26%	30%
6	20%	29%	22%	22%	24%	24%	26%
8	18%	18%	20%	22%	—[2]	11%	—[2]

NOTES: [1] Resulting from dilution of 5.7 SLM of 1.4, 2.4, and 4.0% ozone with air at 4.2 SLM.

[2] Not measured.

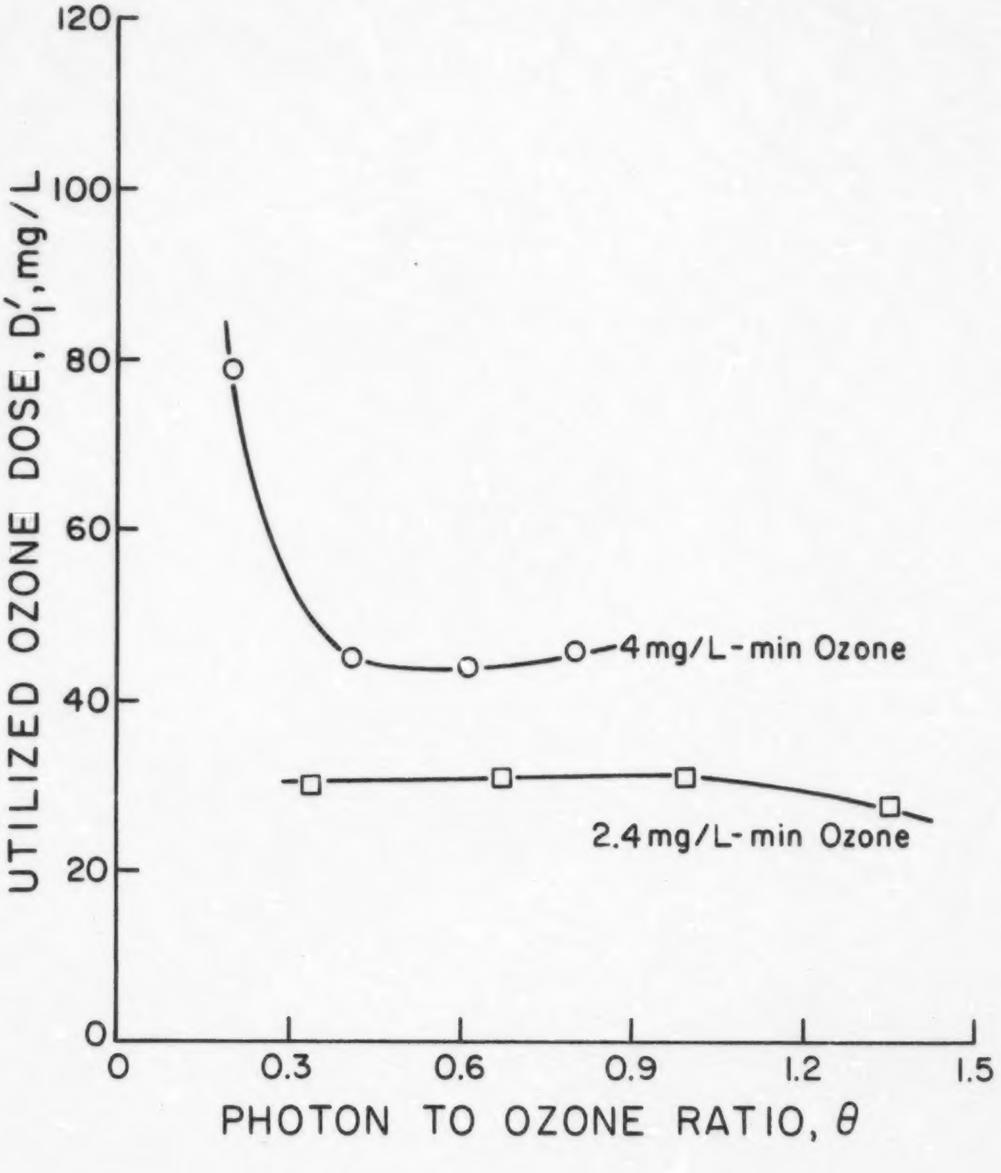

Figure 21. Utilized dose required for 63% removal of TTHMFP (TCSTR - flow runs).

spacing of the two lines is maintained, that is, D_1 (θ) for 4 mg/L-min. is approximately 1.5 times larger than for 2.4 mg/L min. Although no data for 1.4 mg/L-min. appears in Figure 21 because FP removal was not extensive enough and in some cases off-gas concentrations were not available, it seems reasonable to assume from Figure 20 that dosing at 1.4 mg/L min. would also be more efficient on an ozone-utilized basis than at 2.4 mg/L-min., though not so dramatically as between doses of 4 and 2.4. A reasonable generalization seems to be that the lowest ozone dose rate that will accomplish the desired removal in a reasonably-sized vessel will be the most efficient.

When the data in Table 7 is plotted as fraction of ozone removed from gas stream versus number of lamps, each plot shows a sharp break point just above two lamps. This is illustrated for one set of data in Figure 22 which also contains data for a third ozone concentration, 2.8%. This breakpoint is representative of the number of lamps above which mass transfer is only sparingly increased. Since it has already been shown in Figure 21 that FP removal per milligram of ozone transferred from the gas phase does not increase with the number of lamps, it appears that this breakpoint represents optimum operating conditions from an energy consumption point of view. In all but the most drastic conditions (2.8% ozone, 5.7 mg/L min., t_r = 5 minutes), the breakpoint was at 2.4 ± 0.2 lamps. Since the lamps are mounted in pairs, subsequent runs were made with either two or four lamps.

Summary of TCSTR Flow Results--

1) The lowest ozone dose rate that will accomplish the desired THMFP removal in a reasonably-sized vessel will give the most efficient ozone utilization.

2) The primary effect of increasing UV power in the TCSTR above $\theta = 0.4$ in this system is to increase mass transfer by maintaining a lower ozone concentration in the liquid and increasing the concentration of species which react with ozone.

3) The energy-optimized amount of UV power in the TCSTR appears to be 2.4 ± 0.2 lamps or 0.16 W/liter of reactor volume.

4) Batch studies do not necessarily give the same results as flow studies for THMFP removal, and are definitely different in the early stages of treatment.

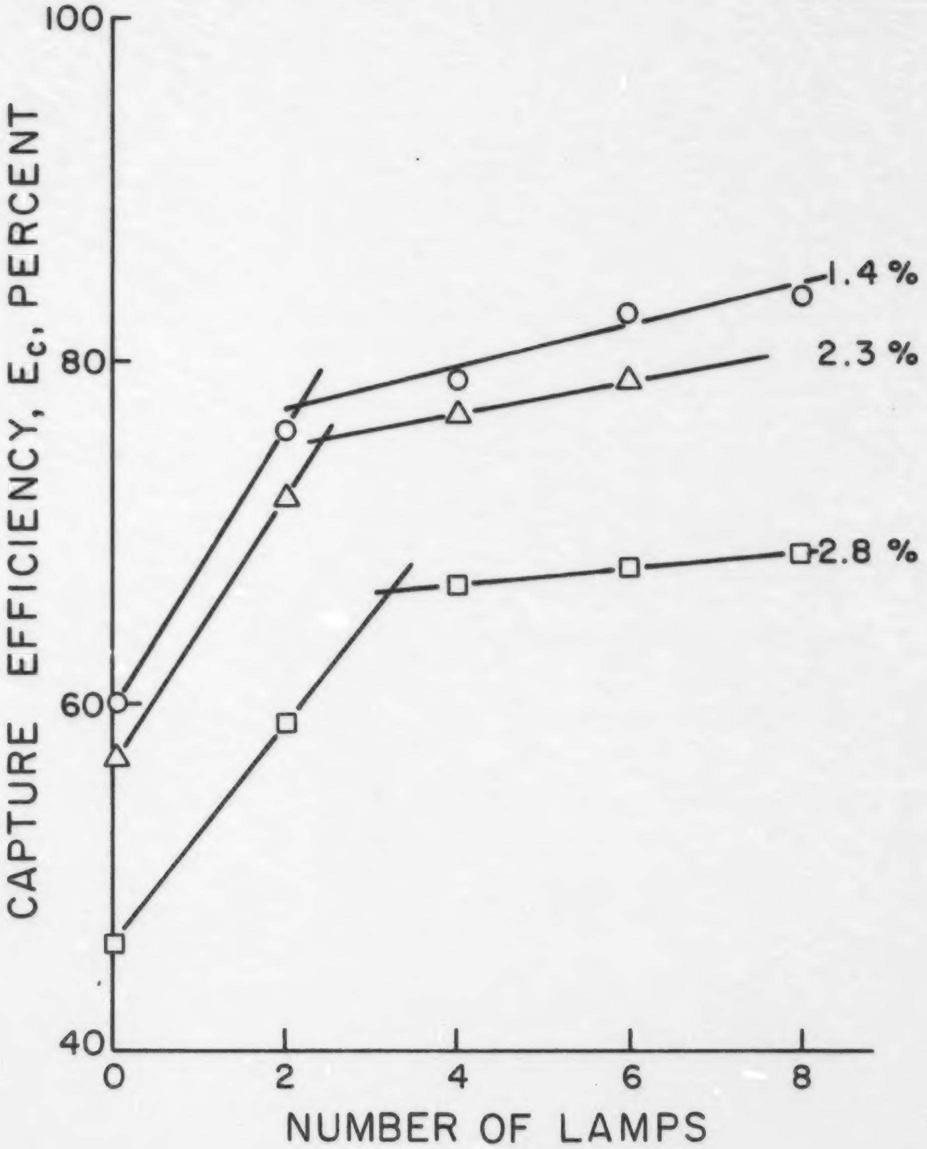

Figure 22. Capture efficiency in TCSTR flow experiments. F_e = 4.0 GPM.

5) TTHMFP is removed from reconstituted lake water more quickly by ozone/UV than is TOC.

6) A dose of 30 mg of ozone consumed per liter of water was adequate to reduce TTHMFP to 1/e of its original value (37% remaining) in the synthetic lake water, using the TCSTR with 2-4 lamps. During that time TOC was reduced to 62% of its original value.

Results of TPR Flow Studies--

The series of experiments which comprise the TPR parametric study included more than sixty separate experiments. Early in the study flow calibration and analytical difficulties were experienced, which necessitated discarding some data and limiting the interpretation of other data. The experiments were run in sets, designated A through L. Of these sets, the experiments comprising sets A through D should only be compared with other experiments in the set, while sets E, F, and G were discarded. Any plots summarizing the data contain only data from experiment sets H through L.

Due to the large number of experiments run, a notation was developed to designate the configuration of a particular experiment. An experiment is described in the notation by first identifying at what point the ozone was applied and where it was vented. Thus, D_{I-IV} means that ozone was applied in the first reactor and vented in the fourth, traveling through reactors II, III and IV with the water and being at least partially remixed when passing through a pipe cap mixer (a 1 inch pipe cap with five 1/8" holes evenly spaced). This type of experimental arrangement was intended to simulate being able to sample at various points along a larger (12 foot) bubble column, in different sections of which UV could be applied or not, as desired. In this notation, D_{I-II} D_{III-IV} means ozone was applied in reactor I, vented (as entirely as possible) in II, and a fresh gas stream applied in III and vented in IV. Correspondingly, D_I means ozone was applied in reactor I and vented there as well.

The notation describing the arrangement of UV lamps is

$$(\text{no. of lamps})L_{(\text{TPR no.})} \quad ,$$

so that IL_I means one lamp in TPR_I, $1L_{II}$ $2L_{III}$ means one lamp in TPR_{II} and two lamps in TPR_{III}, and so forth. By far, the most experiments were run in the configuration D_{I-IV} $1L_I$ or D_{I-IV} $1L_I$ $1L_{II}$.

In the following sections various configurations will be compared for their effectiveness in destroying THMFP. In order to compare those configurations two efficiency terms will be defined. The first, called the capture efficiency, E_c is merely the decimal fraction of applied ozone which does not appear in the off gas, that is, the fraction captured by the system. While of interest for characterization of the reactors, all performance evaluation is based on the amount of ozone consumed, and a parameter called the ozone utilization efficiency, E_u, is useful. This parameter is defined by

$$E_u = \frac{100}{D_u} (1 - FP/FP_o) \quad ,$$

or the percent FP reduction per mg/L of ozone used. This is of course not a true efficiency, since the maximum value is not unity. It should be noted that for a given element of water being treated, E_u will be larger at, say, 40% FP remaining than at 10%, due to the tailing of the removal curve. It is nonetheless a useful parameter. It should be noted that due to the sometimes irregular behavior of FP removal curves in the early stages of treatment, values of E_u derived from experiments where FP destruction was less than about 40% should not be given too much importance. Normalization of this parameter to either TOC or $TTHMFP_o$ is undesirable for the reasons discussed earlier and the fact that the refractoriness of TOC and the FP/TOC ratio vary considerably between water sources.

The experimental sets were designed to be compared "vertically" as well as "horizontally", that is, each day's experiments were designed to test a particular facet of the process, so that in the event of problems such as those encountered or in the event of a gradual change in the humic/fulvic concentrate, some internal consistency would still be preserved. Correspondingly, the following sections analyze the data from each set independently, then an attempt will be made to summarize the conclusions.

SET A

DATE: 10/14/82

PURPOSES: (a) Effect of sequentially increased UV power

(b) Effect of delayed (after contacting) irradiation

CONFIGURATIONS:	$D_{I - IV}$	Ozone only	32B-1
		$1L_I$	32B-2
		$1L_I$ $1L_{II}$	33A-3
		$1L_I$ $1L_{II}$ $1L_{III}$	33A-4
		$1L_I$ $1L_{II}$ $1L_{III}$ $1L_{IV}$	33B-5
		$1L_{II}$ $1L_{IV}$	33B-6

Using the notation generated previously, ozone was introduced in TPR_I through the 3/8" tubular ring contactor (average bubble diameter is 1 cm.) and no gas is vented until TPR_{IV}, that is, the configuration was $D_{I - IV}$. Gas and liquid were remixed upon entering the next TPR by passage through five 1/8" diameter holes in a pipe cap resulting in bubbles of average diameter 4-5 mm. It should be noted that under usual ozone mass transfer considerations, neither the 1 cm bubbles of the ring contactor nor the 4-5 mm bubbles of the pipe cap mixer would be expected to give very efficient mass transfer. In addition, as noted earlier, the superficial velocity of the sparge gas is well below the recommended range.

The results obtained are given in Table 8. An unanticipated liquid flow rate change had to be corrected for in the dose calculations, so the capture efficiencies in the series of one lamp to four lamps do not form as smooth a trend as expected. This problem was corrected in subsequent runs. A definite trend can however be seen in the efficiency ε_u, and delaying irradiation from $1L_I$ $1L_{II}$ to $1L_{II}$ $1L_{IV}$ is seen to lose slightly in both capture efficiency and destruction efficiency. In both of those trends the liquid flow rates in the latter experiments are slower than the former, so while, for example, watts UV/L of reactor volume doesn't change going from $1L_I$ $1L_{II}$ to $1L_{II}$ $1L_{IV}$, watt-minutes/L liquid changes considerably. Similarly, the gain in efficiency in going from one to four lamps may be less significant than it appears.

Conclusions: Some increase in both capture efficiency and utilization efficiency by adding UV power in subsequent reactors. Trade off requires comparison of UV cost per liter of water treated versus ozone cost saved. It is unclear whether delayed irradiation is indicated to be favorable.

TABLE 8. EFFICIENCY DATA FOR SET A

Lamp Configuration ($D_{I} - {IV}$)	Ozone Dose(d) Utilized, Du, mg/L	Capture Efficiency, E_c	Utilization(a)(c) Efficiency, E_u	$\frac{TTHMFP}{TTHMFP_o}$(b)	
				S_4	S_7
0	20.3	0.51	0	0.92	1.00
I	28.2	0.72	1.1	0.68	0.69
I II	30.1	0.69	1.2	0.70	0.63±0.15
I II III	32.6	0.72	1.5	0.64	0.81
I II III IV	38.9	0.75	1.5	0.69	0.40
II IV	38.8	0.66	1.1	0.87	0.57

(a) Not a "true" efficiency, that is, not $E_{u, max} = 1$. This measure of efficiency is only appropriate since the feedwater remains approximately constant from one experiment to the next. Measured on effluent from TPR_{IV}.

(b) Sampling point S_4 is between TPR_{II} and TPR_{III}; Sampling point S_7 is after TPR_{IV}.

(c) Because of the flowmeter calibration problem, described in the text, comparison with E_u from data sets collected on other days may not be valid.

(d) Liquid flow rate was 0.55 - 0.93 gpm, ozone sparge gas contained 2% ozone by weight.

TABLE 9. EFFICIENCY DATA FOR SET B

Lamp Configuration ($D_{I - IV}$)	Ozone Dose (c) Utilized D_u, mg/L	Capture Efficiency, E_c	Utilization (a) Efficiency, E_u (b)	$\frac{TTHMFP}{TTHMFP_o}$	
				S_4	S_7
O	6.2	0.38	2.7	0.82	0.83
I	9.4	0.56	1.8	0.93	0.83
II	11.1	0.68	2.0	0.87	0.78
I II	12.1	0.74	2.1	0.85	0.75
2 I	10.4	0.64	1.8	0.98	0.81

(a) Values should not be compared outside this data set because of flowmeter calibration problems. See text for discussion. S_3 values are based on total D_u.

(b) E_u evaluated at S_7.

(c) Liquid flow rate was 2 gpm in this set of experiments compared to 0.55 - 0.93 gpm in the previous set. Ozone concentration in the feed gas was 2% by weight.

SET B

DATE: 10/18/82

PURPOSES: (a) Compare increased power in one TPR with adding lamps in subsequent reactors

(b) Second comparison of delayed irradiation (increased liquid flow rate)

CONFIGURATIONS: D_{I-IV}	Ozone only	34A-1
	$1L_I$	34B-2
	$1L_{II}$	34B-3
	$1L_I$ $1L_{II}$	35A-4
	$2L_I$	35A-5

Set B was run with 2% ozone as was Set A, but the liquid flow rate was increased to 2 gpm. Data is given in Table 9. While the capture efficiencies are, for the most part, lower than the previous set presumably because of the difference in flow rate and ozone dose rate, the ratio of E_c for $1L_I$ to ozone only is roughly the same as before, as is the ratio of E_u of $1L_I$ and $1L_I$ $1L_{II}$. Increased UV power in one TPR does not do as much good as adding the lamp sequentially.

Conclusions: In contrast to Set A, the $1L_{II}$ configuration gives slightly better results than $1L_I$ but with only 20±3% FP removal, cannot be given too much weight. The configuration $1L_I$ $1L_{II}$ is better than either one lamp configuration in both capture and utilization, and $2L_I$ is significantly poorer than $1L_I$ $1L_{II}$ in both respects.

SET C

DATE: 10/22/82

PURPOSES: (a) To verify equilibration times for experimental configurations.

(b) To establish approximate error bounds for parametric measurements.

CONFIGURATIONS: D_{I-IV}	Ozone only	36A-1
	$1L_I$ $1L_{II}$ after 4 reactor volumes	36A-2
	" " 8 " "	36B-3
	" " 12 " "	36B-4
	" " 16 " "	36B-5
	$1L_I$ " 4 " "	37A-6
	" " 8 " "	37A-7

The data indicated that slight changes may still be taking place in TOC/TOC_o and BKI/M even at $16V_r$ (reactor volumes). However the following figures represent the percent change between $4V_r$ and $16V_r$ when a trend exists and the average spread of the four measurements, taken at S_5.

Parameter	% change $4V_r - 16V_r$	Avg. value ± spread
TOC/TOC_o	5	0.73 ± 0.03
$TTHMFP/TTHMFP_o$	0	0.73 ± 0.03
HBI	0	0.3 ± 0.1 mg/L
BKI/M	50	0.6 ± 0.2 mg/L
H_2O_2	0	0.5 ± 0.1 mg/L
$[O_3]g$, out	0	4.5 ± 0.1 mg/L
$[O_3]g$, in	0	16.4 ± 0 mg/L

Therefore the expected error in TOC/TOC_o and $TTHMFP/TTHMFP_o$ is a few percent, and in the oxidants, a few tenths of a milligram/L. Perhaps even more interesting is the variation in the calculated parameters E_c and E_u. This variation was found to be $E_c = 0.73 \pm 0.01$ and $E_u = 2.3 \pm 0.3$, or about ± 13%. The above estimate does not refer to the ability to reproduce numerical values on successive days, but merely to the ability to generate the same number throughout the day without changing any parametric settings.

Comparison of E_c and E_u (0.73 ± 0.01 and 2.3 ± 0.3 respectively,) for a utilized dose of 12.0 ± 0.2 mg/L) with those from the $1L_I1_{II}$ configuration from the last experiment (0.74 and 2.1 respectively, for a utilized dose of 12.1 mg/L) would seem to support the above statement, although it must be kept in mind that comparison of data between these sets may not be valid.

A similar analysis on the $1L_I$ configuration for this set (experiment nos. 37A-6 and 37A-7) gives

	S_4	S_7
TOC/TOC_o	0.80 ± 0.00	0.85 ± 0.01
$TTHMFP/TTHMFP_o$	0.79 ± 0.04	0.77 ± 0.01
HBI	1.2 ± 0.2	1.1 ± 0.1 mg/L
BKI/M	1.3 ± 0.0	1.4 ± 0.4 mg/L
H_2O_2	0.0 ± 0.0	0.03 ± 0.03 mg/L
$[O_3]g$, out	-	7.4 ± 0.0 mg/L

with the results that $E_c = 0.55 \pm 0.00$ and $E_u = 2.5 \pm 0.1$, compared with $E_c = 0.56$ and $E_u = 1.8$, where E_u is seen not to compare favorably with previous values.

Conclusions: Within the accuracy of the experiment $4V_r$ appears to be an adequate volume for equilibration. Values of E_c are probably good to a few percent while values of E_u can be expected to have an error spread of several tenths of an E_u unit.

SET D

DATE: 10/25/82

PURPOSE: (a) Comparison of delayed irradiation, particularly C/P configurations.

(b) Effect of additional contact time with ozone gas stream after irradiation.

CONFIGURATIONS:	D_{I-II}	Ozone only	37B-1
		$1L_{III}$	37B-2
		$1L_{II}$ $1L_{III}$	38A-3
		$1L_{II}$	38A-4
		$1L_{I}1L_{II}$	38B-5

Strictly speaking, two different types of C/P experiments were performed in this set. In DI (Delayed Irradiation) experiments, ozone contacting precedes photolysis, but the gas stream is left in intimate contact with the solution, whereas the C/P configuration as originally defined was intended to utilize only liquid-phase reactions by separating the gas and liquid phases before photolysis. Thus the terminology C/P will be reserved for those situations where a gas/liquid separation has taken place before irradiation, and the term DI will be used for the intermediate case. The distinctions between the reaction types become more of a matter of degree, and are summarized thus:

Reaction Type	Characteristics
CP	Contacting and photolysis simultaneous. Ozone and ozone/UV reactions taking place possibly in both liquid and gas phases.
DI	Fast ozonation reactions (ozone demand) can occur in vessels prior to photolysis. Ozone/UV reactions in gas and liquid occur once UV is added.
C/P	Ozonation reactions take place (ozone demand satisfied) after which ozone residual builds up. Gas and liquid phases are separated before photolysis takes place, so that only liquid phase reactions occur.

TABLE 10. EFFICIENCY DATA FOR SET C

Lamp Configuration (D_I - II)	Ozone Dose Utilized, D_u, mg/L	Capture Efficiency, E_c	Utilization Efficiency, E_u (b)(d)		$\frac{TTHMFP}{TTHMFP_o}$	
			S_4 (c)	S_7 (b)	S_4	S_7
0	5.9	0.36	4.2	3.2	0.75	0.81
III	5.4	0.32	4.1	0.7	0.78	0.96
II III	7.8	0.47	0.6	0.6	0.95	0.95
II	7.8	0.46	1.0	1.0	0.92	0.92
I II	8.6	0.53	0.8	0.6	0.93	0.95

(a) Ozone sparge gas concentration was 2% by weight. Liquid flow rate was 2.0 gpm.

(b) It may not be valid to compare $_u$ values with other data sets because of the flowmeter problems discussed in the text.

(c) Based on total ozone usage, D_u.

(d) E_u is evaluated at S_7.

Results of this set were disappointing but instructive. However, the THM values do not appear to be erratic, and it appears rather that due to the low ozone dose there simply was not much destruction of THMFP. The data are shown in Table 10.

Looking first at $1L_{II}$, it is seen that after a value of $E_u = 1.0$ is reached at S_4 no further THMFP decrease occurs in the last two TPR's. The ozone residual, R, leaving TPR_{II} where gas/liquid separation takes place is only 0.25 mg/L while the peroxide value, P, is 1.43 mg/L. At the exit, S_7, R = 0.19 and P = 1.48 so that no net change in oxidants has taken place. In other words, all the ozone in TPR_{II} is either removed in the gas phase or photolysed to peroxide, which then has no ozone with which to react. Consequently, although the FP destruction through reactors I and II is roughly comparable between Set C and Set D, FP reduction stops at that point in the latter.

Also interesting is the comparison between the ozone experiment and that of $1L_{III}$. While roughly comparable destruction of FP is seen at S_3, further treatment with ozone/UV in $1L_{III}$ results in a very great increase in FP. It will be recalled that the general shape of an ozonation batch run FP destruction curve is a sharp decrease in FP followed by an equally sharp rise, generally to $FP/FP_o > 1$, then a gradual diminishing of the ratio as more ozone is used, whereas ozone/UV experiments generally produce curves which rise immediately from $FP/FP_o = 1$ then fall more quickly than ozonation curves. This effect will be referred to later when more examples have been presented.

Comparing the two lamp experiments $1L_I 1L_{II}$ and $1L_{II} 1L_{III}$, one finds very similar results and an oxidant situation which is quite similar to that of $1L_{II}$ above, so that it is not surprising that little FP removal occurs.

Conclusions: The configurations such as D_{I-II} in which the only ozone available is a residual in the liquid fail to show any further removal after the point of gas/liquid separation, and in some cases ($1L_{III}$) even increase FP again. Hydrogen peroxide which formed is wasted if no ozone is present with which it can react. The additional ozone contact time is beneficial, even if there are no further lamps in the system as seen by comparison of $E_u(S_7)/E_u(S_4)$ values of Set B with those of Set D for similar configurations.

SETS E, F, G

These sets have not been analyzed in the manner of the

TABLE 11. EFFICIENCY DATA FOR DATA SET H(a)

Lamp Configuration (D_{I-IV})	Ozone Dose Utilized D_u, mg/L	Capture Efficiency, E_c	Utilization Efficiency, E_u		$\frac{TTHMFP}{TTHMFP_o}$	
			S_4(b)	S_7	S_4	S_7
0	8.8	0.46	1.8	3.2	.84	.72
I	15.7	0.82	1.0	1.5	.84	.76
I II	16.6	0.86	1.6	1.6	.74	.73
I II III	16.9	0.87	1.8	1.5	.70	.74
I II III IV	17.1	0.88	(d)	1.8	(d)	.69

(a) Ozone sparge gas concentration was 2% by weight. Liquid flow rate was 1.7 gpm.

(b) Based on total ozone usage, D_u.

(c) E_u is evaluated at S_7.

(d) TTHMFP not measured for this sampling point.

previous sets, due to the experimental difficulties associated with them, as described earlier in this report.

SET H

DATE: 11/8/82

PURPOSES: Comparison of one to four lamp data with that from other liquid flow rates.

CONFIGURATIONS:

$D_{I} - IV$	Ozone only	43B-1
	$1L_{I}$	43B-2
	$1L_{I}1L_{II}$	44A-3
	$1L_{I}1L_{II}1L_{III}$	44A-4
	$1L_{I}1L_{II}1L_{III}1L_{IV}$	44B-5

Results for Set H are given in Table 11. The jump in capture efficiency compared to previous sets is obvious and significant. Sets A-D were taken before the porous stainless steel sparger was installed, while data sets H - L were all obtained using the porous sparger.

Also notable in Table 11 is the difference in efficiencies at S_4 for 1, 2, and 3 lamps while the efficiencies at S_7 are roughly similar. It should be pointed out that E_u at S_4 for the two lamp and three lamp runs should be the same, so that the difference of 0.2 is probably within experimental error (see previous discussion of experimental error in determination of E_u). A similar value of E_u could probably be assumed for four lamps by reasoning that the first half of the four reactor sequence should be functioning quite similarly in all three cases. Thus, additional removal takes place in TPR_{III} and TPR_{IV} for one lamp, while no additional removal or even regeneration of FP occurs in following experiments. Capture efficiency, however, appears to increase slightly with number of lamps, although the exact amount of increase is comparable or below experimental error.

Conclusions: (a) Porous sparger gives significantly better capture efficiences than ring tube sparger. Little improvement noticed with more than two lamps at this ozone dose.

(b) Utilization efficiency is better at S_4 with two or more lamps than with one lamp. Much less difference at S_7.

SET I

DATE: 11/11/82

PURPOSES: To investigate the effect of pH

CONFIGURATIONS:	D_{I-IV}	Ozone only,	pH = 9.7	45A-1
		" "	pH = 6.9	45B-1
		" "	pH = 4.4	46A-1
		$1L_I$	pH = 9.7	45A-2
		"	pH = 6.9	45B-2
		"	pH = 4.4	46A-2

Comparison of the results for these runs is given in Table 12. For the ozonation experiments it is seen that elevated pH favors ozone capture, presumably due to the base-catalysed decomposition of ozone. However, it does not favor FP destruction, when judged from a utilization efficiency standpoint. This result could be extremely important, since it seems to imply that ozone is more effective against FP than is hydroxyl radical, but the effect of degree of conversion must be kept in mind. That is, it appears to be analogous to the ozone-ozone/UV system comparison(70), where in the initial stages of reaction, ozone appears to be more effective, but then FP/FP_o rises back up and FP destruction due to ozonation is overtaken by that of the ozone/UV system at larger treatment times. Once again a familiar theme arises: ozone/UV (or in this case, hydroxyl radical) appears initially to do more FP generation than FP destruction, compared to ozone, which seems at first to be removing FP, then later begins to generate it. This seems to agree with reports that water which has had the FP lowered by ozone, regenerates FP upon standing. One explanation might be that the ozone attacks the FP site, making that site temporarily unavailable to the chlorinating agent. The unstable ozone intermediate eventually breaks down, yielding one or two carbonyl groups, which contribute as much or more to the total FP than did the original site. In addition, this breakdown may produce hydrogen peroxide as a by-product, thus initiating the free radical reaction. Repeated occurrence of this process eventually converts all FP sites, but the rate of the process is controlled primarily by the rate

TABLE 12. EFFICIENCY DATA FOR SET I: EFFECT OF pH[(a)]

Lamp Config. (D_{I-IV})	pH Influent	pH Effluent	Ozone Dose Utilized,	Capture Efficiency, E_c	Utilization Efficiency, E_u[(b)]	$\frac{TTHMFP}{TTHMFP_o}$ S_4	$\frac{TTHMFP}{TTHMFP_o}$ S_7
0	9.7	9.5	18.3	0.78	1.8	0.72	0.67
0	6.7	7.3	9.4	0.40	2.4	0.81	0.77
0	4.4	4.9	7.3	0.31	3.8	0.75	0.72
I	9.7	9.5	19.4	0.83	1.4	0.69	0.72
I	6.7	8.0	18.6	0.79	0.8	0.83	0.85
I	4.4	4.8	15.6	0.66	1.3	0.80	0.79

(a) Ozone sparge gas 2% by weight, 4.34 SLM^{-1}, giving D = 23.4 mg/L. Liquid flow rate was 1.4 gpm.

(b) Based on total utilized ozone dose, D_u.

at which sites become reactive to ozone, hence the overall slow rate of FP destruction. Hydroxyl radical, on the other hand, immediately adds to aliphatic unsaturation and aromatic rings to produce the type of site which Rook(71) found was the most efficient producer of trihalomethanes. Again, all potential sites must be destroyed before the FP goes to zero, but since hydroxyl radical will react with practically anything, this happens much more rapidly than with the ozonation reaction.

The ozone/UV experiments run in this set demonstrated capture efficiencies which also increased with pH, although much less drastically than the ozonation experiments. This increase may indeed be due to the increased capture of ozone before photolysis could occur, and it can be seen from the oxidant data, presented in Table 13, that the peroxide values increase with decreasing pH. Whether this represents less peroxide formed or merely less mutual O_3/H_2O_2 decomposition is not known. Interpretation is made more difficult by the fact that the $1L_I$/pH 6.7 numbers in both Table 12 and Table 13 appear somewhat anomolous, and are not in very good agreement with those for $1L_I$/pH7 in Table 10, although there is a difference in liquid flow rate.

Conclusions: The pH of the solution has a marked affect on both ozone capture and FP removal during ozonation, the former increasing with pH while the latter decreases when viewed on a "per mg/L of ozone" basis. Ozone capture in the one lamp system was enhanced slightly by increased pH, probably because of increasing basic decomposition before photolysis could occur. No peroxide was found in the ozone/UV experiments at higher pH, but utilization efficiencies at high and low pH values were roughly equal. (Compare with ozone photolysis in dilute acetic acid, sodium acetate solution at various pH, Figure 5-4).

SET J:

DATE: 11/15/82

PURPOSES: (a) To provide additional information about the CP vs. C/P configurations.

(b) To compare with earlier C/P data for a faster flow rate.

CONFIGURATIONS: D_{I-II} $1L_I$ 46B-1

D_{I-II} $1L_{III}$ 46B-2

TABLE 13. OXIDANT DATA FOR DATA SET I

Lamp Config. (D_{I-IV})	pH	D_u	Ozone Concentration, mg/L		Hydrogen Peroxide Concentration, mg/L		Total Oxidant[a] Concentration, mg/L	
			S_4	S_7	S_4	S_7	S_4	S_7
0	9.7	18.3	nd	nd	nd	nd	0.1	nd
0	6.7	9.4	2.6	2.1	nd	nd	2.9	2.0
0	4.4	7.3	3.0	2.5	nd	nd	3.8	3.4
I	9.7	19.4	0.6	0.3	nd	nd	0.2	nd
I	6.7	18.6	0.05	nd	0.9	0.5	1.4	0.8
I	4.4	15.6	2.1	1.5	2.6	2.3	4.8	4.0

(a) As ozone

TABLE 14. EFFICIENCY DATA FOR SET J(a)

Lamp Configuration $(D_{I - II})$	Ozone Dose Utilized, D_u, mg/L	Capture Efficiency E_c	Utilization(b) Efficiency, E_u		TTHMFP/$TTHMFP_o$			
			S_4	S_7	S_3	S_4	S_6	S_7
I	21.7	0.67	0.51	0.92	(c)	0.89	(c)	0.80
III	10.1	0.31	1.9	0.89	0.80	0.81	0.93	0.91

(a) Ozone concentration in sparge gas was 2% by weight, 4.3 SLM^{-1}, liquid flow rate was 1 gpm, giving D = 32.5 mg/L.

(b) Based on D_u.

(c) Not measured.

TABLE 15. OXIDANT DATA FOR SET J

Lamp Configuration (D_I - II)	D_u	Oxidant (method)	Concentration, mg/L, at S_3	S_4	S_6	S_7
I	21.7	R = ozone (HBI)	0.4	0.2	0.2	0.1
I	"	P = peroxide(TiIV)	2.4	1.9	1.8	1.7
I	"	O_t = total (BKI/M)	1.9	2.3	2.1	2.0
IV	10.1	R = ozone (HBI)	1.7	2.8	0.3	0.3
IV	"	P = peroxide(T:IV)	0	0	1.7	1.8
IV	"	O_t = total (BKI/M)	2.1	4.7	2.2	2.2

Sampling for oxidants was performed at all four sampling points to provide a better oxidant profile throughout the system. Calculated efficiencies for Set J are given in Table 14. Capture efficiency for $D_{I - II}$ $1L_{I}$ is about double that for $D_{I - IV}$ $1L_{III}$. Both are in line with previous values. In the $1L_{I}$ experiment, FP destruction is seen to continue through TPR_{III} and TPR_{IV}, while in $1L_{III}$ (the C/P experiment) regeneration of FP takes place until almost all removal (by ozone-only, in TPR_{I} and TPR_{II}) has been reversed. Oxidant data in Table 15 indicate that this regeneration occurs upon photolysis of 2.8 - 0.3 = 2.5 mg/L (52 μM) of ozone to produce 1.7 mg/L (50 μM) of hydrogen peroxide. Considering the efficiencies experienced so far, it seems unlikely that this process was responsible for the regeneration of FP, and the question is raised whether photolysis of the ozone adduct of FP sites is responsible for the regeneration. This process would be the photocatalysed equivalent of the process discussed in conjunction with the previous data set. In experiment 37B-2 ($D_{I - II}$ $1L_{III}$) a similar situation was encountered, where photolysis of 1.9 mg/L (40 μM) ozone gave 0.9 mg/L (26 μM) H_2O_2 while regenerating the FP value from 22% removal to 4% removal.

Conclusions:

(a) The configuration in which ozone continues to be in contact with the solution after irradiation ($D_{I - IV}$) gives significantly greater removal than that where a gas liquid separation ($D_{I - II}$) is performed. This appears to be due to one or more of several causes:

(1) Ozone-adduct photolysis causes regeneration of formation potential removed by ozone reaction.

(2) Insufficient ozone residual remains in the solution after gas-liquid separation to allow ozone/UV reaction to the extent possible when the liquid is irradiated while in the presence of the ozone gas stream.

(3) Increased removal in the $D_{I - IV}$ case may actually be due simply to ozonation of FP sites after the ozone/UV process has ceased.

(b) Capture efficiency is considerably higher in $D_{I - IV}$ configurations than in $D_{I - II}$ configurations.

TABLE 16. EFFICIENCY DATA FOR SET K(a)

Lamp Config. (D_{I-IV})	Sparge Gas Ozone Concentration, Wt.%	Ozone Dose Utilized, D_u, mg/L	Capture Efficiency, E_u	Utilization Efficiency, E_u		$\frac{TTHMFP}{TTHMFP}$	
				S_4	S_7	S_4	S_7
I	2	18.5	0.79	0.49	1.0	0.91	0.81
I II	2	20.1	0.84	0.80	1.3	0.84	0.73
I II	3	35.5	0.84	0.70	1.0	0.75	0.63
I	1	9.4	0.80	0.96	1.3	0.91	0.88
I	0.5	4.8	0.81	1.7	1.0	0.92	0.95

(a) Liquid flow rate was 1.4 gpm; gas flow rate 4.34 SLM^{-1}.

TABLE 17. EFFICIENCY DATA FOR SET L[a]

Lamp Config. (D_{I-IV})	Ozone Concentration in Sparge Gas,	Ozone Dose Utilized, D_u, mg/L	Capture Efficiency, E_c	Utilization Efficiency, E_u	$\frac{TTHMFP}{TTHMFP_o}$	
					S_4	S_7
I	4	49.3	0.75	1.2	0.51	0.42
I II	4	53.3	0.81	1.3	0.41	0.31
I II III	4	53.6	0.82	1.3	0.38	0.28
I II	3	39.3	0.80	1.7	0.50	0.35
I II III	3	40.0	0.82	1.6	0.48	0.37
I II	2	26.5	0.81	1.9	0.63	0.49
I II III	2	27.2	0.82	1.7	0.63	0.54

(a) Liquid flow rate = 1 gpm, gas flow rate 4.34 SLM^{-1}.

SETS K AND L

DATES: 11/18/82 and 11/19/82

PURPOSES: (a) To examine the effect of ozone concentration in the sparge gas.

(b) To collect more data at other flow rates.

(c) To obtain points at higher values of D_u.

CONFIGURATIONS:	SET K:	D_I - IV	$1L_I$	2% ozone	47B-1
			$1L_I1L_{II}$	"	47B-2
			$1L_I1L_{II}$	3% ozone	48A-3
			$1L_I$	1% ozone	48A-4
			$1L_I$	0.5% ozone	48B-5
	SET L:	D_I - IV	$1L_I$	4% ozone	49A-1
			$1L_I1L_{II}$	"	49A-2
			$1L_I1L_{II}L_{III}$	"	49A-3
			$1L_I1L_{II}$	3% ozone	49A-4
			$1L_I1L_{II}1L_{III}$	"	49B-5
			$1L_I1L_{II}$	2% ozone	49B-6
			$1L_I1L_{II}1L_{III}$	"	49B-7

Efficiency data is shown for Set K in Table 16 and for Set L in Table 17. These sets are analyzed together because of their similarity in both purpose and result. It can be seen that the increase from 0.5% to 2% ozone for $1L_I$, and from 2% to 4% for $1L_I1L_{II}$ and $1L_I1L_{II}1L_{III}$ causes very little change in capture efficiency, within the probable error of the experiment. This effect can also be seen in Tables 8 and 11, for other sets of conditions. Only in the case of one lamp and high ozone concentration (4%) is a drop in efficiency noticed. Furthermore only small differences are seen in going from one to three lamps, so that the use of a greater number would not be justified on a capture basis.

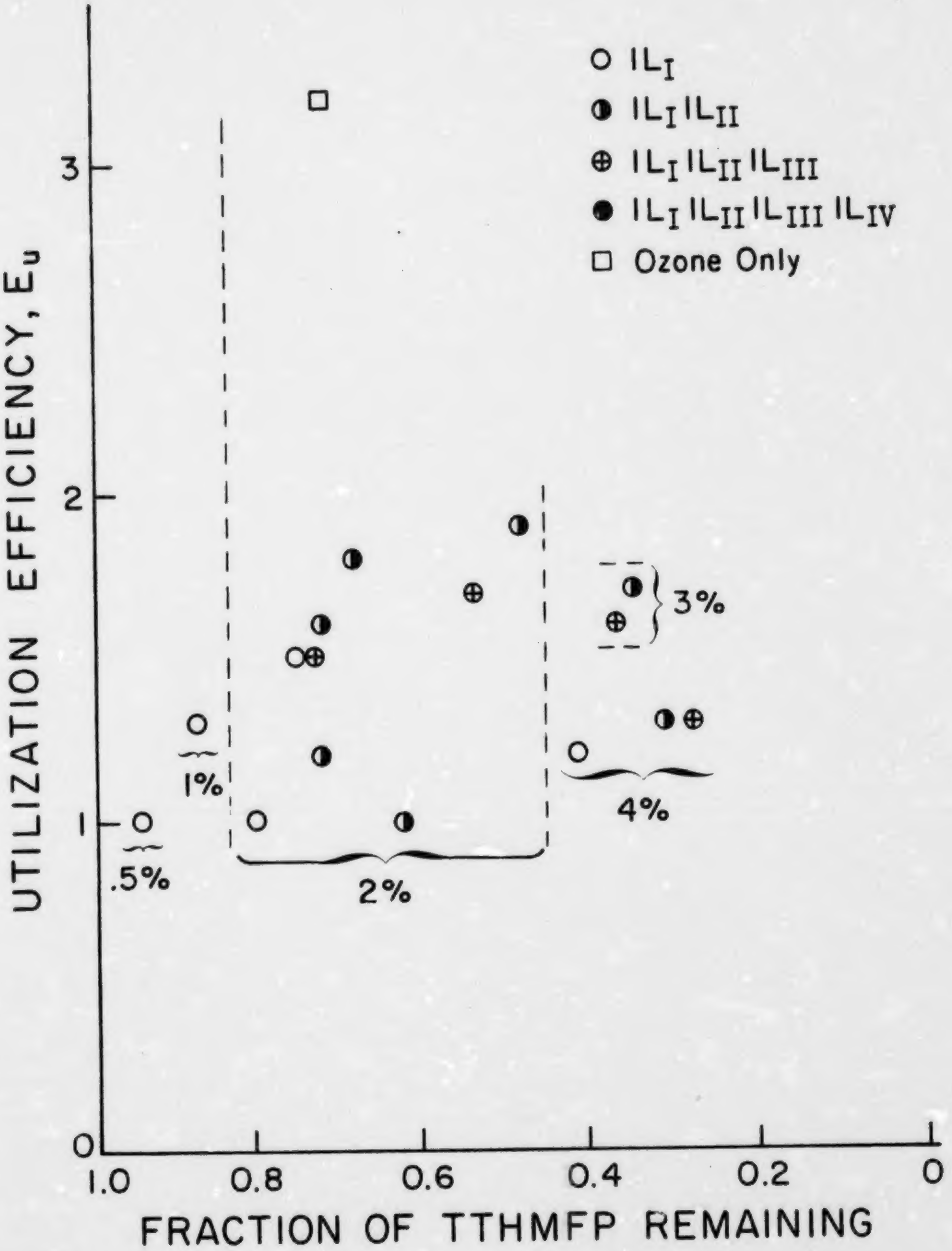

Figure 23. Utilization efficiencies in TPR experiments.

The situation with regard to utilization efficiency is considerably less clear, due to the uncertainty and variability of those numbers. Shown in Figure 23 is a plot of E_u versus fraction of formation potential remaining for Sets H, K and L. The other Sets prior to H are omitted from this plot for reasons of comparability, discussed earlier. Set I is omitted because of the pH variation and Set J because of the D_{I-II} configuration. The one ozone-only point from those sets is included for comparison. This curve has perhaps a fundamental basis, which is rationalized as follows. At the beginning of the reaction the rate of destruction and thus E_u removal is slow because precursor is being regenerated as it is being destroyed. In the middle stages, the "material" (sites) from which precursor sites are formed are being depleted, so the overall FP removal rate is faster. At the end of the reaction, there are fewer precursor sites, so that it becomes more difficult for active species to find them as in any reaction step which is first order in substrate. Thus the shape of the plot of the function E_u versus F/F_o is lower at both ends with a maximum in the middle.

In all series in Tables 16 and 17 except the 0.5% run where two or more ozone concentrations have been used with the same number of lamps, the lowest ozone concentration has resulted in the highest utilization efficiency. This is in accordance with the results found for the TCSTR in the previous section. The only explanation which can presently be offered is that at high dose rates more unreacted ozone is present to compete with substrate for hydroxyl radical, resulting in lowered efficiency by not only scavenging hydroxyl radical but also by destroying ozone which could produce hydroxyl radical.

Conclusions: (a) Except at higher ozone concentrations (4%) the number of lamps has very little effect on the capture efficiency.

(b) There may be a weak correlation between E_u and the extent of FP removal, with a maximum in E_u at a value of FP/FP_o of 0.5 - 0.6.

(c) The utilization efficiency is greatest in the order 1% > 2% > 3% > 4% ozone for a given combination of lamps.

Summary of Results--

In this section, the conclusions from inspection of the individual data sets will be summarized, and an attempt will be

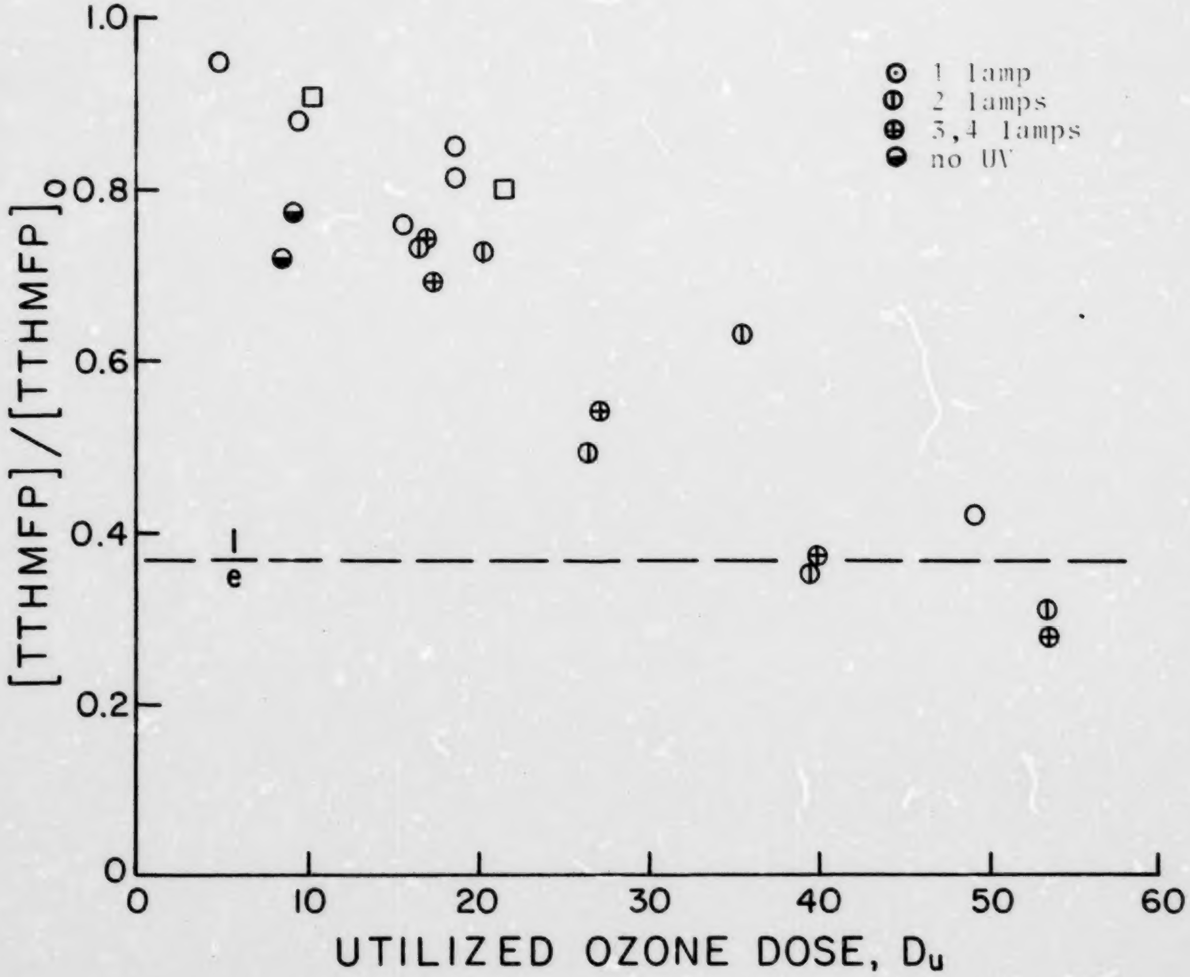

Figure 24. Formation potential removal in TPR experiments.

made to resolve conflicting conclusions. It has already been seen that even with exclusion of data sets known to be questionable, trends are difficult to predict and even more difficult to quantify, because of the considerable scatter in the data.

Shown in Figure 24 is the fraction of FP remaining versus the utilized ozone dose, D_u. It appears from this figure that in the TPR's 40 mg/L of ozone is required to reduce FP to 1/e of its original value for this reconstituted lake water. This is to be compared with a value of 30 mg/L found previously for the TCSTR. The reasons for this difference are unknown, but one possibility is a catalytic effect for the porous stainless steel spargers. One clue to the difference in behavior may be found in the amount of hydrogen peroxide found in the systems. In many TCSTR ozone/UV experiments there was no hydrogen peroxide found, and in the others, a maximum of 0.5 mg/L was present. In the TPR experiments 0-1 mg/L was frequently found before the porous spargers were installed, compared to 1-2 mg/L afterward. Hydraulic retention times in the TCSTR were 5, 10, and 15 minutes, compared with 8-13 minutes in the entire 4 TPR bank. However, peroxide would find more free ozone with which to react in the TCSTR to form more hydroxyl radical. Since this peroxide is not only generated directly but is also a by-product of the reaction between hydroxyl radical and TOC, this "bonus" may not be as well utilized in the TPR system where ozone replenishment of the solution is not so facile.

The results of the TPR parametric studies can thus be summarized as follows:

1) The porous stainless steel sparger increased ozone capture efficiency from 34 ± 2% to 43 ± 3% when used for ozonation, and from 67.7 ± 7.1% (15 values) to 82.5 ± 3.4% (23 values) in ozone/UV configurations.

2) Because of erratic results obtained after its installation, the porous stainless steel sparger should be checked for catalytic ozone decomposition effects and cleaned if necessary before use.

3) At ozone concentrations of 3% or below, only one or two percent of additional ozone capture results from the addition of each lamp in excess of two, provided the porous stainless steel sparger is used.

4) Delayed irradiation (DI), is seen to be about as efficient as CP mode for two lamps, and slightly more efficient in both

capture and utilization with one lamp than in configurations in which irradiation is begun in the first TPR.

5) The extreme case of delayed irradiation, C/P, in which a gas/liquid separation is performed before irradiation, is considerably less favorable than either DI or CP, sometimes even exhibiting a negative effect.

6) Passage of four reactor volumes of equilibrated liquid appears to have provided adequate equilibration time for the TPR experiments. Under these conditions, however, one can expect errors in the values of E_u measuring several tenths of an E_u unit.

7) Quite significant increase in FP removal can take place in TPR_{III} and TPR_{IV}, even though all irradiation takes place in I and II, provided the solution is maintained in contact with the ozone-containing gas stream. This is presumed to be the result of ozone-peroxide reactions and further direct reaction of ozone.

8) During ozonation, elevated pH of the solution enhances ozone capture and decreases utilization efficiency. In the ozone/UV system, elevated pH slightly enhanced ozone capture, but utilization efficiencies were roughly equal at high and low pH.

9) As in the case of the TCSTR, lower ozone dose rates (concentrations) favor greater utilization efficiencies.

10) One lamp each in columns I and II gives better utilization efficiency than one lamp in either column. Increasing to three lamps does not further increase E_u.

11) The highest values of E_u approach 2, meaning 2% of the formation potential destroyed for each mg/L of ozone. In other words, removal of 63% of the TTHMFP requires at least 31 mg/L of ozone. From Figure 6-14 that value is estimated to be closer to 40 mg/L, compared to 30 mg/L in the TCSTR.

12) Values of E_u for ozonation ranged up to 4 but FP removal was not complete enough to accomplish the goals of this project.

SUMMARY OF PARAMETRIC STUDIES

Before proceeding to the results of pilot studies at Longview, Texas, it may be helpful to the reader to briefly summarize the conclusions of the previous three subsections.

1) The TCSTR appears to perform better than the TPR's, requiring 30 mg/L to reach $FP/FP_o = 1/e$ compared with 40 mg/L for the TPR's.

2) In both reactors, the lowest dose rate which would effect the desired removal was also the most efficient.

3) The optimum number of lamps in the TCSTR was 2.4, while in the TPR it was 2 ($1L_I 1L_{II}$) in the $D_{I - IV}$ configuration.

4) Elevated pH during ozonation increased capture efficiency and reduced utilization efficiency. In the ozone/UV system, elevated pH enhanced ozone capture slightly but utilization efficiencies were roughly equal at low and high pH.

5) Utilization efficiencies are considerably higher for ozonation reactions than for ozone/UV, but the desired levels of removal cannot be achieved. This probably accounts for the increased capture efficiency of $1L_{II}$ over $1L_I$.

Comparison of the ozone and ozone/UV TPR results show that although ozone capture is considerably less with ozone than with ozone/UV, the utilization efficiency, that is, the amount of FP destruction per amount of ozone used, was much greater, being in the range of $E_u = 2 - 4$ for ozone as opposed to 1 - 2 for ozone/UV. The feature of the TPR experiments which allowed the recognition of the probable roles of the two processes was the ability to sample the reaction mixture, then perform another unit process on it and sample again. The utility of this feature is illustrated in a general way in the data in Table 18, where the ratio of values of E_u at S_5 and S_3 have been tabulated. Figure 10 shows where these sampling points are located with respect to the various TPR's. The ratio $E_u(S_7)/E_u(S_4)$ is greater than 1 in 80% of all cases in the $D_{I - IV}$ column of Table 18 where no lamps appear in TPR's III and IV. In some of these cases significant ozone and/or hydrogen peroxide concentrations were found going into TPR_{III}, but their concentrations varied widely and the tendency to remain or disappear was erratic. However, in the $D_{I - II}$ experiments, although they too contained hydrogen peroxide and ozone in the influent to TPR's III and IV, 86% of the ratios $E_u(S_7/E_u(S_4)$ were ≤ 1.0, indicating no further decrease or even an increase in FP in TPR_{III} and TPR_{IV}. Furthermore, the largest decreases were in the $D_{I - II}$ $1L_{III}$ experiments where very little ozone is present in TPR_{III}. The above data, the ratio of E_u for ozonation compared to ozone/UV experiments, and inspection of

TABLE 18. EFFECT OF SECOND PAIR OF TPR'S ON OZONE UTILIZATION EFFICIENCY.

Percent Ozone in Sparge Gas	Nbr. of Lamps	D_I - IV			D_I - II		
		D_u	$E_u(S_7)/E_u(S_4)$	Data Set[(a)]	D_u	$E_u(S_7)/E_u(S_4)$	Data Set[(a)]
4	1	49.3	1.2	L			
	2	53.3	1.2	L			
	3	53.6	1.1	L			
3	2	35.5	1.4	K			
	2	39.3	1.3	L			
	3	40.0	1.2	L			
	0	6.2	0.93	B	5.9	0.76	D
		8.8	1.8	H			
		20.3	0	A			
	1	9.0	0.93-1.05	C	5.4	(0.17)	J (III)
		9.4	2.6	B	7.8	(1.0)	J (II)
		11.1	(1.7)	B (II)	10.1	(0.47)	J (III)
		15.7	1.5	H			
		18.5	2.0	K	21.7	1.8	J
		28.2	1.0	A			
2	2	10.4	(9.0)	B (21)	7.8	(1.0)	D (II,III)
		12.0	0.89	C	8.6	0.75	D
		12.1	1.8	B			
		16.6	1.0	H			
		20.1	1.6	K			
		26.5	1.4	L			
		30.1	1.2	A			
		38.8	(3.7)	A (II,IV)			
	3	16.9	0.83	H			
		27.2	1.2	L			
		32.6	1.4	A			
	4	17.1	1	H			
		38.9	1.9	A			
1	1	9.4	1.4	K			
0.5	1	4.8	0.59	K			

(a) And lamp configuration, if different from one lamp per reactor, starting with TPR_I.

the data from the individual experiments has led to the following hypothesis about what is occurring in this system.

The first effect of ozonation is to immediately and efficiently react with precursor sites. This is seen in Figure 12 of this report and in Figure 26 of the final report EPA-600/2-80-110 from project R-804640(1). In the former, 20% of the formation potential, about 1/4 μmole/L of FP sites, is lost in 2.5 minutes, or at an ozone dose of 3.5 mg/L (70 μM) ozone. In the latter example given above, an ozone dose of 2.1 mg/L (40 μM) after 5 minutes eliminated 35% of the formation potential (about 1 μM sites) in water with a DOC of about 12 mg/L (1 mM). Selectivity in the latter experiment was such that about 4% of the ozone molecules successfully killed precursor sites which only represented 0.1% of the carbon atoms in the humic/fulvic material.

The effect of the "ozone/UV reaction", that is, of hydroxyl radical, is to hydroxylate aromatic rings and unsaturated carbon-carbon bonds, and probably, by hydrogen abstraction in the presence of water, even aliphatic systems. This reaction produces precursors by conversion to m-dihydroxybenzene moieties as well as other precursor functionalities, as long as the raw materials are present for that conversion. The ultimate fate of the ozone/FP intermediate, however, can vary. Upon further reaction it may collapse to carbonyl compounds, as in the case of ozonides. In aqueous solution these reactions often lead to the production of hydrogen peroxide. This collapse is consistent with various reports that upon standing or distribution ozonated water may regain part of its formation potential. Upon photolysis ($D_{I-II}\,{}^{1}L_{III}$) it appears to undergo a similar fate, either directly or by further ozone photolysis to free radical products which then have the effect of the "ozone/UV" system. Finally, ozone which undergoes base-catalysed or peroxide-catalysed decomposition enters the free radical branch of the reaction, via hydroxyl radical, as shown by Hoigne and Bader(39) and Staehelin and Hoigne(35), and contribute precursor by hydroxylation and abstraction mechanisms.

Earlier in the project it was hoped that the specificity of the ozone/UV process could be manipulated by control of process variables such as photolysis wavelength. This has not proven to be the case, primarily because ozone photolysis at 254 nm leads directly to hydrogen peroxide which in turn reacts with ozone to produce hydroxyl radical, one of the most nonspecific species known with respect to its reactions with organic compounds. In addition, much lower absorption coefficients and quantum yields at longer wavelengths , coupled with the fact that most O(^{3}P) reactions with organics resemble hydroxyl radical reactions(30) make 0(^{3}P) production impractical.

Specificity apparently has been found however in the form of ozonation itself, provided the FP generation reactions could be suppressed. Although the C/P configurations did not work well in the parametric studies, the DI configurations in which ozone was contacted prior to photolysis then left in contact during the photolysis step, appeared promising. It was decided to begin pilot studies on CP and DI configurations using the TCSTR already in place, while the TPR region was converted to four six-foot TPR's, each with its own porous stainless steel sparger.

RESULTS OF PILOT STUDIES AT LONGVIEW, TEXAS

The pilot plant was in almost continuous operation from April 4, 1983 to November 30, 1983, a period of eight months. During that time the plant was shut down only to correct malfunctions or reconfigure a particular section. During this period, conditions have been changed several times to observe the effects on treatment of actual presed and clarifier water from the Sabine River Water Treatment Plant (SRWTP) and to test hypotheses about the treatment process. Although for clarity this data is presented in this report as separate experiments, it represents continuous operation during 179 days of the 229-day period (78%). It should be recalled from the experimental section that "presed" water has been treated with alum and some permanganate, then settled in a clarifier. The pH of this water is usually maintained around 4.7 - 5.0. "Clarifier" water has been treated with lime and a small amount of powdered activated carbon, then settled in a clarifier. The pH of this water is generally around 9. Both feedwaters are filtered through a mixed-media filter in the "Waterboy" before use in the pilot plant.

The format used below is that of individual experiments, in order to facilitate discussion of the results, even though the pilot plant was in almost continuous operation.

Throughout this discussion, the symbol F/F_o will be used to represent the TTHMFP after some specified treatment, divided by that before the treatment. The abbreviation FP will be used for formation potential when used in a general way. Experiments A - E were aborted for a variety of experimental reasons.

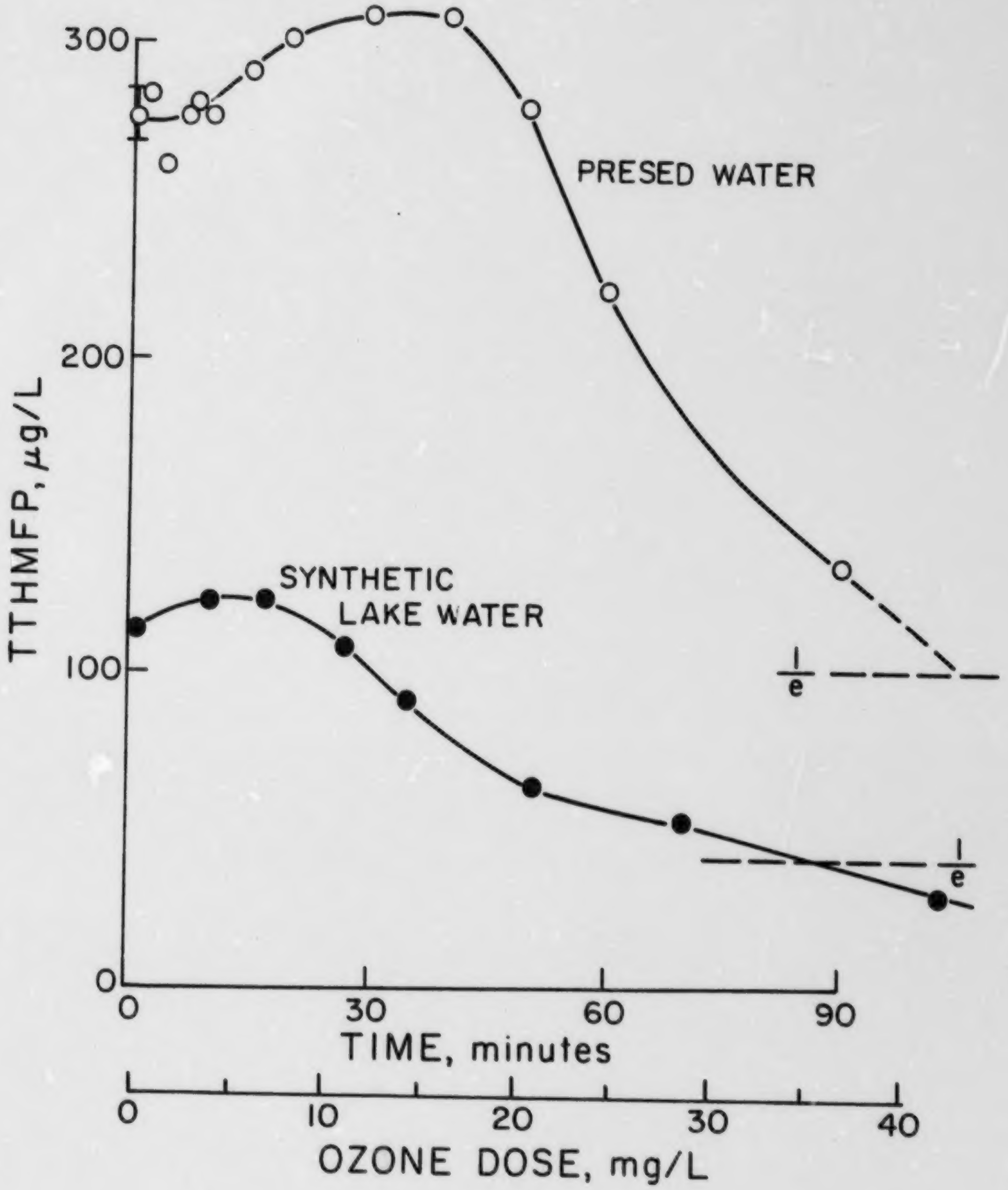

Figure 25. THMFP removal using simultaneous contacting and photolysis in CSTR.

Experiment F

This was a batch experiment run on presed water using simultaneous contacting of 0.41 mg/L-min of ozone and irradiation with two lamps (CP mode, approximately 10.6 W/80L = 0.13 W/L). A treatment time of 87 minutes (ozone dose = 35.7 mg/L) was required to reduce TTHMFP to 50% of its original value, and a dose of about 48 mg/L would have been required to reach 101 mg/L TTHMFP (removal to 1/e of the original value). Shown with this data for comparison in Figure 25 is a batch run performed previously on the synthetic lake water. The ozone dose scale applies to both experiments while the time scale applies only to the run using presed water. Although quantitatively quite different, some similarity is seen between the curves. An ozone dose D_1 of 36 mg/L for removal of FP to 1/e was required in the synthetic lake water experiment (in which the TOC was 2.1 mg/L compared to around 3 mg/L in the presed water), indicating that presed water was somewhat more difficult to treat than the synthetic lake water.

Experiment G

Considerable clouding of the lamp wells in the TCSTR was noticed during earlier series of flow runs. To investigate this problem further, a run was made on presed water in the flow CP mode with two lamps and an ozone dose of 10.8 mg/L. Samples were taken each morning for one week and analysed at the end of the experiment for TTHMFP. Shown in Figure 26 is the normalized TTHMFP, that is, FP in the trailer effluent divided by that in the influent. After three or four days at this dose rate (10.8 mg/L) performance begins to change, probably shifting from ozone/UV to ozonation behavior. The dotted line in Figure 26 represents the value of F/F_o which is predicted from the batch data shown in Figure 25 for ozone/UV.

At this point due to the lamp well coating problem and to the appearance of a pink color in the effluent (presumably permanganate), the trailer was switched from feedwater obtained from the presedimentation basin (pH = 4.7) to clarifier water, which has a pH of around 9. The lamp wells were cleaned and the trailer was put back into operation at an even higher ozone dose rate in the flow CP mode with the following conditions:

water flow = 2.5 gal/min
ozone concentration = 1.7%
ozone flow = 14.3 SCFH - 1.0 L/min to monitor
2 lamps in TPR = 1.8 W/L

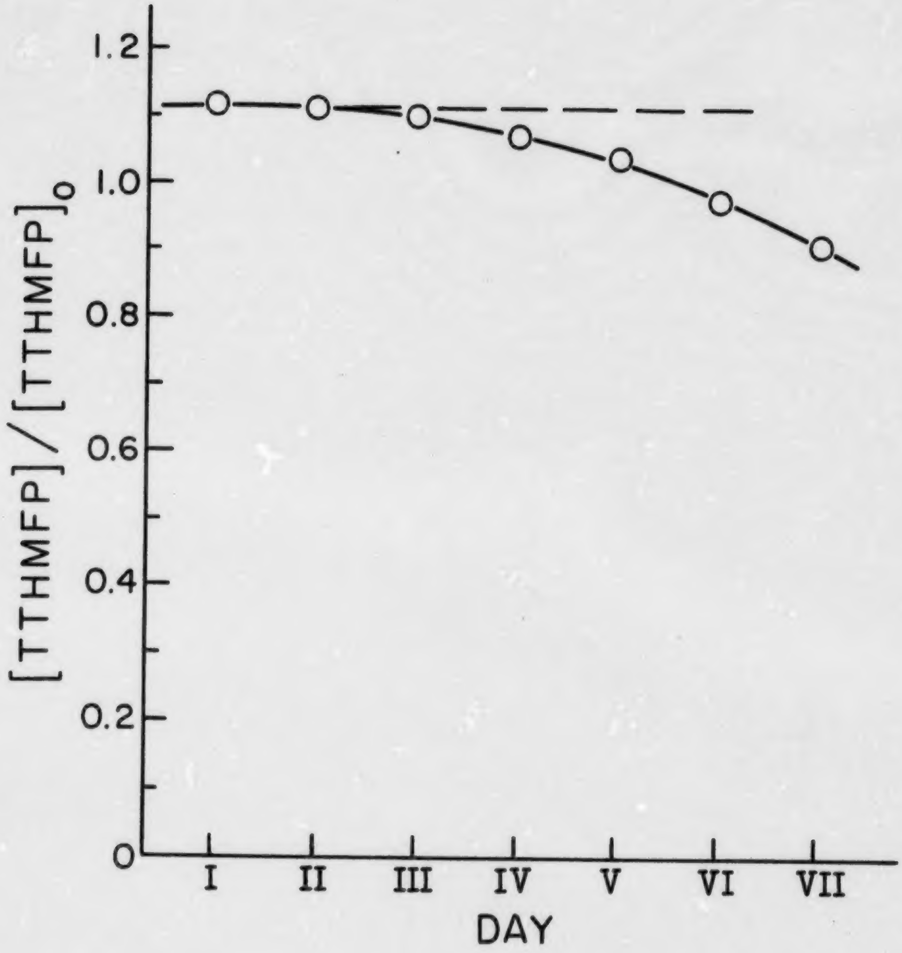

Figure 26. Change of normalized TTHMFP (C/C_o) with time during lamp well coating experiment. Dotted line is value predicted from Figure 25.

Under these conditions the ozone dose is 16.0 mg/L. The system was run for four days under those conditions with the following results:

DAY	TTHMFP,IN mg/L	TTHMFP, OUT mg/L	F/F_o
1	387.1 ± 16.0	298.2 ± 12.2	0.77 ± 0.03
2	346.4 ± 0.9	264.3 ± 13.2	0.76 ± 0.04
3	410.9 ± 3.5	262.7 ± 15.3	0.64 ± 0.04
4	391.5 ± 13.0	316.0 ± 7.4	0.81 ± 0.05

A similar ozone dose used in the CP mode on presed water resulted in a F/F_o of 1.11.

When the quartz wells were removed after this experiment, considerably less coating had formed than with presed water, but the reason for the variation in treatment efficiency during the last three days is not known. Lamp wells were cleaned before continuing.

Experiment H

This experiment was designed to investigate TTHMFP reduction in the DI mode as a function of ozone dose. This was accomplished by holding the gas flow constant and turning up the ozone generator power by one unit each day. After this experiment, each set of conditions was allowed to equilibrate for one day to avoid transient conditions such as peroxide buildup which might form initially then subside with time. Samples were taken of the water as it entered the TCSTR (IN), between the TCSTR and TPR (MID), and after the TPR (OUT). The measured values are tabulated in Table 19 and the normalized values are plotted in Figure 27. From the above discussion it is seen that the sample labeled MID corresponds to ozone-only (although with a short contact time) while that labeled OUT is the actual DI sample, a small but seemingly real difference is seen between MID and OUT, but diminishes beginning with the point at about D = 10 mg/L. At this point, the operator reported noticing the appearance of the buildup on the lamp wells as indicated by a color change of the light.

TABLE 19: DATA FROM EXPERIMENT H

Day	Utilized ozone dose, mg/L	TTHMFP, μg/L[a] IN	MID	OUT
1	2.0	365 ± 6	308 ± 14	304 ± 8
2	3.3	352 ± 8	290 ± 7	273 ± 13
3	5.2	(290 ± 2)[b]	308 ± 6	294 ± 6
4	7.5	370 ± 13	317 ± 9	290 ± 2
5	9.9	363 ± 7	290 ± 3	278 ± 10
6	11.6	356 ± 3	260 ± 1	260 ± 10
7	12.9	383 ± 4	239 ± 2	250 ± 10
8	13.6	384 ± 5	228 ± 2	225 ± 2

(a) IN represents influent to TCSTR, MID is taken between TCSTR and TPR, and OUT is after the TPR.

(b) Value thought to be in error.

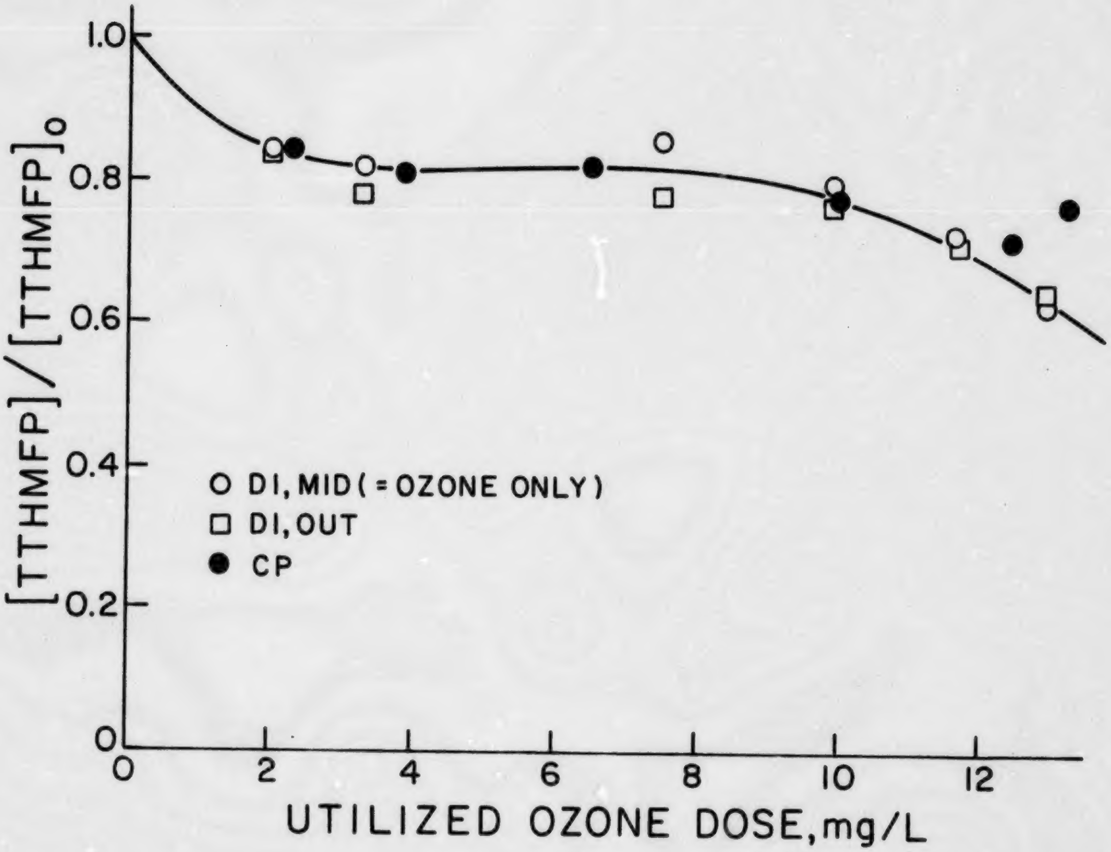

Figure 27. Effect of ozone dose on TTHMFP removal in DI and CP modes.

This data appears more promising than that indicated by previous Figures in terms of projected dose for TTHMFP removal to 1/e. using either ozone or ozone/UV. It is possible that ozone/UV would be even more effective in the absence of the lamp coating buildup. In any case it appears that not only is buildup slower with clarified water than with presed water in CP mode, but that ozone utilization is better as well.

Experiment J

Also shown in Figure 27 are the results of experiment J, which was run in CP mode, again making a daily incremental increase in the generator power. The data is seen to very closely follow that of the DI configurations, up to a dose of about 8 mg/L, where the plot of the latter turns downward. When experiment J was discontinued, the lamp wells were removed, inspected, and cleaned. The coating was present but not as severe as before, so that the extent to which it affected the last few points (dosages of 12.4 and 13.2 mg/L) is not certain. The rerunning of a few points with higher ozone concentrations was indicated, to insure that performance was not seriously affected by lamp well coating.

Experiment K.

This is a rerun of Experiment H (clarifier water, DI mode) with the modification that smaller increments of ozone dose are used. The object of this experiment was to get greater resolution of the treatment curve in the region of lower ozone dose, in order to see any advantage which might be gained by the DI configuration. Since the pH of the incoming water is around 9 ($t_{1/2}$ of ozone = 200 seconds) it is necessary to stay close to the ozone demand level of the water to avoid an ozone residual which would then be photolysed or suffer other secondary reactions, if the strategy of maximization of direct ozonation reactions is to be successful. When the data are superimposed on those from Experiment H (Figure 25), where it is seen that there is essentially no difference between the two sets of results when expressed as fraction of TTHMFP remaining, $TTHMFP/TTHMFP_0 = F/F_0$. Thus, under these conditions precursor production appears to equal destruction in the region from 2 to 9 mg/L of ozone dose.

Experiment L

This experiment was run on clarifier water in the tubular reactors with simultaneous contacting and photolysis and is the first test of the TPR's after installation of the porous frit spargers. The system could only be investigated at low dose rate due to the limited amount of gas which could be forced through the frits with the available pressure from the ozone generator. Since low dose rate does not appear to be effective when the free-radical mode is used, this experiment was discontinued after only a few days, and the same conditions used with presed water in Experiment P. Less than 10% removal of TTHMFP was seen in Experiment L.

Experiment M.

This was a TPR "almost-batch" ozonation experiment run on clarifier water which had been acidified to 5.6 x 10^{-2} N with sulfuric acid (pH 1-2). Flow rate through the 28 liter TPR was 1.9 liter/minute, just adequate to allow sampling of the effluent. At pH 2 the half life of ozone is 1000 times longer than at pH 8, or in other words, the auto-initiation of the free radical mode is 1000 times slower. Thus if one were to be able to "titrate" the precursor sites with ozone as was suggested previously, it should be seen in this experiment. Instead of the expected result, a sharp spike followed by a gradual decrease in THMFP was found. Although the experiment was poorly designed (drastic pH change due to flow during the experiment, poor sampling, etc.). No sharp decrease in FP with low ozone doses was seen. Thus the data seems contradictory to the hypothesis about ozone reacting with THMFP sites while ·OH generates them.

Experiment N

Experiment N was a mass transfer experiment on a 6' TPR. The data was not very good, exhibiting a great deal of scatter, but did indicate poor mass transfer, presumably because of the low gas flow rates which were attainable through the porous frits. The superficial velocity was much lower than recommended (0.094 cm/sec compared to "not less than 4 cm/sec" as recommended by one chemical engineering text [14]). This data did however indicate that in previous experiments in the 6' TPR the utilized dosage may have been considerably lower than applied dosage. In the case of the batch ozonation discussed previously, that means that the maximum in TTHMFP may have occurred at even lower dosage than 0.4 mg/L. It is not known how much ozone, if any, may have been lost to decomposition on the frit.

No experiment was named O because of possible confusion in sample labeling in the field.

Experiment P

In order to test the TPR C/P configuration on presed water experiment P was begun. It ran for only four days before the ozone monitor began to malfunction and had to be repaired. The results were as expected, with very little removal being effected by the low dose rate. When the ozone monitor was repaired, this configuration was dropped in favor of the DI mode on presed water, where the low pH might emphasize the direct ozonation reactions.

Experiment Q

This was a low-dosage DI mode experiment using the TCSTR for contacting and one 3' TPR with two lamps for photolysis. Dosage was increased slowly each day, again to determine if a minimum existed in the F/F_o vs Dose curve. The value of F/F_o stayed around unity up to the highest dose used, 5.7 mg/L applied, and again, no minimum found. At this point the ozone monitor again malfunctioned due apparently to low source intensity and was repaired by adjusting the lamp position.

Experiment R

This experiment was begun to test the conditions of Experiment Q at higher dose rate. It had only run for three days when the ozone monitor failed again. It was repaired this time by fashioning a teflon o-ring to secure other pieces in their proper place. No additional information was gained from experiment R.

Experiment S

Due to the failure of the low pH experiments (presed water) to find a minimum in the F/F_o vs Dose curve, and to rapid coating of the lamp wells when using presed water, the pilot plant feedwater was switched back to clarifier water (pH 9) and the ozone dose increased to that which earlier experiments (e.g., Experiment H) had indicated would effect significant removal. At this time compositing of samples was begun, with two 100 ml samples a day being added, up to 700 ml, making 2 composite samples per week from each sampling point. After only three days of operation, the ozone monitor failed again, due to the elastomer of the armature seal being degraded by ozone. This time the monitor was repaired using a replacement armature from EEMCO, the manufacturer of the solenoid valve in the PCI ozone monitor. No replacement parts were available from PCI other than the entire valve at a cost of $75.00. The replacement armature was sent by EEMCO at no charge. Experiment S was resumed and it was found that 25 ± 4% removal of TTHMFP was obtained using a 11.3 ± 0.5 mg/L ozone dose (applied). These are the combined results of four composite samples over a twelve-day period, with the utilized dose being typically 75-85% of that applied. While this appears at first to be rather low utilization for the 3600 rpm turbine contactor, the data of Kosak-Channing and Helz(47) show the concentration of ozone in the liquid in equilibrium with the feed gas to be < 7 mg/L and with the off gas to be < 1.5 mg/L at that temperature (31°C), which correspond to 62% and 13% of the applied dose rate, respectively. Thus the utilized rate is actually greater than the solubility and is undoubtedly due to the removal of ozone from solution due to fast reaction and perhaps decomposition other than chemically induced. This TTHMFP removal, 25 ± 4% for a dose of 11.3 mg/L (8.8 mg/L utilized) is in excellent agreement with the corresponding Experiment H where a removal of 23% was experienced with a utilized dose between 3 and 10 mg/L (Figure 27). At this point the ozone dose was increased as described in the next experiment.

Experiment T

This experiment is separate from the previous one only in that the power at the ozone generator was increased, giving an increased dose rate of 12.1 mg/L and later 12.4 mg/L and 11.1 mg/L applied (9.4, 10.3 and 10.2 mg/L utilized). In the first two samples, 40% removal was experienced, while in the third, removal dropped to 32%. The values found in Experiment H were 21%, 23%, and 23% respectively. More difference was seen between the FP removal after ozonation only and after photolysis than in Experiment H. Formation potential removals in Experiments T are significantly better than Experiment H. Photolysis of some ozone is undoubtedly taking place in the TPR in Experiment T.

Experiment U

The ozone monitor malfunctioned again, this time because the elastomer armature seal degraded rapidly and dissolved to a sticky substance, sealing the valve in the reference position. The old armature was cleaned and put back into service. A different person at EEMCO said that they had several failures of that particular elastomer and sent the correct part this time. Experiment U is essentially a continuation of T with the ozone generator power turned up from 80 to 90%. After running like that for five days, the ozone generator failed, losing pressure.

A preliminary examination indicates that when the liquid oxygen tank ran out of oxygen, the ozone generator was no longer pressurized and the vacuum from the TCSTR turbine pulled in the O-ring seals which separate the ozone generating portion from the cooling water. Evidence of severe arcing was present on the top contact plate and the electrical connecting rods. This appears to be a serious design flaw in this combination of TII tube-type ozone generator and turbine contactor. The liquid oxygen level gauge on the supply tank proved unreliable, still reading 60% full when the cylinder ran out.

Two plate-type Grace/Union Carbide ozone generators were borrowed from the Environmental Sciences Program at the University of Texas at Dallas, one of which was used to replace the TII generator while it was repaired. The other generator was installed in a second process stream as described below.

At this point the use of letter designations for experiments was terminated. After repairs were made, the trailer was reconfigured to run in DI mode using the TCSTR on one stream and CP mode in the TPR`s (with new frits) on a second. Flow dropped steadily in the TPR's over a period of three days until almost no gas was flowing, and that part of the experiment was discontinued. The plant was operated in DI mode with the TCSTR for almost three weeks (8/26 - 9/13/83) at which time it was shut down in order to replace the troublesome frits with other spargers, and to run some reactor characterization experiments. It was restarted and run for five days, when the results of some THMFP analyses indicated that the TPR's were not operating as thought. Closer investigation revealed that ozone decomposition appeared to be taking place in both the inlet and to a greater extent, the outlet ozone lines connected to the TPR, so that not only was the feed concentration probably not that which was indicated by the ozone monitor, but the off-gas concentrations were incorrect as well.

A test manifold was arranged such that the ozone/oxygen mixture from the generator was sent to a switching valve. In one position (called "blank" in Table 20 below), the valve sent the ozone mixture directly to the ozone monitor while in the other position (labeled "sample" in Table 20) the ozone was first sent through a suspect piece of tubing, then to the monitor. It is seen that considerable ozone decomposition is taking place in tubes a and c, while tubes b, d, and e do not appear to cause ozone decomposition. All are 304 stainless 3/8" O.D. and the longest (a) is less than four feet long. Tube c is about two feet long. Tubes a, b, c and e have gotten

TABLE 20. OZONE DECOMPOSITION IN STAINLESS STEEL TUBING

ACTION(a)	Monitor Reading, % ozone Blank	 Sample	% ozone Lost
1) tube "a" placed in sample side	2.05, 2.08(b)	0.78, 0.319(c)	62%, 85%
2) tube "a" removed from sample side	2.852,2.263(b) 2.260,2.254(d)	2.123,2.302(c)	2%
3) tube "a" replaced in sample line	1.841,1.849(b) 1.849(d)	1.239,1.156, 1.102(c)	37%
4) tube "b" placed in sample line	1.901,1.912(b)	1.879 1.907(c)	1%
5) tube "c" placed in sample line	1.609(b)	1.235,1.238(c)	23%
6) tube "d" placed in sample line	1.632,1.563(b) 1.565	1.590(c)	0%
7) tube "e" placed in sample line	1.481,1.501(b)	1.503,1.490, 1.484,1.520(c)	1%

---

a) Tube "a" was from off gas line in trailer, "b" from feed gas line to TPR_I, "c" from feed gas line to TPR_{II}, "d" from feed gas rotameter manifold, "e" from off gas sampling line.

b) Concentration of ozone in test gas before diverting to "sample" position.

c) Concentration of ozone in test gas having passed through tubing piece being tested.

d) Concentration of ozone in test gas after diverting to "sample" position.

TABLE 21. FORMATION POTENTIAL DATA FOR EXPERIMENT W(a)(b)

Ozone dose, mg/L		Total Trihalomethane Formation Potential, g/L				
		Influent	After Ozonation		After UV	
Applied	Utilized	FP_o	FP	FP/FP_o	FP	FP/FP_o
32.1	13.9	275	205	0.75	166	0.60
49.9	29.6	261	201	0.77	108	0.41
70.9	48.3	279	101	0.36	72	0.26

a) Configuration is ozonation in TCSTR, followed by $2L_I2L_{II}$ in TPR's.

b) Liquid flow rate = 0.84 GPM, gas flow 17.6 SCFH of 0.98, 1.52 and 2.16% ozone, respectively.

wet inside by water backing up, then been exposed to ozone. No explanation for the decomposition can be offered at this time other than catalytic ozone decomposition.

It is not known how long this error in concentration measurement had been present, but inspection of the data collected prior to discovery indicates that the problem was discovered almost as soon as it occurred. Evidence for this is the fact that the ratio of feed gas to off gas concentrations appears reasonable prior to the data which indicated the problem. The net effect of ozone loss in either feed gas or off gas lines would be to cause the utilization efficiency to appear lower, so that the values obtained would at least be lower bounds to the actual efficiencies.

After the loss of ozone was discovered, the plant was left running in the TCSTR CP mode with 2 lamps while aluminum tubing was obtained to replace the stainless steel. During this period (10/7 - 10/10/83), 39% removal (from 406 µg/L to 246 µg/L TTHMFP) was obtained using an applied dose of 32.5 mg/L of ozone. Utilized dose could not be calculated because off-gas sampling plumbing had been removed for replacement.

When the aluminum tubing arrived, the TPR feed and sampling lines were rebuilt, checking the whole line for ozone decomposition after each additional piece was in place. When the entire system was in place and showed no ozone loss, and the TPR's were briefly characterized with respect to ozone capture, the system was operated for 10 days with split streams going to a TCSTR CP (4L) and TPR CP ($1L_{I}2L_{II}2L_{III}2L_{IV}$) configurations. Two sets of samples (10/11 - 10/17/83) and (10/18 - 10/19) were taken. Formation potential removal in the first was 11% in the TCSTR and -9% in the TPR's for a dose of 16.9 and 12.1 mg/L respectively. It was learned however that the Sabine River Water Plant had been shut down on 10/14 - 10/16, so that during that time, the composition of the feedwater to the pilot plant was unknown. In the second sample set (10/18 - 10/19) however, removals of 37% (17.1 mg/L ozone applied) and 34% (13.3 mg/L ozone applied) were obtained in the TCSTR and TPR configurations, respectively, starting with an FP of 437 µg/L. Although parts had not yet arrived to plumb the off-gas sampling line for continuous operation, the capture efficiencies measured at the beginning of the experiment indicate that utilization could be expected to be 75% and 80% in the TCSTR and TPR`s, respectively, so that utilized doses were thought to be 12.8 and 10.6 mg/L respectively. This brought the TCSTR results in line with Experiment H and the TPR results between those of Experiments H and T.

TABLE 22. FORMATION POTENTIAL DATA FOR EXPERIMENT X[a][b]

Ozone Dose, mg/L		TTHMFP		
		Influent	Effluent	
Applied	Utilized	FP_o	FP	FP/FP_o
33.2	28.4	300	107	.36
52.6	43.9	312	70	.22
59.6	47.9	317	72	.23

a) TCSTR CP (4L)

b) Liquid flow rate = 0.84 GPM, gas flow of 17.6 SCFH of 1.0, 1.6, and 1.8 ozone, respectively.

TABLE 23. FORMATION POTENTIAL DATA FOR EXPERIMENT Y(a)(b)

Experiment Number	Influent FP_o, g/L	After TPR_I				After TPR_{II}				After TPR_{III}			
		D_a	D_u	FP_1	FP_1/FP_o	D_a	D_u	FP_2	FP_2/FP_o	D_a	D_u	FP_3	FP_3/FP_o
Y_1	332	5.1	3.5	334	1.01	11.9	8.1	346	1.04	19.4	13.2	339	1.02
Y_2	332	9.4	6.6	274	0.83	22.2	15.6	283	0.85	37.0	26.0	207	0.62
Y_3	332	14.9	10.8	139	0.42	34.8	25.2	222	0.67	56.6	41.0	122	0.37
Y_4	332	19.5	14.2	299	0.90	43.8	32.0	161	0.48	70.6	51.6	87	0.26

a) TPR CP configuration $2L_I2L_{II}2L_{III}$.

b) All FP data in g/L TTHMFP. All D_a (applied ozone dose) and D_u (utilized ozone dose) data in mg/L. FP_i/FP_o dimensionless. All ozone dosages cumulative across a line in the table.

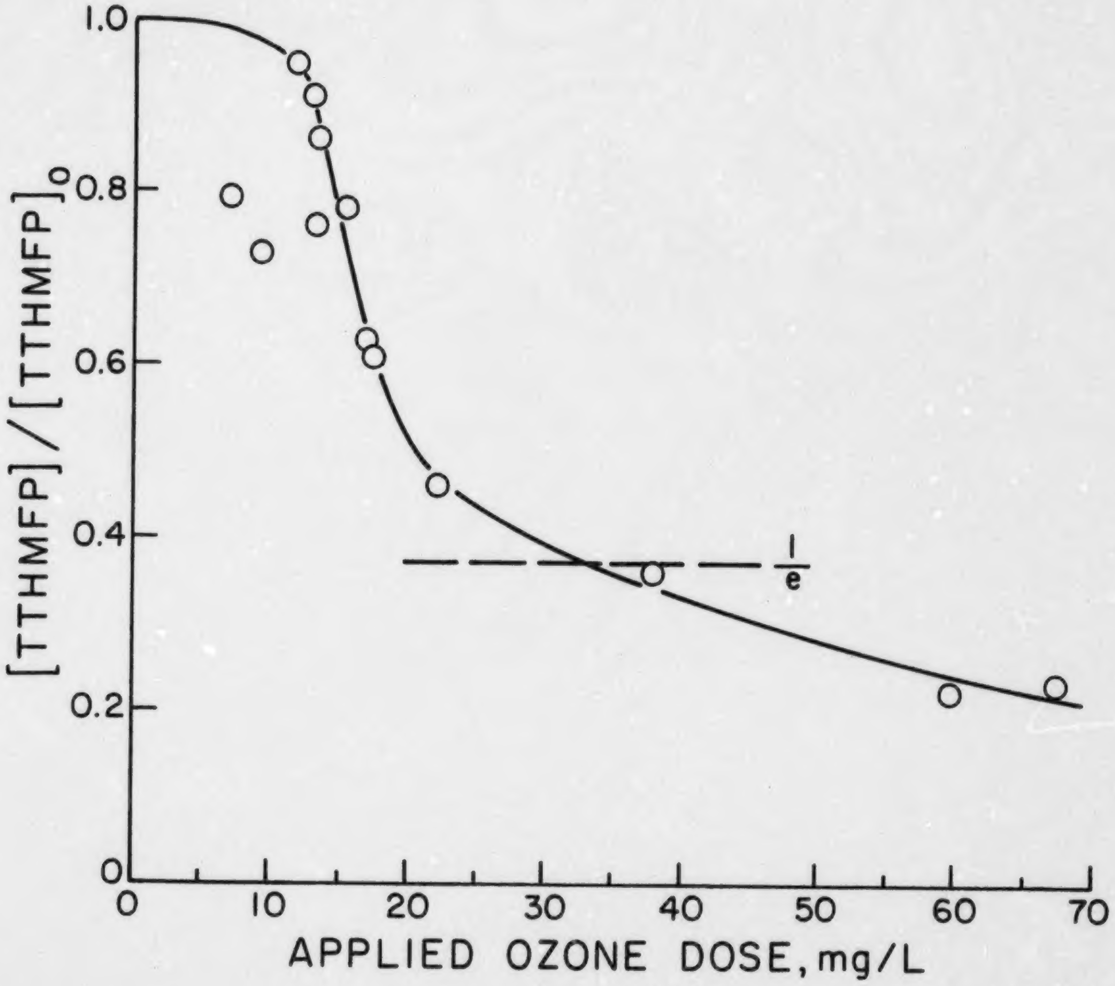

Figure 28. TTHMFP removal using TCSTR CP(4L) configuration.

More data was to be collected using these parallel configurations, but when an operator again allowed the system to run out of oxygen, water backed up into the system, and despite the presence of check valves in the gas lines, severely damaged both ozone generators. The original ozone generator was repaired and the TCSTR CP (4L) configuration put back into operation for four weeks. Formation potential removals varied during that period from 9% (13.1 mg/L ozone applied) to 54% at 22.4 mg/L applied. Figure 28 shows a plot of FP/FP_0 versus applied ozone dose for the TCSTR CP (4L) configuration during the period 10/18 - 11/29/83. Points representing the three highest ozone doses are from experiments described below, and discussion of Figure 28 will be delayed until those data are presented.

Three last sets of experiments were run during November in order to obtain data at higher ozone doses, compare TCSTR CP with TCSTR DI, and to obtain further data with the TPR configurations. The ozone off-gas sampling line was repaired, another ozone generator borrowed (the original ozone generator had again malfunctioned), and the following experiments run.

Experiment W

This was a TCSTR DI $2L_I2L_{II}$ configuration. Data is shown in Table 21 where a significant difference is seen between the FP of the water after ozonation alone, and after irradiation. Also of interest is the fact that with ozonation alone, 48 mg/L is sufficient to decrease the FP to FP_0/e (37% remaining). This data is discussed below.

Experiment X

The data for this TCSTR CP (4L) experiment has already been shown in Figure 28 and is given in Table 22. Notable is the fact that FP/FP_0 reaches a plateau just above a value of 0.20, compared with Figures 12, 14, 15 and 17 through 19. In only one case (4 mg/L min. ozone, 120 mg ozone dose, two lamps, Figure 14) does FP/FP_0 drop significantly below 0.20, and only then at a very high ozone dose. From Table 22 one concludes that in the TCSTR CP (4L) configuration, 27 mg/L of ozone is required to reduce FP/FP_0 to 1/e.

Experiment Y

Due to numerous experimental difficulties, this was the only real test of the TPR's at ozone doses which give FP removal greater than 50%. The run of 10/18 - 10/19 appears to have given valid data but the largest ozone dose was 13.3 mg/L

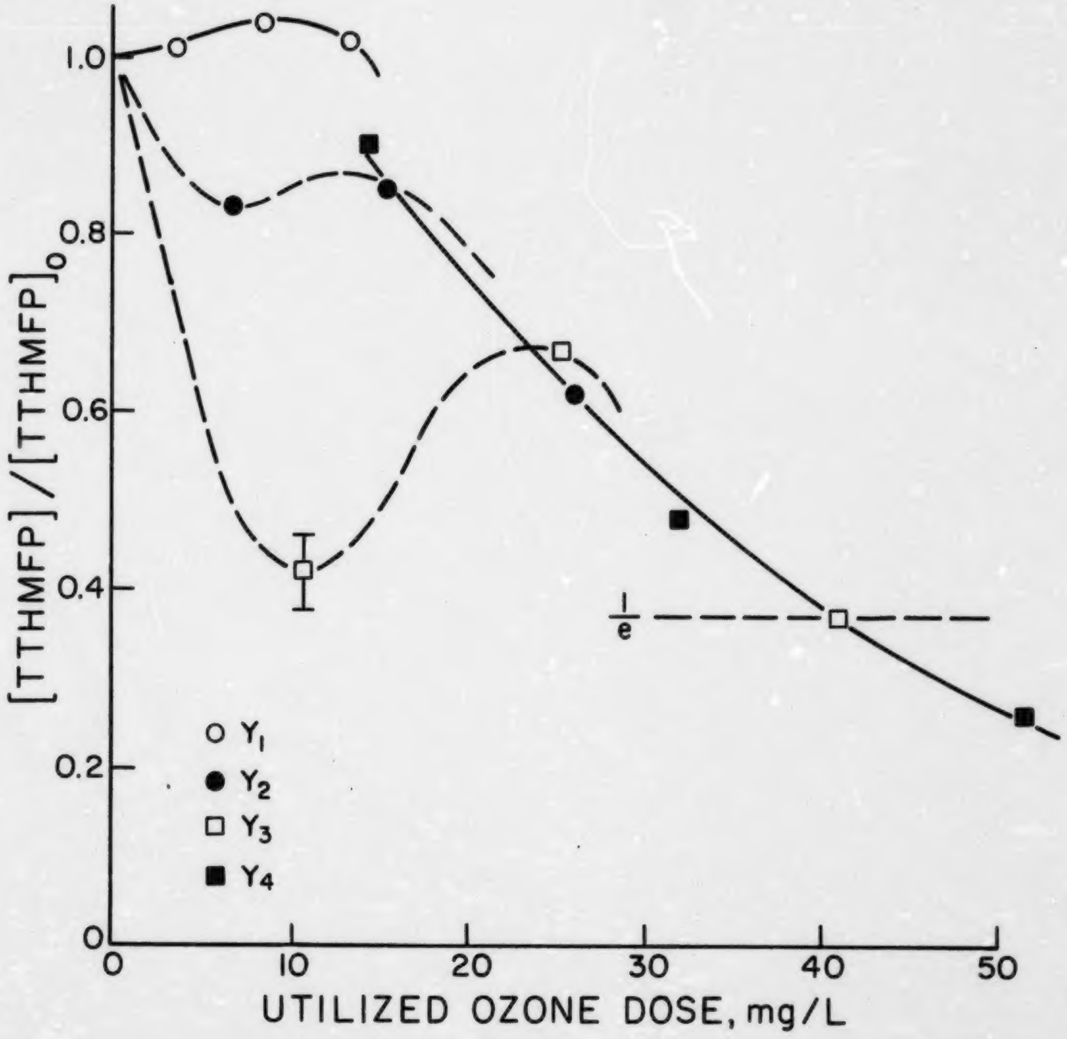

Figure 29. Formation potential removal in the tubular photochemical reactors.

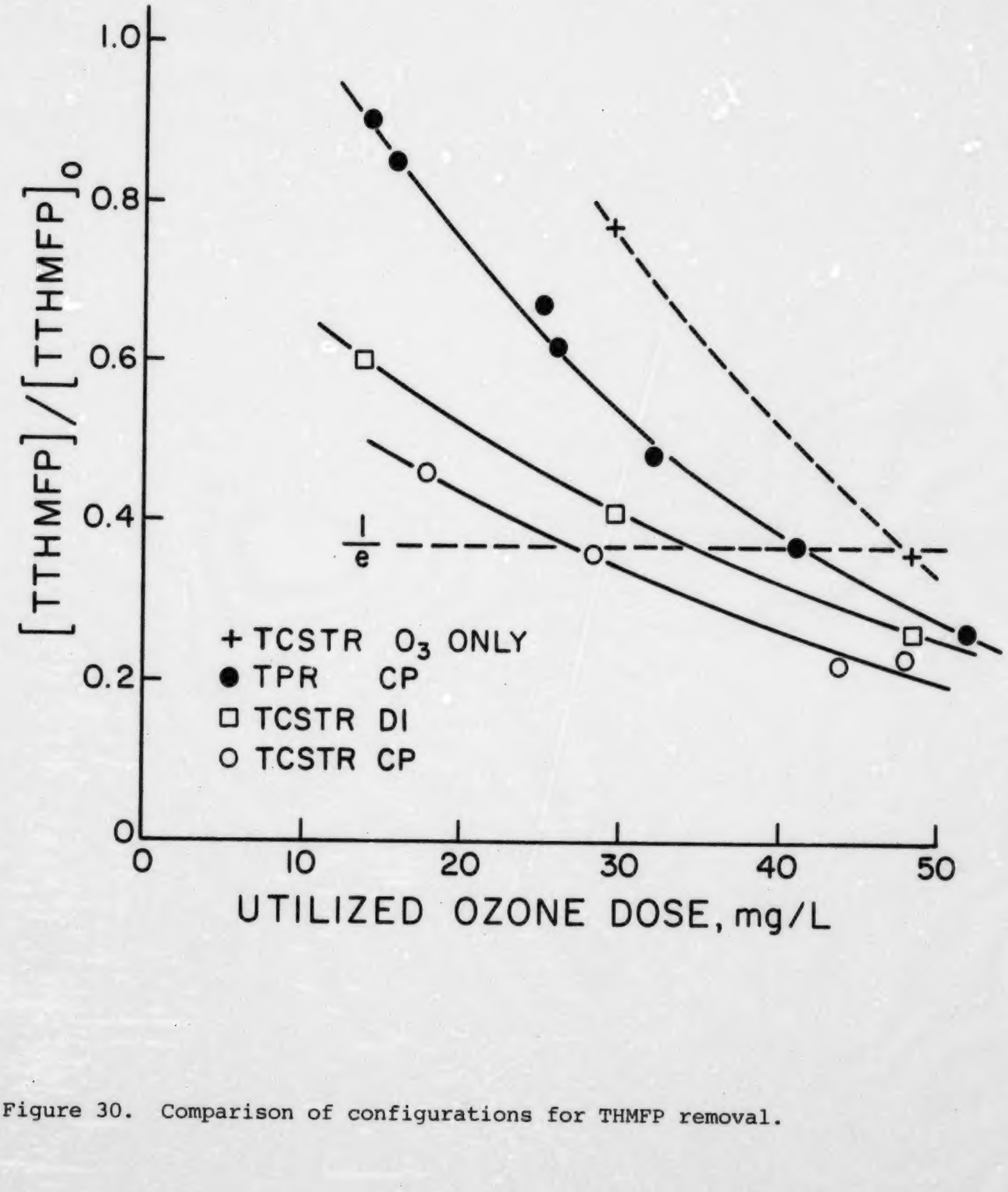

Figure 30. Comparison of configurations for THMFP removal.

(applied). Formation potential data for Experiment Y is given in Table 23, and plotted versus the utilized ozone dose, D_u, in Figure 29. Immediately noticeable is the "dip" exhibited in the Y_2 and Y_3 curves. It is this elusive feature which these investigators were searching for in earlier experiments at lower ozone doses. It is almost inconceivable that it is the result of data scatter. The error bars shown for that point in Figure 29 are for duplicate 25 ml analyses of a several hundred milliliter sample, and represents the largest error bounds in Figure 29 (all others are ± 2% or less). Furthermore, all experiments seem ultimately to approach the same removal curve at higher dose rates. However, until this phenomenon can be verified experimentally, and is understood and/or can be produced at will in water treatment, one must conclude that a utilized ozone dose of 41 mg/L was required to achieve removal to $FP/FP_o = 1/e$ in this TPR configuration.

Figure 29 also provides a good example of why one should not give too much importance to removal versus ozone dose values for the early stages of FP removal. Thus, when the higher-dosage experiments are plotted together, as in Figure 30 where TCSTR CP (4L), TCSTR DI ($2L_I 2L_{II}$), and TPR ($2L_I 2L_{II} 2L_{III}$) are all shown versus the utilized dose, D_u, a clearer picture of their relative efficiencies for THMFP destruction emerges. Also included, although not directly comparable, are the removals achieved with the ozonation portion of the TCSTR DI experiments. They are not directly comparable because there was undoubtedly some ozone remaining in both liquid and gas when the samples were taken and quenched. Thus, the actual ozone dose required is probably somewhat less than that shown.

The required dosages, D_1, to reduce FP/FP_o to 1/e (37%) of its original value are summarized below:

TCSTR-CP(4L)	$D_1 = 27$ mg/L
TCSTR-DI ($2L_I 2L_{II}$)	$D_1 = 34$ mg/L
TPR-CP ($2L_I 2L_{II} 2L_{III}$)	$D_1 = 41$ mg/L
TCSTR - ozone only	$D_1 = 48$ mg/L

where the ozone-only is subject to the qualifications stated above. Of the ozone/UV configurations, required UV power increases in the order of decreasing efficiency, although the synthetic lake water work indicates that if a full parametric study had been also done on real water, somewhat less UV power might have proven adequate.

In the parametric studies using synthetic lake water, TOC was measured routinely. Those results proved to be relatively uninteresting, disappearance curves being approximately exponential and decreasing more slowly than did THMFP. Due to time constraints and frequent malfunctions of the TOC analyser in the last year, TOC was not routinely measured during pilot operation. It was, however, measured on samples from experiments W, X, and Y, and shows some interesting differences between configurations.

Table 24 and 25 list TOC data which was collected on these experiments, along with calculated values of TOC/TOC_o and a parameter R defined as the percent reduction in TTHMFP divided by the percent reduction in TOC. The larger the value of this parameter, the more selectively FP is destroyed over TOC, a supposed advantage in process optimization. If either TOC or TTHMFP increases over the initial value, then $R < 0$ and the numerical value is meaningless.

The data in these two tables clearly partitions into three subsets, according to configuration. Values of TOC_o in parentheses are calculated from TTHMFP/TOC = 209 g/mg, determined from the TOC_o value of sample X_2, since the other samples were either not taken or were used up before TOC was measured. This procedure is justified since samples W_1 - W_3 and X_1 - X_2 were all taken from the same water source within a period of ten hours. The differences exhibited by the subsets far exceeds the error introduced by the above estimation of TOC_o values.

Experiment W, where the water was ozonated with doses of 13.9 - 48.3 mg/L before irradiation, shows high values of R ($3 < R < 7.5$) and all of the TOC/TOC_o values in the range of 0.88 to 1.27, with 50% of the R values less than zero. Experiment X, where ozonation (in the same dose range as W) and irradiation took place simultaneously, shows greater than 50% TOC destruction in all cases and quite regular values of R, with $1.2 \leq R \leq 1.5$. Experiment Y was simultaneous ozonation and contacting in the TPRs and with one exception, exhibit TOC destruction of $37 \pm 12\%$ (11 values) over an ozone dose range of 3.5 to 51.6 mg/L.

There appear to be two factors influencing these results. The first, referred to earlier, is the problem associated with using a photo-oxidative TOC method such as is used in the Dohrmann DC-54 to follow the course of a photo-oxidation

TABLE 24. TOC REMOVAL IN THE TCSTR SYSTEM[a]

Experiment Number		After Ozonation			After Ozone/UV		
	TOC_o	TOC	TOC/TOC_o	$R = \frac{(FP/FP_o)}{(TOC/TOC_o)}$	TOC	TOC/TOC_o	$R = \frac{(FP/FP_o)}{(TOC/TOC_o)}$
W_1	(1.32)	1.21±.03	0.92	3.1	1.16±.20	0.88	3.3
W_2	(1.25)	1.39±.01	1.11	< 0	1.15±.03	0.92	7.4
W_3	(1.33)	1.64±.02	1.23	< 0	1.69±.01	1.27	< 0
X_1	(1.44)	-------NA-----------			0.71±.03	0.47	1.2
X_2	1.49±.02	-------NA-----------			0.73±.02	0.49	1.5
X_3	1.64±.03	-------NA-----------			0.74±.01	0.45	1.4

a) All TOC values in mg/L

TABLE 25. TOC REMOVAL IN TPR SYSTEM(a)

Experiment Number	TOC_1	TPR_I $\frac{TOC}{TOC_o}$	R_1	TOC_2	TPR_{II} $\frac{TOC}{TOC_o}$	R_2	TOC_3	TPR_{III} $\frac{TOC}{TOC_o}$	R_3
Y_1	1.67±.03	0.78	< 0	1.40±.00	0.66	< 0	1.29±.05	0.61	< 0
Y_2	1.60±.07	0.75	0.70	1.43±.01	0.67	0.45	1.24±.03	0.58	0.90
Y_3	2.20±.00	1.03	< 0	1.15±.00	0.54	0.72	0.93±.01	0.44	1.13
Y_4	1.72±.02	0.81	0.53	1.21±.13	0.57	1.21	1.09±.04	0.51	1.51

(a) All TOC values in mg TOC/L $TOC_o = 2.13 \pm 0.10$ mg/L.

reaction. Persulfate photolysis in the TOC analyser ultimately produces hydroxyl radical which converts TOC to carbon dioxide in the same manner as is desired of the ozone/UV process. Natural organic substances which are more refractory to hydroxyl radical may not be detected in the TOC analysis as run until some ozone/UV treatment has occurred. The TOC increase which is observed is the difference between the amount of TOC which was destroyed and that which was "made visible" to the analyzer by photo-oxidative pretreatment. This effect has been seen throughout this project, on reconstituted lake water as well as Sabine River water.

The second effect is that of ozonation versus ozone/UV. Ozone adds quickly to sites with which it can react. The second order reaction rate constant of ozone with phenol is 1.3 $\pm$ 0.2 x 10^3 $M^{-1}s^{-1}$ (10) while that for the phenoxide anion is 1.4 $\pm$ 0.4 x 10^9 (10), which is in the diffusion controlled range. At pH 9, less than one pH unit below the pK_a for phenol of 9.9, greater than 10% of the phenol is present as phenoxide, and even at pH 8, Hoigne and Bader (10) give the effective rate constant as 1.8 x 10^7. This is to be compared with the base catalysed rate constant of 70 $M^{-1}s^{-1}$ (35) and that of the peroxy anion, HO_2, of 2.8 $\pm$ 0.5 x 10^6 M^{-1} s^{-1}. The latter is made effectively much slower by the fact that the pK_a of hydrogen peroxide is 11.6, meaning that about 0.25% of the peroxide is present as the anion. Therefore, as a simplified example, for 10% phenol groups in 2 mg/L of humic material, at pH 9, with 1 mg/L of hydrogen peroxide present, the respective pseudo first order rate constants for ozonation, base-catalyzed decomposition, and peroxide-catalyzed decomposition would be 4 x 10^2, 7 x 10^{-4}, and 2 x 10^{-1}, respectively, indicating that reaction of ozone with phenoxide groups is 10^3 faster than indirect ozonation reactions.

Although many counter-arguments to the above calculations can be presented, such as the actual fraction, identity, and rate constants of the phenolic constituents in humic material, and what portion of the total FP they constitute, it is clear that the direct reaction, even at pH, 9 is quite significant for the destruction of formation potential, but probably not for the immediate destruction of TOC. By the time the water in Experiment W reaches the UV lamps, there is very little ozone residual to be photolysed, which leads to the conclusion that the additional FP removal seen upon irradiation is probably not due to ozone photolysis, but to the photolysis of something else.

On the other hand, when ozonation and photolysis are carried out simultaneously (Experiment X) a brute force reduction of TOC results, taking a certain amount of THMFP with it. The TPR's are an intermediate case since irradiation takes place in the bottom half but not the top. Thus good THMFP removal can be obtained using ozone only, without having to "burn out" all of the TOC, but apparently at a higher ozone requirement than with ozone/UV. These investigators still feel strongly that if the regeneration of FP upon ozonation could be suppressed, good FP removal could be obtained at low ozone doses without UV, although not with the benefit of removal of other organic pollutants, as is enjoyed with ozone/UV. Finally, the data in Tables 23 and 24 are clear evidence for a distinct difference in mechanism between ozone and ozone/UV.

Matrix Effects in Photolytic Ozonation

The effect of the presence of various species in the water has been considered and is broken down into the following:

a) organic material

b) Alkalinity

c) pH

d) Chloride

e) iron and manganese

Water quality parameters measured at the Sabine River Water Treatment Plant are given in Appendix A.

Organic Material--

The natural organic material in the water occupies a unique position in this study since it is at once the substrate and its own interference. Experience has shown that if any property may be transferable between systems, it is fraction of FP removed per mg of ozone dose, rather than g or mmol/L of THMFP removed per mg of ozone dose. As will be seen below TOC not a good parameter with which to normalize FP removal data. Furthermore one should not use a photooxidative TOC analyser in a photooxidation study. It was shown in a previous section that for similar ozone doses and similar TTHMFP removals, TOC removals can vary as much as 100% with the configuration used.

Perhaps the most important and most frequently overlooked effect of TOC is that hydroxyl radical reactions (and ozonations to a lesser extent)with organic compounds tend to regenerate hydrogen peroxide which can react with ozone to produce more hydroxyl radicals or can itself photolyse to a limited extent to produce hydroxyl radicals. It is not presently known how these complex effects balance out in real systems, but it was seen for example in the studies of Baxendale and Wilson(16), that hydrogen peroxide regeneration can approach 100%. The question of the balance of these reactions and how it can be put to use is quite worthy of further investigation.

Alkalinity--

The effects of carbonate and bicarbonate in an ozonation system are well understood(6,43). An additional complication when hydrogen peroxide is present was uncovered in the present study (Section 5). Carbonate and bicarbonate serve to stabilize ozone in two ways. First, as is well known, they scavenge hydroxyl radical preventing its wasteful attack on ozone. Secondly, the product of that scavenging apparently reacts selectively with peroxide, thereby preventing the ozone/peroxide reaction. While these reactions are desirable if it is the direct ozone reaction which one desires, they can interfere severely if one is trying to maximize hydroxyl radical reactions.

Values for finished water alkalinity are given in Table A-1 of Appendix A. It is instructive to calculate the proportion of hydroxyl radicals scavenged by alkalinity and TOC, respectively. Using the average values of carbonate and bicarbonate alkalinity and $1 \times 10^9\ M^{-1}s^{-1}$ as a conservative average rate constant for the reaction of hydroxyl radical with organics(27).

$$k_{69}[CO_3^{=}] = 4.2 \times 10^8\ M^{-1}s^{-1}\ (5 \times 10^{-5} M) = 2.1 \times 10^3\ s^{-1}$$

$$k_{67}\ [HCO_3^{-}] = 1.5 \times 10^7\ M^{-1}s^{-1}\ (2.8 \times 10^{-4} M) = 4.2 \times 10^3\ s^{-1}$$

$$k_{6,TOC}[TOC] = 1 \times 10^9\ M^{-1}s^{-1}\ (1.7 \times 10^{-4} M) = 1.7 \times 10^5\ s^{-1}$$

Thus, less than 4% of the hydroxyl radicals produced will be scavenged by carbonate/bicarbonate at the concentrations present in the feed water, and no noticeable effect due to small alkalinity variations is anticipated. Calculations of the type shown above may be used to correct estimated ozone dose requirements in waters of extremely high alkalinity.

Effect of pH--

Staehelin and Hoigne$^{(6)}$ have shown that the initiation step of the base-catalysed ozone decomposition of ozone is considerably slower than has been reported by most investigators, due to the latters' failure to suppress secondary reactions during their experiments. Thus, the effect of pH is of considerably more importance for ozonation than for photolytic ozonation. This was seen in the data on reconstituted lake water, presented earlier, where although high pH aided mass transfer it resulted in a lower utilization efficiency, presumably shifting the mechanism away from direct ozonation toward the free radical mechanism. Once again, it is instructive to compare the base catalysed reaction at pH 9 with the direct reaction. Using the pseudo-first order expression for base-catalyzed decomposition from Staehelin and Hoigne$^{(6)}$, compared with a typical phenolic compound (estimated at 10% of the TOC)

$$k_{OH^-} = 1.75 \times 10^{pH-14}\ s^{-1} = 1.75 \times 10^{-3}\ s^{-1}$$

$$k_{org} = 1 \times 10^{3}\ M^{-1}\ s^{-1}\ (1/10 \times 1.7 \times 10^{-4} M) = 1.7 \times 10^{-2}\ s^{-1}$$

and for the 10% of the phenolic groups ionized at pH 9

$$k_{org} = 1 \times 10^{9}\ M^{-1}\ s^{-1}\ (1/100 \times 1.7 \times 10^{-4} M) = 1.7 \times 10^{3}\ s^{-1}$$

For photolytic ozonation however, the effect is even smaller. From a typical ozone/UV experiment, (21-A, four lamps, Table 5) transfer rate was 2.1 mg/L-min, pH = 7, and ozone residual 0.4 mg/L (interpolated), the base catalysed reaction would account for only an insignificant fraction of the ozone transferred. At pH 9, the ozone residual can be assumed to be less than or equal to the above value for a similar dose, and thus for Experiment X_1 (Table 6), 1.29 mg/L-min is transferred but only $1.75 \times 10^{-3}\ s^{-1} \times 0.4$ mg/L x 60 s/min = 4.2×10^{-2} mg/L-min (3%) can be accounted for by base-catalysed decomposition. We thus conclude that pH is relatively unimportant in a correctly designed (enough UV power) ozone/UV system, except as it affects secondary reactions and, of course, the small amount of direct ozonation of dissociated phenolic moieties. This conclusion is supported by the pH data of the previous section.

Effect of chloride--

The only known effects of chloride would be a "salting-out" effect on mass transfer and hydroxyl radical scavenging. The former is unimportant at the ionic strengths encountered in this feed water(47). The latter may be estimated from the rate constant, $k=10^{7} M^{-1} s^{-1}$ (40) and some average chloride concentration, e.g., 75 mg/L, leading to a pseudo-first order rate constant of $2.1 \times 10^{4} s^{-1}$. This number represents about 13% of a similarly-derived rate constant for reaction between hydroxyl and TOC, above, and thus could be important. For example, the high chloride value on September 23 (210 mg/L) would bring k_{Cl^-} up to 35% of k_{TOC}.

Comparison of the pilot plant data for THMFP removal with chloride content of the water fails to provide any verification of a chloride effect, even during the highest chloride surges (Figure A-1, Appendix A). However, the pilot plant was running in the DI mode during all of the major surges, and this mode would be expected to exhibit less of an effect than would the CP mode.

Iron and Manganese--

The data obtained by the monitoring of iron and manganese by SRWTP personnel was incomplete, but that which was taken failed to provide any evidence of a correlation between iron or manganese content of the water and treatment efficiency of the process. The following observations were made, however.

Laboratory experiments were run in which 0, 0.5, 1.0, and 5.0 mg/L of Mn^{+2} was added to a solution initially containing 10 mg/L of ozone and 30 mg/L of ethanol which was then photolysed for thirty minutes with samples withdrawn at 2, 5, 10 and 30 minutes. The first order (log) plot of the disappearance curves thus obtained were linear and virtually superimposable, indicating no effect of manganese levels far above those which are encountered in potable water.

Iron is known to participate in some ozone and peroxide reactions. However, the presence of ozone insures that virtually all iron is in the +3 state, eliminating Fenton-type reactions. Furthermore, the reactors and piping are of stainless steel and probably provide more opportunity for catalysis than the small quantity of iron present in the feed water.

One effect of iron and manganese which was noticed was the buildup of a light brown material on the quartz lamp wells with time. This material was immediately soluble in dilute hydrochloric acid and when analysed, was found to be 25% iron and 6% manganese. When allowed to accumulate for only a few days the effect of this coating can be seen on the photolytic ozonation process (see Experiment G , above). When allowed to accumulate for two weeks, radiometric measurements indicated that the UV intensity was reduced by a factor of three over that obtained through the sheath after it was cleaned. This effect is important with respect to maintenance, and every attempt should be made during the design of a photoreactor to accommodate facile lampwell cleaning.

To summarize, it can be said that there was no experimental evidence of the matrix affecting the efficiency of the photolytic ozonation process other than the maintenance problem described above.

Summary of Pilot Study Results and Conclusions

1) The TCSTR with simultaneous contacting (CP) and photolysis appears to perform better than the TPR's, with the TCSTR-delayed irradiation (DI) configuration falling in between. All three were more effective than ozone alone.

2) Ozone doses required for THMFP removal to 1/e of the original value are given in Table 26.

3) The optimum number of lamps in the TCSTR-CP configuration was 2-4 (0.13 - 0.27 W/L).

4) The lowest ozone dose rate which achieved the desired extent of FP removal was the most efficient.

5) Ozone utilization efficiency in the ozone/UV reaction was relatively insensitive to pH and other measured matrix components in this water.

6) As also shown in the previous mechanistic discussions, there is a fundamental difference in mechanism between the ozone and ozone/UV processes for THMFP removal.

TABLE 26. Ozone Dose Requirements[a] of the Configurations Tested.

	Sabine River Water, Longview, Texas	Reconstituted Cross Lake Water
TCSTR-CP	27 mg/L	30 mg/L
TCSTR-DI	34 mg/L	-
TPR-CP	41 mg/L	40 mg/L
TCSTR-ozone only	48 mg/L	

(a) for destruction of TTHMFP to 1/e of its original value.

Correspondence between required doses for Sabine River water and reconstituted Cross Lake water support the validity of using the reconstituted water in the parametric study.

SECTION 7

COST ANALYSIS

It was shown in the pilot study that an ozone dose of 27 mg/L was required to reduce the TTHMFP of clarified Sabine River water to 1/e (37%) of its original value (300 to 400 g/L) when treated in the turbine/continuously stirred tank reactor (TCSTR) in the CP (simultaneous ozone contacting and photolysis) mode with four UV lamps (0.27 watts/L). It is of interest to project an approximate treatment cost for this process, for comparison with other THM removal/prevention strategies. This section describes such a cost estimate.

As stated in earlier sections, based on limited experience, the most transferable treatment characteristic of ozone/UV process for the TTHMFP of natural organics in water containing 1-4 mg/L of natural organic carbon, is the fraction of TTHMFP removed per mg/L of ozone dose, provided that removal is greater than 50% (e.g., Figure 25). In many systems, removal seems to plateau at about 80% removal, so the following calculations were carried out for 60, 70 and 80% removal. By using the appropriate extent of removal, one may make a preliminary estimate of the treatment cost to reduce the TTHMFP of this particular water from its original value to, for example, the MCL of 100 g/L. It must be remembered that for a different water source this calculation is only an approximation. For a more accurate cost estimate, the required ozone dose should be determined by experiment for that particular water. These calculations are based on information pertaining to capital, as well as maintenance and operation costs for small water systems (< 1 MGD), which was obtained from USEPA, Drinking Water Research Division, Cincinnati, Ohio. This information along with suggested interest rates, extrapolation procedures, etc., is given in Appendix B. Where necessary, interpolations or small extrapolations have been made using the relationship

$$T = LQ^n$$

where T is the tabulated cost figure, Q is the capacity in MGD, and L and n are parameters to be evaluated from individual data

TABLE 27. CAPITAL COST[a] FOR THMFP REMOVAL USING PHOTOLYTIC OZONATION[b]

Plant Capacity MGD	Desired Removal	Ozone Dose Required	CAPITAL COST, DOLLARS				
			Ozone Contactor	Ozone generation and feed	UV[c] lamps	Mixer	Total
0.1	60%	24 mg/L	$ 4,200	$153,960	$4,600	$8,100	$170,860
"	70%	35 mg/L	4,200	174,200	4,600	8,100	191,100
"	80%	50 mg/L	4,200	200,000	4,600	8,100	216,900
0.5	60%	24 mg/L	7,700	268,915	18,000	10,400	305,015
"	70%	35 mg/L	7,700	336,650	18,000	10,400	372,750
"	80%	50 mg/L	7,700	425,000	18,000	10,400	461,100

(a) 1983 dollars.

(b) Based on figures given in Appendix B.

(c) The equivalent of 1.63 lamps relative to the data in Appendix B.

TABLE 28. OPERATING AND MAINTENANCE COSTS, \$/YEAR(a)

Plant Capacity, MGD	Desired THMFP Removal	Amortized Capital Cost(b)	Ozone Generation and Feed		UV Lamp		Mixing		Total	
			\$0.05/kwh	\$0.10/kwh	\$0.05/kwh	\$0.10/kwh	\$0.05/kwh	\$0.10/kwh	\$0.05/kwh	\$0.10/kwh
0.1	60	\$ 55,746	\$15,000	\$17,500	\$1,300	\$1,630	\$3,600	\$4,100	\$ 75,646	\$ 78,976
"	70	62,350	17,500	20,500	1,300	1,630	3,600	4,100	84,750	88,580
"	80	70,767	19,700	23,900	1,300	1,630	3,600	4,100	95,367	100,397
0.5	60	99,516	30,000	39,000	6,601	8,232	4,200	4,500	140,317	151,248
"	70	121,616	37,500	52,000	6,601	8,232	4,200	4,500	169,917	186,348
"	80	150,442	48,300	67,900	6,601	8,232	4,200	4,500	209,543	231,074

(a) Based on figures given in Appendix B, 1983 dollars.

(b) Twenty years at 8%. Principal tabulated in Table 27.

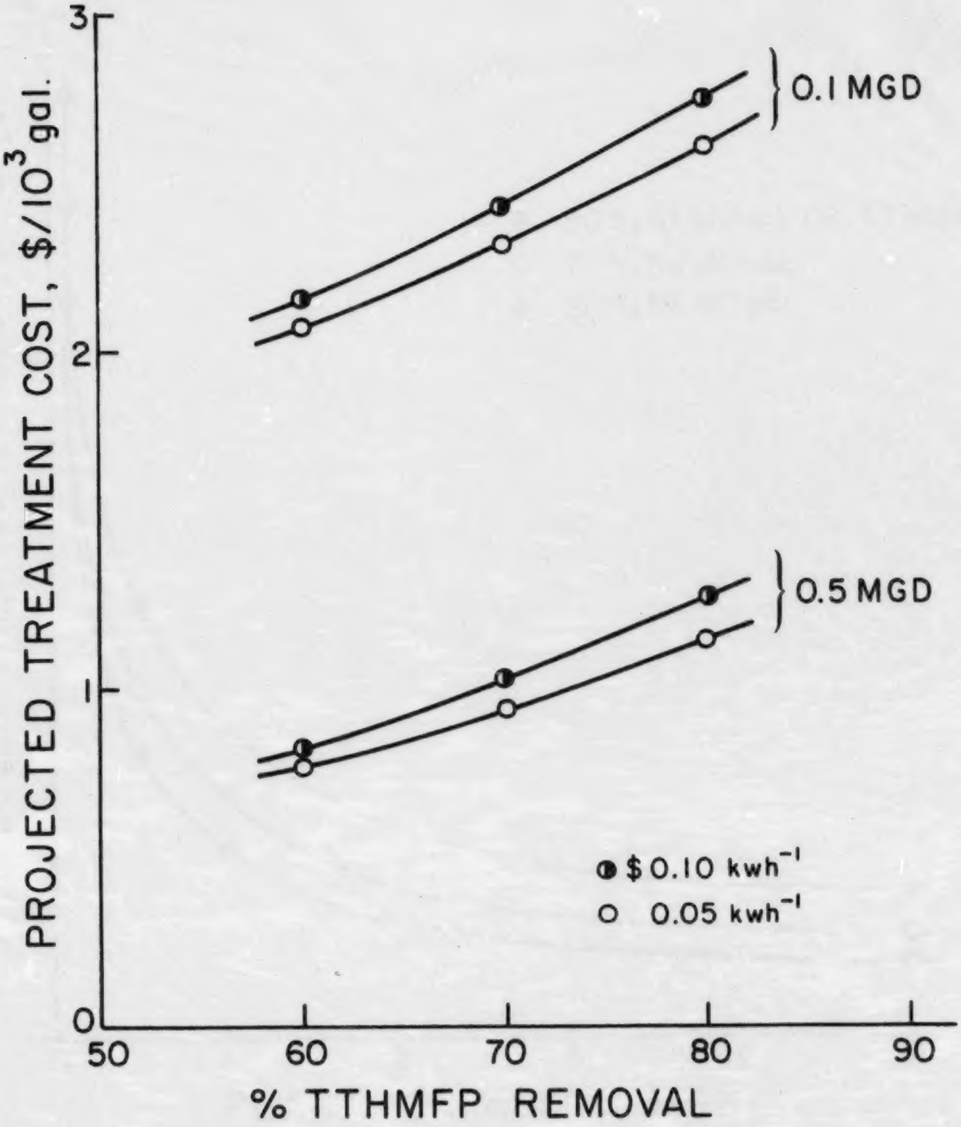

Figure 31. Projected treatment costs as a function of TTHMFP removal.

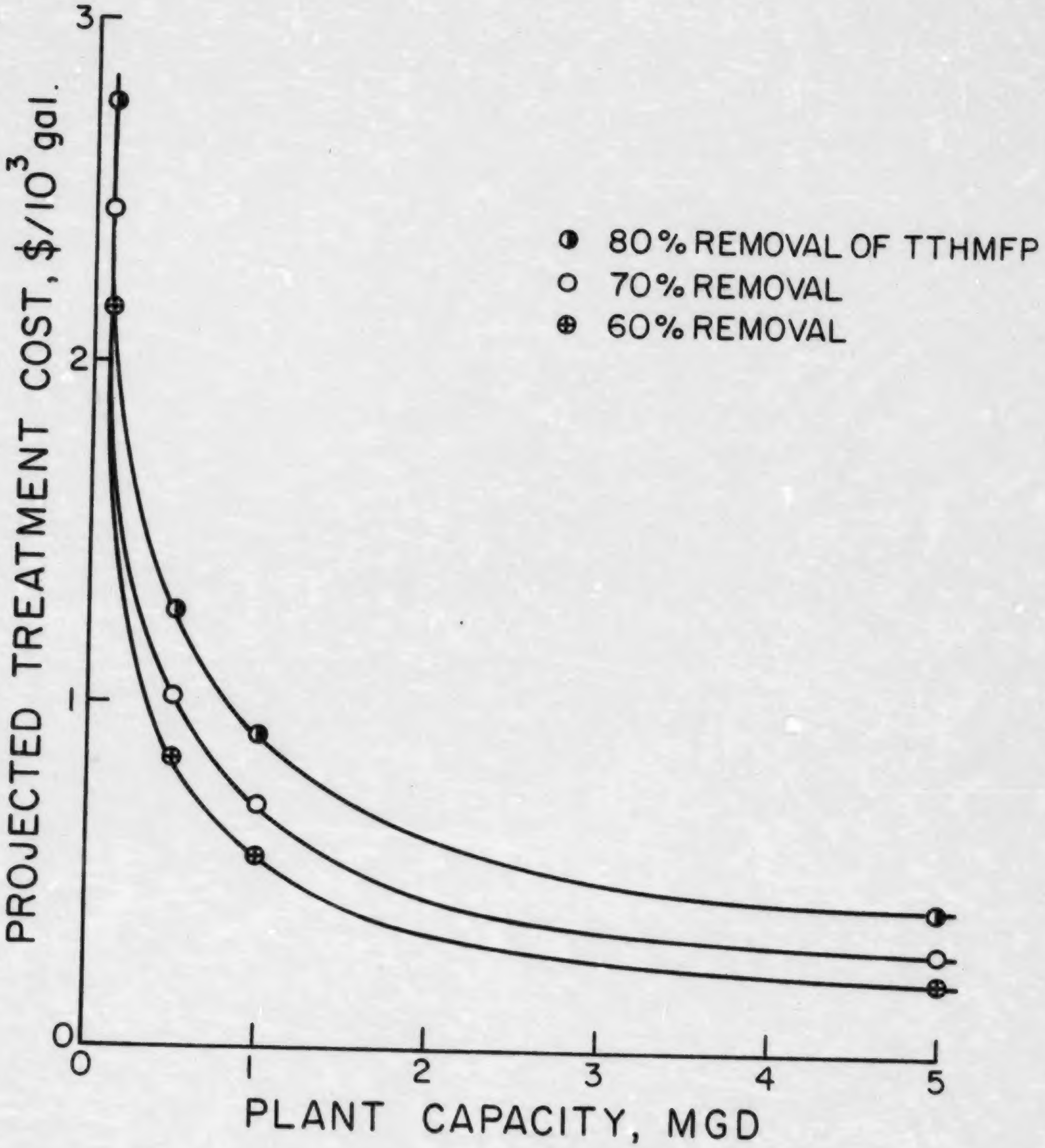

Figure 32. Projected treatment costs for systems up to 5 MGD (electrical cost of $0.10 per kwh assumed).

TABLE 29. PROJECTED TREATMENT COSTS[a]

Plant Capacity, MGD	Desired THMFP Removal	Treatment Cost, per thousand gallons @ $0.05/kwh	Treatment Cost, per thousand gallons @ $0.10/kwh
0.1	60%	$2.07	$2.16
"	70%	2.32	2.43
"	80%	2.61	2.75
0.5	60%	0.77	0.83
"	70%	0.93	1.02
"	80%	1.15	1.27

(a) Calculated from the values in Tables 27 and 28.

points. Capital costs are subjected to a multiplicative factor of 1.4 to cover engineering, contractors overhead and profit, site preparation, interest during construction, and legal and administrative fees (Appendix B).

Projected capital costs are shown in Table 27 for plants of 0.1 and 0.5 MGD obtaining 60, 70 and 80% THMFP removal. Yearly operation and maintenance costs are given in Table 28, where the amortized capital cost was computed using a municipal bond interest rate of 8% compounded over twenty years. Operating costs are computed at \$0.05 and \$0.10 per kilowatt-hour. Finally, the resulting treatment costs per thousand gallons are collected in Table 29 and shown in Figure 31 as a fraction of desired removal of THMFP.

It is of interest to compare the contribution of various factors to the total cost. From Table 27 it can be seen that 88 - 92% of the capital cost is ozone generation and feed equipment, while UV lamps and related equipment accounts for only 2 - 6%, and mixing for 2 - 5%. Similarly from Table 28, UV and mixing account for a 6 to 16% and 6-18% of the operating costs, so that their average contribution to the total cost is around 5-9% each. Contactor cost in Table 27 as supplied by EPA from ozonation cost data was not give as a function of ozone dose. In the presence of UV, contactor size is even less critical from a mass transfer standpoint. Reference to the Summary of Results at the end of Section 6 shows that the increase in THM removal efficiency realized by the addition of UV and mixing is about 75% and 50%, respectively, compared to the ozone-only and TPR results.

The projected costs are seen to be strongly dependent on plant capacity in the range of 0.1 to 0.5 MGD. This is shown more clearly in Figure 32, where the solid lines represents the function $T = LQ^n$, evaluated for the case of \$0.10 per kwh for 60, 70 and 80% TTHMFP removal. It can be seen that the treatment cost does not begin to level out until a capacity of a few MGD is reached, so that for example at 70% removal the projected cost drops from \$2.43 to \$0.29 per thousand gallons in going from 0.1 MGD to 5.0 MGD capacity.

In order to assess the validity of extrapolation to larger systems, suppliers of ozonation equipment were contacted and asked about ozone generation and feed equipment costs for systems in the size range 20-1000 lb/day. The hardware costs thus obtained were fit to the exponential equation given above, then extrapolated upwards (in plant capacity) for comparison with installed costs for actual large systems installed in recent years. A conversion factor for hardware costs to installed costs was obtained from this comparison. When applied to the manufacturer-supplied hardware costs, the resulting value predicted the EPA-supplied cost figures (including the factor of 1.4) within 10-15%, thus indicating some validity of the above extrapolation.

SUMMARY OF COST ANALYSIS

1) Projected treatment costs per thousand gallons are given in Table 30.

2) The dominant term in the capital cost is ozone generation and feed equipment, contributing 88 to 92% of the total capital cost which in turn represents about 65% of the total treatment cost. Thus advances in equipment efficiency can lower treatment costs significantly.

3) Ozone generation and feed operating costs represents 20 to 25% of the total treatment cost and thus this portion of the treatment cost can also benefit from improvements in equipment efficiency.

4) UV and mixing each account for 5 to 9% of the total operating cost but result in ozone utilization efficiency improvements of 50% or greater.

5) There is an exponentially decreasing effect of plant size on projected treatment cost, which drops from $2.43 to $0.29 per thousand gallons in going from a 0.1 MGD to a 5 MGD plant (70% removal, $0.10 per kwh).

TABLE 30. Projected Treatment Costs[a] as a Function of TTHMFP Removal.

Plant Capacity	60% Removal	70% Removal	80% Removal
0.1 MGD	$ 2.16	$2.43	$2.75
0.5 MGD	0.83	1.02	1.27
1.0 MGD	0.55	0.70	0.91
5.0 MGD	0.21	0.29	0.42

(a) in $ per thousand gallons.

SECTION 8

BYPRODUCTS OF PHOTOLYTIC OZONATION

Of interest in the development of any new water treatment process is the nature of byproducts which may be formed during its use. Toxicity and mutagenicity testing of concentrates derived from treated versus nontreated water are valuable screening procedures for new water treatment technologies. Zoeteman et al(51) found that Rhine River water which had been chlorinated showed increased mutagenicity as measured by the Ames test over water which had been treated with chlorine dioxide which in turn showed greater mutagenicity than untreated water. Ozonation on the other hand, reduced Ames mutagenicity over that of untreated water. Combination of ultraviolet irradiation with the above processes heightened the effect over that of the chemical process alone. The investigation of the effect of ozonation or photolytic ozonation followed by chlorination would be an important facet of the closer examination of the ozone/UV process before its adoption into actual practice on potable waters, but was beyond the scope of the present investigation. Described in the following section are studies carried out during this project to determine the existence of identifiable byproducts formed during the photolytic ozonation process.

From the results of Section 5, it should be expected that many of the byproducts of photolytic ozonation should be similar to those formed upon ozonation. It is also to be expected that most of the byproducts from the ozonation and photolytic ozonation of humic macromolecules will be too large and complex to be characterized using currently available techniques. The approach which has been taken in this project was to concentrate on those smaller products which possibly were identifiable by GC/MS techniques, in particular concentrating on components which appeared in treated water but not in untreated water. The main thrust of the investigation was the trapping of products on macroreticular resins, followed by elution and characterization.

EXPERIMENTAL TECHNIQUES AND EQUIPMENT

The macroreticular resins used were XAD-4 and XAD-8 (Rohm and Haas). XAD-4, like XAD-2 and Chromosorb 102, is a polystyrene-divinylbenzene copolymer which is particularly effective at removing nonpolar organic compounds from water while allowing salts to pass through it(52,53). XAD-8 is an acrylic ester polymer which is more suitable for the removal of polar organic compounds and has been used extensively either alone or in combination with XAD-4 for the concentration of natural organic material from water(54-58). These resins were carefully cleaned by soaking in 0.1 N sodium hydroxide for 24 hours, rinsing with deionized, carbon-filtered water (Millipore) until neutral, Soxhlet-extracted with methanol, ethyl ether, acetonitrile, and methanol again for 24 hours each, then rinsed with distilled water, 0.1 N sodium hydroxide, and dilute phosphoric acid at pH 2. All inorganic chemicals were of reagent grade, and organic solvents were pesticide grade, and were used without further purification.

The resins were slurry-packed by gravity into glass columns whose length to diameter ratio always exceeded 25. The water sample was allowed to drain by gravity through the column at a linear velocity of 2.7 meter/hour (4.5 cm/min) or less. The ratio of water sample to resin volume used was 20 in the first experiment and 40 in the second. Remaining details of the experiments are described individually below.

Final analysis of the samples was by GC/FID, HPLC, and GC/MS/DS. The HPLC work has not yielded any results of interest and is not reported here. The gas chromotograph used was a Hewlett Packard 5840 equipped with FID and EC detectors and a 30 m x 0.25 mm SE-54 fused silica capillary column (J & W Scientific).

GC/MS/DS work was done on a Ribermag R10-10 c GC/MS System with EI,NCI and PCI capability and a mass range of 1500 amu. The data system is a PDP-8a with disk drive. A Grob on-column injector was used in conjunction with a 30 meter x 0.25 mm SE-54 capillary column (J&W Scientific), in the Carlo Erba gas chromatograph. Derivatization of acids for gas chromatography was by the method of Bethge and Lindstrom (59), modified to produce the ethyl esters by the substitution of ethyl bromide for benzyl bromide. In this method the pH of the sample is adjusted to 9 with tetrabutylammonium hydroxide, after which the solvent is removed by gentle warming with a stream of inert gas blowing on the surface of the sample. The residue is taken back up in a small quantity of acetonitrile containing a slight excess of ethyl bromide and allowed to stand at room temperature for one hour. After some preliminary experimentation, two experiments were conducted which yielded results of interest.

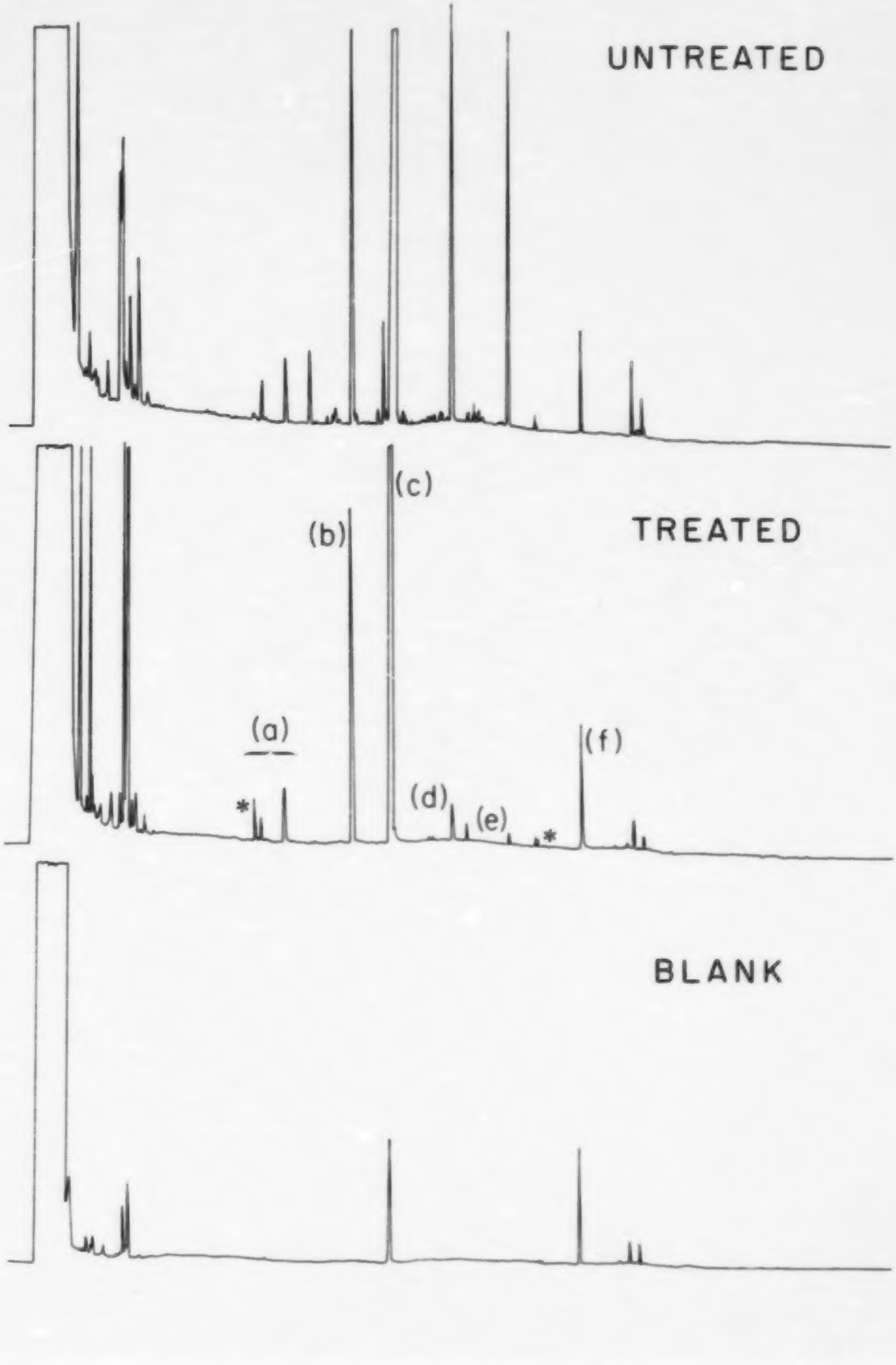

Figure 33. GC/FID chromatogram of derivatized methanol extract from Experiment I.

Experiment I

The pilot plant was operating in the DI mode (see data set D, Section 6 for explanation of configurations), with a utilized ozone dose of 17.7 mg/L. Formation potential removal was from 318 to 227 g/L (29%) while TOC was reduced by about 35%. The molar ratio of ozone used to TOC eliminated was 4.4. Thirty liters of treated and untreated water were acidified to pH 1.8 with phosphoric acid and each successively put through two columns of 0.75 liters each of mixed (50:50) XAD-4/XAD-8, on-site at the pilot plant. The resins were transported to the laboratory, the water used to cover the resin during transportation was drained off and replaced with 700 ml of methanol. After standing 24 hours, the methanol was drained off and replaced with 400 ml of benzene for another 24 hours. Because of the addition of this elution solvent, a resin clean-up step with benzene was added to the resin preparation procedure. A blank was run on a slightly smaller scale, with resin cleanup and elution identical to above but with no water sample in contact with the resin.

Experiment II

The pilot plant was running in the CP mode (see data set D, Section 6 for explanation) for this experiment with an ozone dose of 47.9 mg/L and four UV lamps (21.2 watts/80 liters). Formation potential removal was 77% (317 down to 72 μg/L) while TOC removal was 55% (1.64 down to 0.74 μg/L). Four-liter portions of treated and untreated water were adjusted to pH 10 with 0.1 N sodium hydroxide and run through 90 ml of mixed resin. The resin was allowed to drain for thirty minutes, then 200 ml of ethyl ether was added and allowed to stand in contact with the resin for one hour, then drained. The column was left in contact with methanol overnight, and washed with 500 ml of additional methanol to remove remaining ether. The effluent waters from the previous step were adjusted to pH 2 with phosphoric acid and put back through the column. A 100 ml portion of ether was left in contact with the resin for thirty minutes, then rinsed out with an additional 60ml of ether. A blank was run as before.

Sample Work-Up, Analytical Details and Results

Although low molecular weight carboxylic acids are known to be products of ozonation of many organic compounds, they are probably of minor interest from a public health point of view. Therefore, in these experiments, the focus was on the slightly less polar products which might be produced, hence less polar elution solvents were used rather than, for example 0.1 N

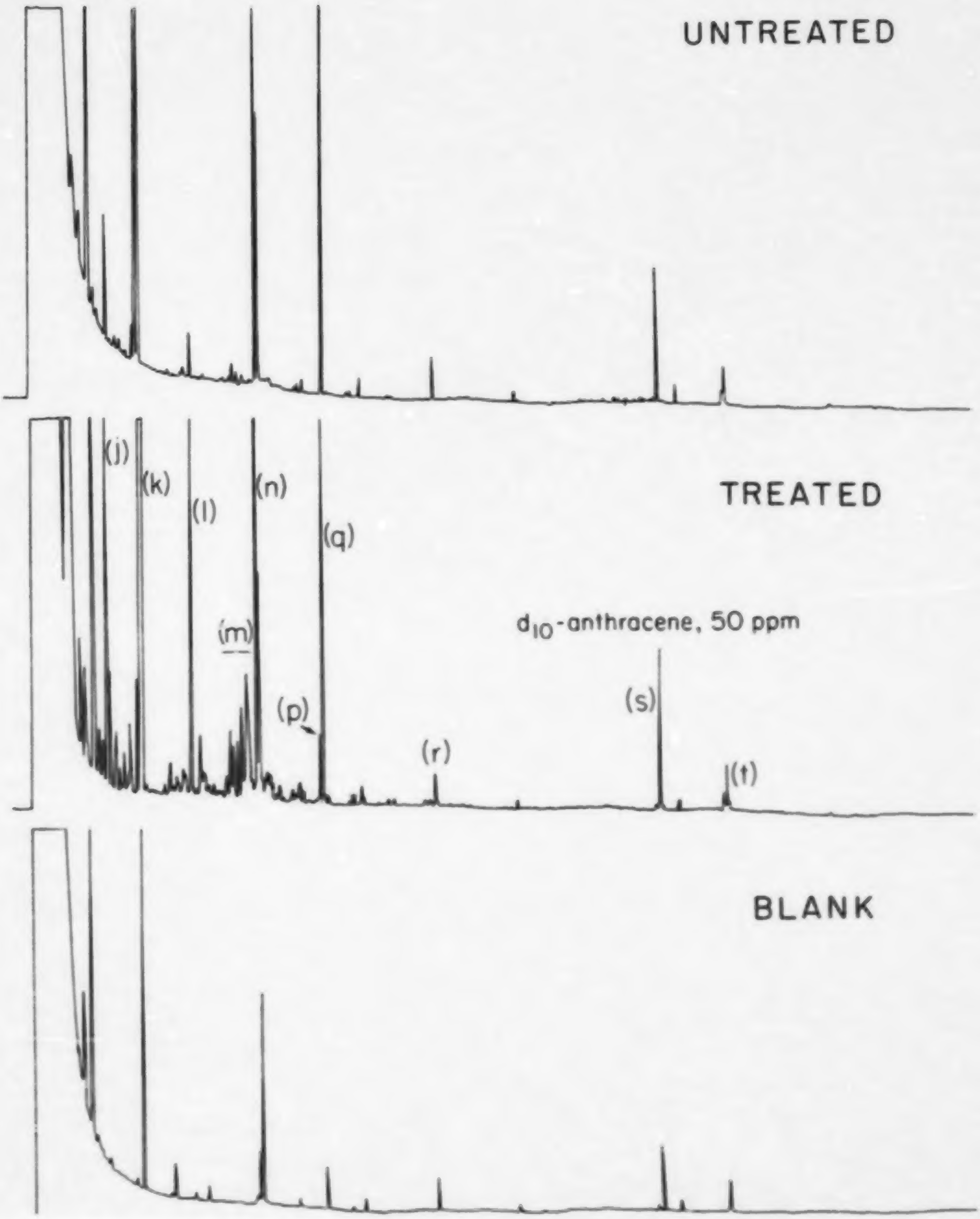

Figure 34. GC/FID chromatogram of ether extract from Experiment II.

alkali.

In experiment I the methanol fraction was derivatized with a resulting overall concentration factor of 1.3×10^3. This fraction was analyzed by GC/FID and GC/MS. As seen from the GC/FID chromatograms in Figure 33, there is very little qualitative difference between the treated and untreated water sample extracts. While several peaks have apparently diminished due to the photolytic ozonation treatment, only two small new peaks have appeared. These peaks are marked with an asterisk (*) in Figure 33 and represent 9 ppb and 2 ppb respectively in the original sample, assuming equal FID response factors with the internal standard, 50 mg/L of d_{10} - anthracene (peak f).

The base/neutral ether extract from experiment II was also analyzed by GC/FID and GC/MS. The GC/FID chromatograms are shown in Figure 34. Considerable differences are seen between the treated and untreated samples in the early region (before and after peak j), in peak(s) k, l, m, and several smaller peaks. Also noticeable is the disappearance of several small peaks just prior to the to the internal standard, d_{10} - anthracene (50 ppm in the extract). Because of the concentration factor (1200) these small peaks represent concentrations of less than 1 ppb in the original water. It was shown in previous reports(1,72) that one advantage of photolytic ozonation is the removal of micropollutants, even at the ppb level, during water treatment for THMFP removal. Preliminary GC/MS data interpretation reveals that the group of compounds belongs to a homologous series which may contain alkyl benzene functionalities. GC/MS data for this experiment will also be published in the open literature at a later date.

SECTION 9

QUALITY ASSURANCE PRACTICES

In order to insure the continued validity of data collected in this investigation, certain quality assurance practices were instigated during the course of the project. A narrative statement concerning those quality assurance practices was required by EPA during the third year of the project. This statement is given in Appendix C.

Of the analytical procedures employed during the project, three stand out as most in need of quality assurance checks. These are the gas chromatographic measurement of trihalomethanes, in the closely related trihalomethane formation potential of treated and untreated waters, and the accurate measurement of gas flow rates in the pilot plant trailer.

When the pilot plant was moved to Longview, Texas, the mass flowmeter used at SumX Corporation was no longer available to the project, and various rotameters in the pilot plant had to be relied upon for gas flow measurement. Rotameter calibration can vary considerably from that supplied by the manufacturer, depending on differences of inlet and outlet pressures from that used in the original calibration, etc. The rotameters used in the trailer for the calculation of ozone doses were whenever possible those which were mounted on the ozone generators. Although those rotameters were less finely graduated than those in the gas lines downstream, they would always be subject to the same feed gas pressure, regulated in the generator itself, and thus be less subject to variation due to operating conditions.

These rotameters were calibrated by the use of a wet test meter in the line and the following correlations found.

For feed to the TCSTR in the range of operation (10-20 SCFH) the linear correlation

$$R_{\text{actual}}\ (\text{SCFH}) = 6.95 + 0.55\ R_{\text{apparent}}$$

was used, leading for example, to the following values:

$R_{apparent}$	R_{actual}
10.0 SCFH	12.1 SCFH
15.0 SCFH	15.9 SCFH
20.0 SCFH	17.6 SCFH

The raw data were corrected by the appropriate amounts for calculation of ozone dosages.

In the TPR system, the flow was frequently too low for good reading accuracy on the generator rotameter, and individual control of each TPR was desired, so that the smaller in-line rotameters were calibrated individually. Actual flows were found to be 1.10, 1.11, and 1.16 times the calibrated value at 30, 50 and 70 divisions respectively (1.11, 1.81, and 2.43 SLM). Although not strictly linear, a linear correlation was fit to the factors. However, in the final data analysis, the correction factor used was 1.1. Since rotameter readings were primarily in the lower to middle (26 to 52 divisions) of the above range, the resulting error introduced (0 - 1% of the corrected flow) is well within experimental error from other sources.

One method used to maintain quality assurance for trihalomethane analysis was to plot day-to-day response of the electron capture detector to individual compounds. This plot is shown in Figure 35. With the exception of the low values on August 5, detector response was fairly constant until October 13. When high values were obtained on that date, new standards were made up, including the internal standard in the extraction solvent. This solution was made up at a different concentration than before to aid resolution from some interfering peaks. Since the values in Figure 35 were back-calculated from values which were normalized to the internal standard, they still include the ratio of THM concentration to internal standard concentration, and thus group around a different value after the new internal standard solution was made up. Due to the decreasing value of the $CHClBr_2$ integral and the onset of appearance of error messages of detector saturation after October 25, the use of multi-point calibration curves each time THM's were analysed was instigated, rather than the single-point mid-range calibration which had been used previously.

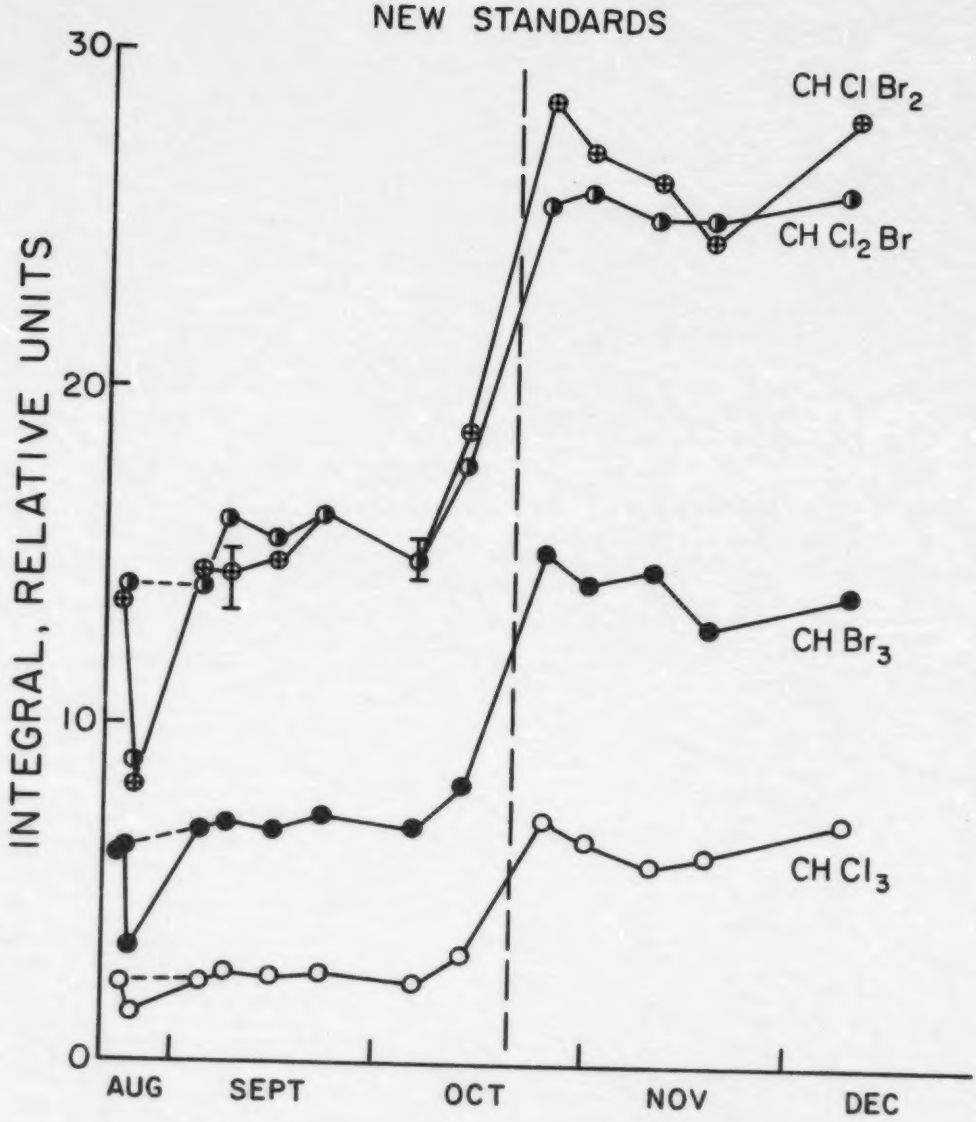

Figure 35. Day-to-day electron-capture detector response of individual trihalomethanes.

TABLE 31. EFFECT OF STORAGE ON TTHMFP ANALYSIS

Date of Sample Chlorination	Nontreated Water	Treated Water	C/C_o
5/24	364 ± 18	262 ± 3	0.72 ± 0.06
6/15	380 ± 10	299 ± 6	0.79 ± 0.04
6/17	336 ± 18	276 ± 5	0.82 ± 0.07
6/20	340 ± 6	259 ± 7	0.76 ± 0.04
6/21	350 ± 6	264 ± 7	0.75 ± 0.04
6/22	325 ± 2	262 ± 1	0.81 ± 0.01
6/23	320 ± 7	254 ± 6	0.79 ± 0.04
Average	345 ± 21 (6%)	268 ± 15 (6%)	0.78 ± 0.04 (5%)

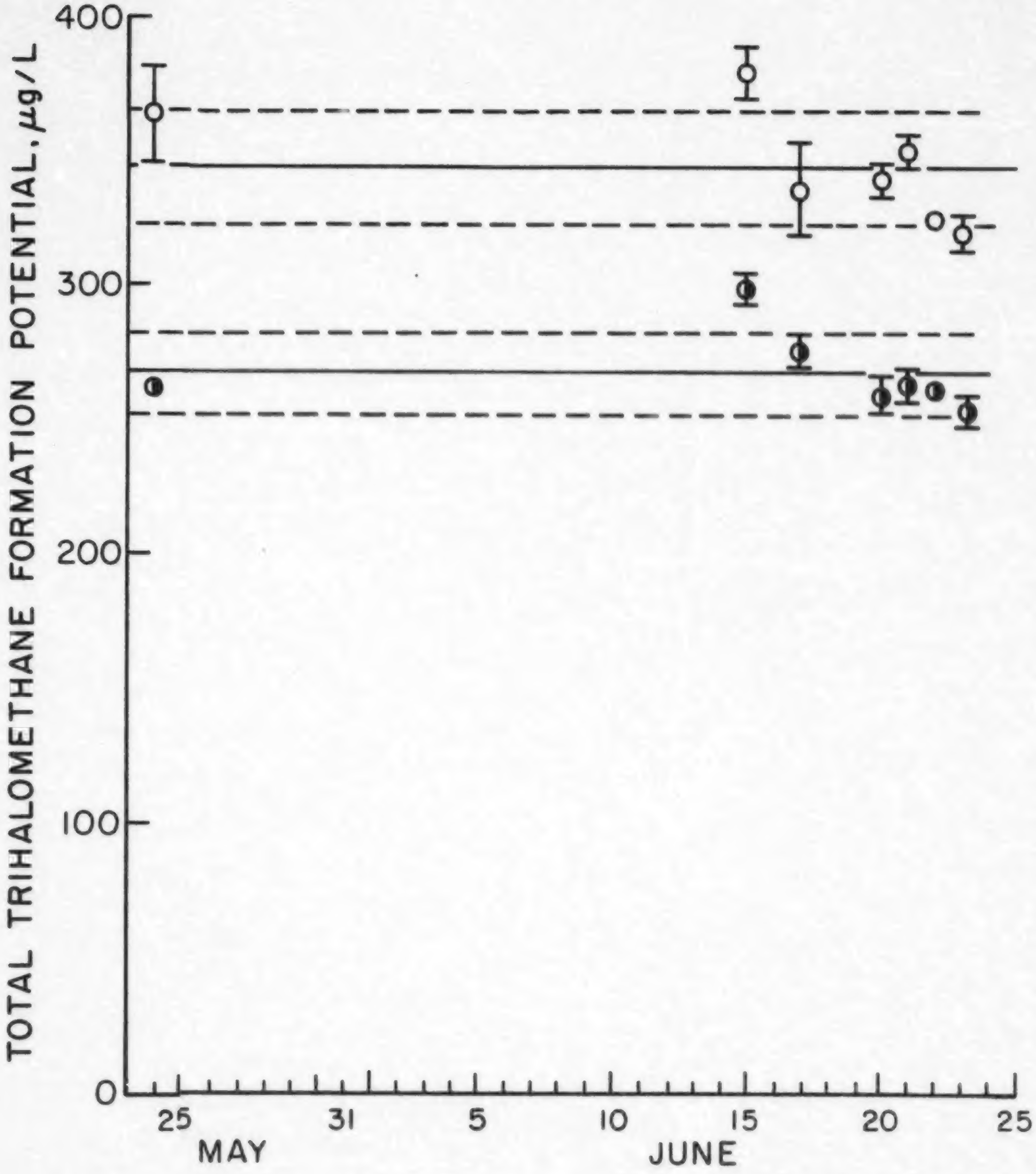

Figure 36. Effect of sample storage on total trihalomethane formation potential.

As a check on day to day reproducibility of THMFP analysis, large samples of both treated and untreated (by ozone/UV) water were collected periodically, from which chlorinated samples were prepared every few days. This was intended to serve not only as QA on the THMFP analysis method, but also as an investigation of sample stability upon refrigerated storage, since no preservatives were added other than the small amount (10^{-4}M) of sodium sulfite added upon sampling as an ozone quenching agent.

The data from one such study is shown in Table 31. The sample was taken on 5/19/83, brought to the laboratory on ice on 5/21, and refrigerated. A portion of the sample was chlorinated on the first working day after that (5/24), then the rest stored in the cold room for three weeks. Beginning on 6/15, portions of the sample were chlorinated every day or two for nine days, and analysed one week later. These data are shown graphically in Figure 36, along with the precision of replicate measurements (error bars), and the average and standard deviation of all measurements (solid and dotted lines) for a treated and non treated sample. The replicate precision is seen in most cases to be 2 to 3%, while the "accuracy" of later measurements is about ± 6% relative to the initial measurement. There may in fact be a slight tendency of TTHMFP to decrease upon storage, and samples should be analysed as quickly as is practicable. The accuracy of calculated TTHMFP/TTHMFP_0 values is slightly better than the measured concentrations, being around ± 5%. This data indicates that precision and accuracy for THMFP measurements are in an acceptable range. Although sample storage does not appear to drastically affect the measurements, THMFP analysis should be performed as soon after sampling as possible.

REFERENCE

1. Glaze, W. H., G. R. Peyton, F. Y. Huang, J.L.Burleson, and P.C. Jones. Oxidation of Water Supply Refractory Species by Ozone with Ultraviolet Radiation, Final Report, EPA-600/2-80-110, August 1980.

2. Lin, C. L., and W. B. DeMore, J. Photochem 2 (1973/74) 161.

3. Taube, H., Trans, Farad. Soc., 53 (1957) 656.

4. Taube, H., and W.C. Bray, J. Am. Chem. Soc 62 (1940) 3357.

5. Leitus,E., J. D. Zeff, M. M. Smith, and D. G. Crosby, "An Investigation into the Chemistry of the UV-Ozone Purification Process", Final Report to NSF, ENV 76-24652, 1980.

6. Staehelin, J., and J. Hoigne, Environ. Sci. Technol., 16 (1982) 676.

7. Gilbert,E., "Ozone/chlorine Dioxide Oxidation Products of Organic Materials", EPA/IOA, Ozone Press International, Cleveland, 1978, p. 227.

8. Gilbert,E., "Hydroperoxide and Organic Formation by Ozonation of Organic Compounds in Aqueous Solution", paper presented at Sixth Ozone World Congress, Washington, D. C., May, 1983.

9. Gilbert, E., Water Research 14 (1980) 1637

10. Niki, E., Y. Yamamoto, H. Shiokama, and Y. Kamiya, "Ozonation of Phenol in Water", presented at IOA Ozone. Technology Symposium and Exposition,Los Angeles, CA 1979.

11. Hoigne, J., and H. Bader, Water Res. 17 (1983) 173.

12. Hoigne, J., and H. Bader, Water Res. 17 (1983) 185.

13. Hoigne, J. and H. Bader, Water Res. 10 (1976) 377.

14. Vahidi, B., J. Wallace, A. Alladin, and J. Fernandes, Paper presented at the 6th Ozone World Congress, Washington, D. C., May 26, 1983.

15. Namba, K., and S. Nakayama, J. Chem. Soc., Japan, (1982) 55, 3339.

16. Baxendale, J. H., and J.A. Wilson, Trans. Farad. Soc., 53 (1957) 344.

17. Danckwerts, P.V., Ind. Eng. Chem. 434 (1951) 1460.

18. Whitman, W. G., Chem & Met. Eng. 29 (1923) 147.

19. Lewis, W. K. and W. G. Whitman, Ind.Eng. Chem 16 (1924) 1215.

20. Froment, G. F., and K.B. Bischoff, "Chemical Reactor Analysis and Design", Wiley, New York, 1979, p. 305.

21. Horak , J. and J. Pasek, "Design of Industrial Chemical Reactors from Laboratory Data", Heyden, Philadelphia, 1978, p. 323.

22. Tournier, A., and X. Deglise, J. Photochem. 18 (1982) 47.

23. Jacob, S. M. and J. S. Dranoff, AICHE J. 16 (1970) 359.

24. Irazoqui, H. A., J. Cerda, and A. E. Cassano, AICHEJ. 19 (1973) 460.

25. Staehelin, J. and J. Hoigne, World Ozone Congress, IOA, Washington, D. C. May 1983.

26. Bailey, P. S. "Ozonation in Organic Chemistry," Vol. I, Academic Press, N.Y., 1978, p. 113.

27. Farhataziz and A. B. Ross, "Selected Specific Rates of Reactions of Transients from Water in Aqueous Solution, III" NSRDS-NBS 59, 1977, p. 81.

28. Eberhardt, M. K., J. Am. Chem. Soc. 103 (1981) 3876.

29. Jacob, N., I. Balikrishnan, and M. P. Reddy, J. Phys. Chem., 81 (1977) 17.

30. Sawyer, D. T., and J. S. Valentine, Acc. Chem. Res. 14 (1981) 393.

31. Czapski, G., and B.H.J. Bielski, J. Phys. Chem. 67 (1963) 2180.

32. Czapski, G. and Dorfman, L. M., J. Phys. Chem, 68 (1964) 1169.

33. Glaze, W.H., J.L. Wallace, K.L. Dickson, D.P. Wilcox, K.R. Johansson, Eichin Chang, A.W. Busch, B.G. Scalf, R.K. Noack, D.P. Smith Jr., Municipal Environmental Research Laboratory, Office of Research and Development, Cincinnati, OH., 1982, Report No. EPA-600/52-82-046.

34. Prengle, H. W., Jr., Hewes,G. G. III, and Mank, C. E., Proceedings of 2nd International Symposium on Ozone Technology, R. G. Rice, P. Richet and M. A. Vincent, eds, International Ozone Institute, Syracuse, N.Y., 1975, p. 224.

35. Yocum, F. H., paper presented to 86th National Meeting of American Institute of Chemical Engineers, April 1-5, 1979.

36. Prengle, H.W.,Jr., Envir. Sci. Technol. 17 (1983) 743.

37. Bader, H., and J. Hoigne, Ozone: Science and Engineering 4 (1982) 169.

38. Bader, H., and J. Hoigne, Water Res. 15 (1981) 449.

39. Flamm, D. L., Environ. Sci. Technol., 11 (1977) 978.

40. Hart, E. J.,K. Sehested, and J. Holcman, Anal. Chem. 55 (1983) 46.

41. Parker, G.A., in "Colorimetric Determination of Nonmetals", D. R. Boltz and J. A. Howell, eds. Wiley, 1978, p. 301.

42. Masschelein, W. J., M. Denis, R. Ledent Water & Sewage Works, August 1977, p 69.

43. Weeks, J. L. and J. Rabani, J. Phys. Chem. 70 (1966) 21.

44. Behard, D. G. Czapski, and I. Duchovny, J. Phys. Chem. 74 (1970) 226.

45. Dainton, F.S. and P. Fowles, Proc. Roy. Soc. A 287 (1965) 295.

46. Dainton, F. S. in discussion following the paper of R. G. W. Norrish in "Fast Reactions and Primary Processes in Chemical Kinetics", Proceedings of 5th Nobel Symposium, August 1967, Stockholm, Wiley, New York, 1967, p. 67.

47. Kosak-Channing, L.F., and G. R. Helz, Environ. Sci. Technol., 17 (1983) 145.

48. Froment, G.F., and K.B. Bischoff, "Chemical Reactor Analysis and Design", Wiley, New York, 1979, p.

49. Vahidi, B., J. Wallace, A. Alladin, and J. Fernandes, paper presented at the 6th Ozone World Congress, Washington DC, May 26, 1983.

50. Huie, R.E., and J. T. Herron, Prog. React. Kin.

51. Zoftman, B.C.J., J. Hrubec, E. DeGreef, and H.J. Kool, Environ. Health Perspectives 46 (1982) 197.

52. Glaze, W.H., G.R. Peyton, R. Rawley, Environ. Sci. Technol. 11 (1977) 685.

53. Glaze, W.H., G.R. Peyton, F.Y. Saleh, F.Y. Huang, Intern, J. Environ. Anal. Chem. 7 (1979) 143.

54. Glaze, W.H., F.Y. Saleh, W. Kinstley, In "Water chlorination, Environmental Import and Health Effects", Vol. 3, R.L. Jolley, W.A. Brungs, R.B. Cummings, eds. Ann Arbor Science, 1980, p. 99.

55. Thurman, E.M. and R.L. Malcolm, Environ. Sci. Technol. 15 (1981) 463.

56. Leenheer, J.A., Environ. Sci. Technol. 15 (1981) 578.

57. Llao, W., R.F. Christman, J.D. Johnson and D.S. Millington, Environ. Sci. Technol. 16 (1982) 403.

58. Miller, J.W. and P.C. Uden, Environ Sci. Technol. 17 (1983) 150.

59. Bethge, P.O. and K. Lindstrom, Analyst 99 (1974) 137.

60. Forni, L., D. Bahneman, and E. Hart, J. Phys. Chem., 86 (1982) 255.

61. Bahneman D., and E. Hart, J. Phys. Chem. 86 (1982) 252.

62. Kuppenol, W.H., J. Butler, and J.W. van Leeuwen, Photochem. Photobiol. 28 (1978) 653.

63. Czapski, G. and Y.A. Ilan, Photochem. Photobiol. 28 (1978) 651.

64. Christensen, H., K. Sehested, and H. Corfitzan, J. Phys. Chem., 86 (1982) 1588.

65. Chin, D.H., G. Chiericato, Jr., E.J. Nanni, Jr., and D.T. Sawyer, J. Am. Chem. Soc. 104 (1982) 1296.

66. Bielski, B.H.J., Photochem. Photobiol. 18 (1978) 645.

67. Bielski, B.H.J. and A.O. Allen, J. Phys. Chem. 81 (1977) 1048.

68. Sehested, K., Holcman, and E. Hart, J. Phys. Chem. 87 (1983) 1951.

69. Ross, A.B., and P. Neta, Rate Constants for Reactions of Inorganic Radicals in Aqueous Solution", NSRDS - NBS -65, 1979, p.5.

70. Glaze, W.H., G.R. Peyton, S. Lin, F.Y. Huang, and J.L. Burleson, Environ. Sci. Technol. 16 (1982) 454. 71. Rook, J.J., In "Water Chlorination - Environmental Impact and Health Effects", R.L. Jolley, W.A. Brung, R.B. Cummings, Eds.; Ann Arbor Science, Ann Arbor, Mich. 1980, Vol. 3, p. 85.

72. Peyton, G.R., F.Y. Huang, J.L. Burleson, and W.H. Glaze, Environ. Sci. Technol. 16 (1982) 448.

APPENDIX A

WATER QUALITY DATA FROM SABINE RIVER WATER TREATMENT PLANT.

Parameters routinely measured on a daily basis at the water plant included alkalinity, hardness, chloride and pH. The pH of the clarifier water used for pilot operation varied between 8.8 and 9.2. Rather than present eight months of data, an average range has been established for each parameter and values which fall outside of this range tabulated with their dates. The average ranges for alkalinity (carbonate/bicarbonate), and hardness, as taken from the daily plant data, are 3-7/20-35 mg/L as $CaCO_3$ and 9-110 mg/L as $CaCO_3$, respectively. Chloride data show a trend over the period of operation with several superimposed spikes and is plotted in Figure A-1 rather than tabulated. To date no correlation has been found between water quality data and process efficiency.

One interesting relationship was noted, however, between the water quality parameters measured at the treatment plant. If the total alkalinity, hardness and 1.65 x the chloride (to convert to a sodium chloride basis) are summed, that quantity is closely related to total residue as measured in the UTD laboratories. That relationship is shown in Figure A-2 for eight samples taken throughout October and November, 1983. Ratios of the TDS to the summed water quality parameters vary from 0.90 to 1.01 for the samples analysed, with a strong dependence of the ratio of the chloride concentration.

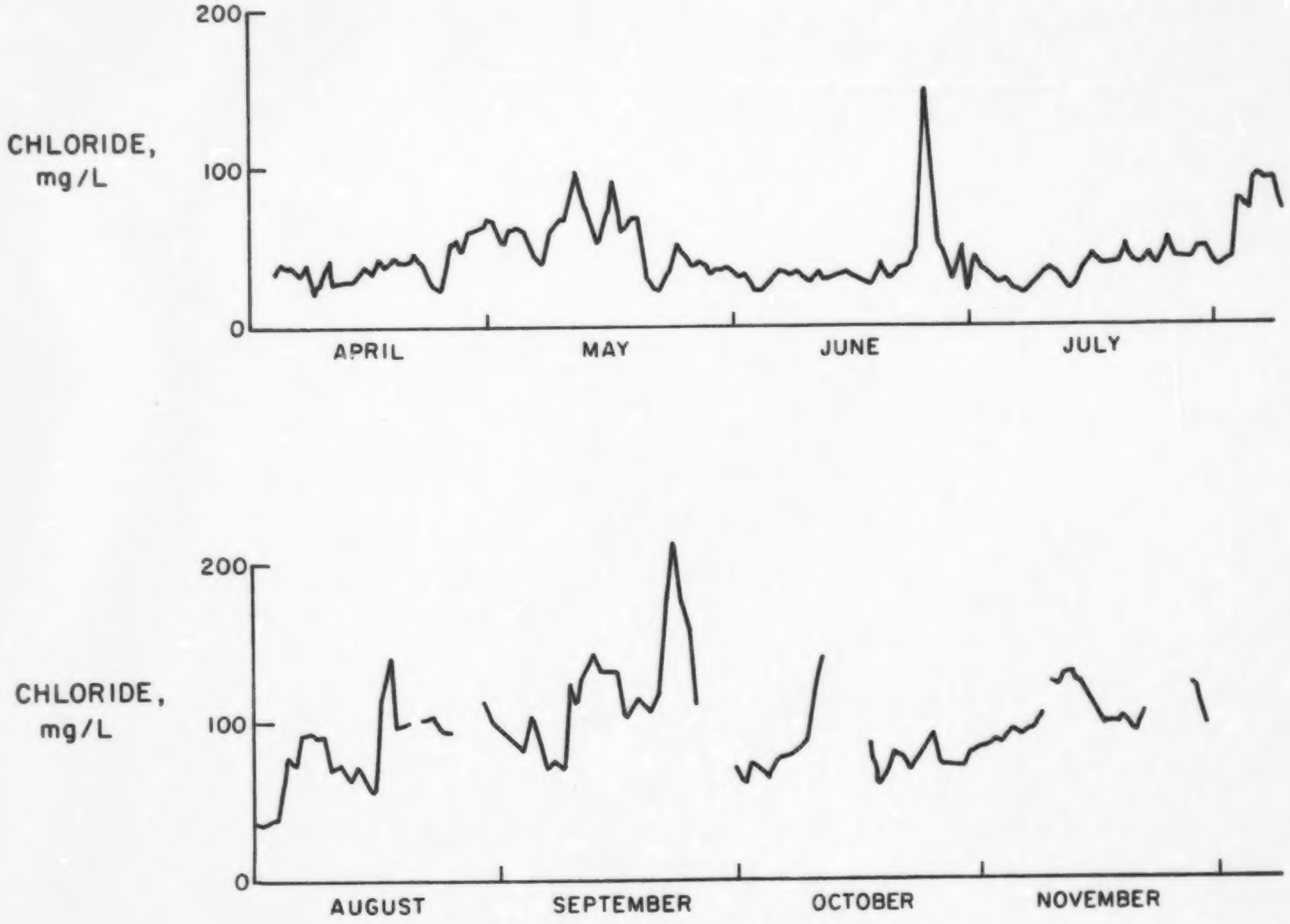

Figure A-1. Chloride content of finished water during pilot operation.

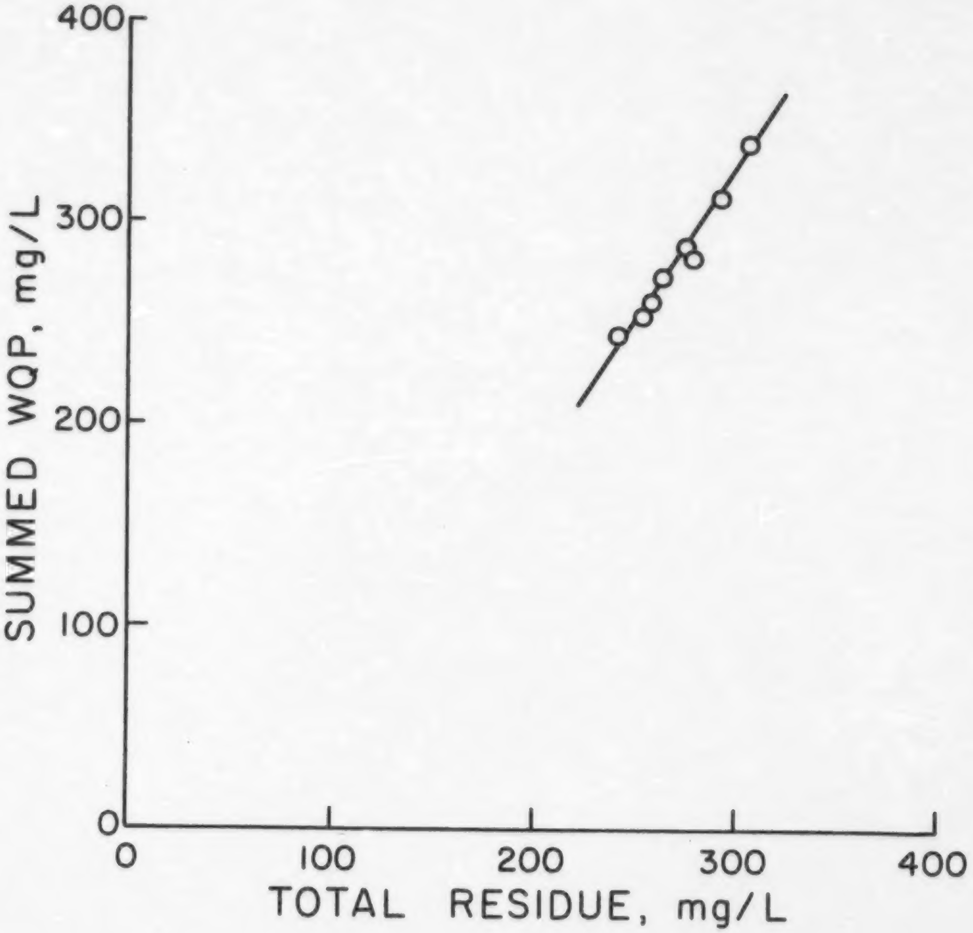

Figure A-2. Correlation of summed water quality parameters with total residue.

TABLE A-1. ALKALINITY DATA OUTSIDE OF NORMAL RANGE(a)(b)

Date, 1983	Carbonate Alkalinity,(a) mg/L	Bicarbonate Alkalinity,(a) mg/L
4/4	*	17
4/9	*	19
4/30	8	*
5/27	10	36
5/29	8	*
6/6	*	36
6/27	*	36
6/30	8	*
7/5	*	34
7/7	8	34
7/8	*	35
7/12	*	38
7/13	*	40
8/3	*	40
8/4	*	38
8/5	2	40
8/12	8	*
8/15	8	*
8/16	*	37
8/23	*	36
8/24	*	38
8/26	*	38
9/1	2	40
9/4	*	36
9/8	2	*
9/12	1	37
9/13	1	*
9/15	1	*
9/19	1	37
9/20	0	*
9/21	2	*
10/3	*	38
10/4	*	40
10/5	*	37
10/6	2	38
10/7	2	43
10/8	2	40

Date, 1983	Carbonate Alkalinity,(a) mg/L	Bicarbonate Alkalinity,(a) mg/L
10/10	1	40
10/11	2	38
10/12	1	40
10/18	2	
10/19	2	
10/20	2	
10/21	1	38
10/22	1	36
10/25	1	*
10/26	2	36
10/27	0	*
10/28	2	*
10/29	2	*
10/31	*	37
11/1	2	36
11/2	*	36
11/3	*	36
11/18	1	36
11/19	0	37
11/20	0	*
11/21	*	36
11/28	*	40

Notes:

a) Normal range, carbonate alkalinity: 3-7, bicarbonate alkalinity, 20-35 mg/L, * indicates within normal range.

b) Monthly average began to shift slightly in June to where the monthly average was 30-40 in September, October, and November with very few exceptions.

TABLE A-2. HARDNESS DATA OUTSIDE OF NORMAL RANGE[a]

Date, 1983	Hardness, mg/L
4/4	80
4/6	70
4/8	112
4/13	116
4/15	112
4/22	112
4/24	120
4/26	120
5/9	114
5/10	86
5/14	80
5/31	80
6/1	80
6/10	59
6/17	63
6/30	130
9/25	120
10/12	120

a) Normal range 90-110 mg/L as $CaCO_3$. The "normal range" bracketed 93% of the measured values during the period 4/1/83 - 12/1/83.

APPENDIX B

TREATMENT COST INFORMATION

The following information was obtained from USEPA, Drinking Water Research Division, Municipal Environmental Research Laboratory, Cincinnati, Ohio, for purposes of treatment cost projection.

Amortization rate: 8% for 20 years
Labor cost : $15 per hour

CONTINUOUSLY STIRRED TANK REACTOR SYSTEMS

Construction Costs

Ozone Contactor

0.1 MGD	98 cu. ft.	Cost = $4,200
0.5 MGD	490 cu. ft.	Cost = $7,700

Source: "Estimating Water Treatment Costs",
Ozone contactor costs, updated to 1983.

Ozone Generation and Feed System

	Ozone Dosage		
	5 mg/L	20 mg/L	50 mg/L
0.1 MGD	$120,000	$150,000	$200,000
0.5 MGD	$160,000	$270,000	$425,000

Source: Current project on "Small Water System Costs"

UV Lamps

	No. of Lamps/Reactor at 13 Watts Each	
	Two	Four
0.1 MGD	$ 5,400	$ 9,000
0.5 MGD	$21,900	$43,800

Source: Current project on "Small Water System Costs"

Mixers

Use energy input equivalent to G-600.

0.1 MGD	$ 8,100
0.5 MGD	$10,400

Source: "Estimating Water Treatment Costs", Rapid mix costs at G = 600 (manufactured equipment cost only) updated to 1983.

Operation and Maintenance Costs

Ozone Generation and Feed System

Plant Capacity-MGD	Ozone Dosage-mg/L	Annual Cost = $/Yr At $0.05/kwh	At $0.10/kwh
0.1	5	$11,700/Yr	$12,500/Yr
0.1	20	14,400	16,300
0.1	50	19,700	23,900
0.5	5	15,800	18,100
0.5	20	27,900	35,600
0.5	50	48,300	67,900

Note: Annual cost includes electrical energy, maintenance material, and labor.

UV Lamps

Plant Capacity-MGD	Number of Lamps/Reactor	Annual Cost - $/Yr $0.05/kwh	$0.10/kwh
0.1	2	$ 1,600/Yr	$ 2,000/Yr
0.1	4	3,200	4,000
0.5	2	8,100	10,100

0.5	4	17,100	21,000

Note: These costs include annual lamp replacement, as well as electrical energy.

Turbine Mixer

	Annual Cost - $/Yr	
	$0.05/kwh	$0.10/kwh
0.1 MGD	$3,600/Yr	$4,100/Yr
0.5 MGD	4,200	4,500

TUBULAR PHOTOCHEMICAL REACTOR SYSTEM

Construction Costs

Ozone Contactors

0.1 MGD	4 at 35 cu. ft. =	$22,400
0.5 MGD	4 at 175 cu. ft. =	$61,600

Ozone Generation and Feed Systems

Use same costs as presented for Continuously Stirred Tank Reactor System.

UV Lamps

0.1 MGD	$17,500
0.5 MGD	$84,900

Operation and Maintenance Costs

Ozone Generation and Feed Systems

Same as for Continuously Stirred Tank Reactor Systems.

UV Lamps

	Annual Cost - $/Yr	
	$0.05/kwh	$0.10/kwh
0.1 MGD	$ 6,400/Yr	$ 8,000/Yr
0.5 MGD	32,100	40,000

Note: These costs include annual lamp replacement, as well as electrical energy.

Note that a multiplier must be applied to the construction costs to accommodate other costs such as engineering, contractors overhead and profit, on-site piping, roads, and electrical, interest during construction, and legal and administrative costs. This multiplier will vary with project cost and the specific site under consideration. For this project, it was recommended that a multiplier of 35 to 40% be applied to the construction costs.

For extrapolations and interpolations the relationship

$$\$ = LQ^n ,$$

was used, where $\$$ = cost,

Q = capacity,

and L and n are parameters.

APPENDIX C

NARRATIVE STATEMENT CONCERNING QUALITY ASSURANCE PRACTICES

SUBMITTED JUNE 23, 1983

PARAMETERS TO BE MEASURED

The parameters to be measured in this study fall into one of three groups:

1. Parameters measured in the UTD laboratories.
2. Operating parameters measured in the pilot plant trailer.
3. Parameters measured routinely by Sabine River Water Treatment Plant personnel and copied from their records.

In the first group fall trihalomethane (THM) measurement, trihalomethane formation potential (THMFP), total organic carbon (TOC), the oxidants (ozone, hydrogen peroxide and total), residual chlorine, and pH. The second group includes water flow, gas flow, ozone concentration, and water temperature. The third group consists of conductivity, pH, alkalinity, and iron.

INTENDED USE OF THE DATA AND ASSOCIATED ACCEPTANCE CRITERIA FOR DATA QUALITY

From the group 1 parameters, by far the most important parameter is THMFP, which includes the formation and then measurement of THMs. The parameter TTHMFP is used directly to assess the effectiveness of various treatment conditions by determination of the TTHMFP reduction compared to the extent of treatment required. The acceptance criterion for TTHMs on the EPA quality assurance performance evaluation is ±20% of the true value, but an acceptance criterion has not been developed for TTHMFP.

TOC is measured occasionally, but is a much less useful parameter than it was earlier in the project, due to the day-to-day variability of the composition of the Sabine River compared with the more constant composition of the humic/fulvic concen-trate used earlier. While TOC is of general interest for comparison to other water systems, its actual quantitative significance is uncertain and it is not measured with the regularity that it was before. EPA QA acceptance criteria are not known for TOC, but as described below, the precision is a few percent.

Oxidant measurement is used primarily for mechanistic interpretation and will also be used in the part of the study involving the identification of intermediate products. Colorimetric measurement of oxidants in natural water systems is subject to more uncertainty than in lab systems made up in purified water, due to interferences from colored components of the natural organic material. Correspondingly, oxidant data in natural water is used in a more descriptive rather than quantitative manner. Acceptance criteria have not been developed for these measurements, but project requirements are discussed in the next section.

The residual chlorine measurement is used to determine the chlorine dose in the TTHMFP measurement, as well as to ascertain that a chlorine residual exists at the end of the chlorination period in that test. Measurement of pH is used in the preparation of solutions, determination of pH change upon reaction, and in other ways common to chemical investigation.

The second group of parameters, exclusive of water temperature, combine to determine the ozone dose (ozone applied per unit volume of water treated), which is the basis for all treatment effectiveness criteria. Water temperature will be measured in the pilot plant, but since the water to be treated is stored in an aluminum basin with an average hydraulic retention time of greater than three hours, the water temperature is more representative of ambient temperature inside the trailer than of anything else. Acceptance criteria for these in-plant measurements have not been developed, but their quantitative effect on results is discussed in a later section.

The third group of parameters are analyses performed by water plant personnel. They may find use in comparison of matrix effects during continuous operation, but their use in any other than a descriptive manner is uncertain at this point.

PROJECT REQUIREMENTS FOR PRECISION, ACCURACY, REPRESENTATIVENESS, COMPLETENESS, COMPARABILITY, AND HOW THESE WILL BE DETERMINED

The most important measurements in the pilot-scale study are those of TTHMFP and the operating parameters which are measured in the trailer. The most important measurements in the active species study are those of the oxidants. These parameters will be dealt with separately, below.

1. TTHMFP - In order that a set of operating conditions may be chosen over another, results of TTHMF determinations must be compared from experiment to experiment. This means that for TTHMFP, comparability is of primary importance in these measurements. In addition, precision must be good enough that a distinction between values from two different runs can be made. Compared to many analytical procedures, TTHMFP is not an especially precise procedure. It is felt by these investigators that a precision of ±5% would be within the limits of experimental error imposed by the other measurements involved and would be acceptable. It is shown in Section 7-2 below that the precision of individual measurements with replicate samples seems to be better than this value.

The term "accuracy" needs some definition in the context of TTHMFP measurement. Since conditions for the measurement of TTHMFP are not standardized(1), the amount of precursor converted to THMs may vary with the test conditions and the term "accuracy" becomes ill-defined. Our approach has been to chlorinate with a higher dose than would be used in a plant (30 mg/L applied) in order to obtain as much information as possible about the effect of ozonation and ozone/V on precursor formation and destruction.

A measure of comparability may be given by the measurement of TTHMFP on the same sample on consecutive days. If the value changes then either the TTHMFP measurement is not reproducibile and is out of control, or sample storage is affecting the results. If the value does not change, however, then a statement can be made about the reproducibility of the measurement from day to day, and therefore about comparability. This test is currently being conducted. Representativeness is assured by 1) allowing experimental conditions to equilibrate for at least 24 hours before sampling, 2) taking a large sample from which smaller replicate samples are poured up back in the laboratory, and 3) the fact that the whole stream is sampled rather than only a limited portion as when sampling a river or lake.

2. Parameters Measured in the Trailer. - The precision and accuracy with which these parameters are measured will be reflected directly in that of the calculated results. Therefore, a precision of ±5% would be desirable where possible. This presents no problem in the ozone concentration measurement where 1-2% precision is regularly seen, or in liquid flow measurement (2 seconds variation out of 40 sec = 5% range or ±2.5%), while in the measurement of low gas flows by a rotameter, the range of readibility is about 0.1 SLM (±0.05 SLM) out of 1.0 - 1.5 SLM, or 7 - 10% range (±3.5 - 5%).

Accuracy, however, may be more of a problem than precision. Liquid flow rate measurement accuracy can be easily determined by filling the bucket to the mark and weighing it. The quartz crystal clock used to time the measurement has required no resetting in the last year in order to stay with local time standards (radio). Measurement of ozone concentration by the spectrophotometric monitor was checked chemically once so far, but the difficulties encountered in that measurement make it questionable whether the accuracy of the measurement is comparable to that of the ozone monitor being calibrated. The problem is also fairly serious in the case of rotameter accuracy determination, where the calibration of the rotameter changes with inlet and outlet pressure and therefore with operating conditions. We will attempt to check the accuracy of these two measurements under conditions identical to those used in the pilot plant experiments, using direct displacement of water for flow measurements, and chemical means to check ozone concentrations reported by the ozone monitor.

3. Oxidants - Precision requirements for the oxidant data are estimated at ±0.2 mg/L for concentrations of 1 mg/L and above. Below that level, as good precision as possible is needed for mechanistic interpretation. Early work has shown that this kind of precision is obtained with these methods when used in water which has no colorimetric interference. This work is described in detail in earlier progress reports and is discussed below. As the mechanistic work on this project continues, more precision data will be generated.

It is of course desirable that oxidant measurements also be as accurate as possible, but for studies where the interconversion of oxidants is of interest, the fact that the various oxidant values are calibrated against the same method

(BKI) helps to assure internal consistency. The BKI method has in turn been calibrated against the UV absorbance method for an absolute calibration, using what appears to be the best value (2) of the extinction coefficient (3) for ozone which has been published to date.

Analytical results which are taken from the SRWTP plant records will be understood to be of unknown quality, since no rigorous QA program is known to be in place at that plant.

PROCEDURES FOR SELECTION OF SAMPLES OR SAMPLING SITES AND COLLECTION OR PREPARATION OF SAMPLES

Samples taken in the trailer are grab samples which are either taken daily along with a concurrent reading of operating parameters, or are composited to a weekly sample. Sampling sites are before, between, and after unit processes in the trailer. Ozone is quenched immediately with sodium sulfite and samples are stored in the refrigerator until chlorination or other analysis, usually less than ten days. Samples to be transferred from Longview to Dallas are packed in ice and transported by private vehicle (3 hours). Triplicate vials are prepared for TTHMFP analysis as described in Section 6 below. Oxidant samples in the trailer or laboratory are analyzed immediately, as are those for residual chlorine. No ozone quench solution is added to samples to be analyzed for conductivity, pH, or alkalinity.

PROCEDURES FOR SAMPLING, HANDLING, IDENTIFICATION, PRESERVATION, TRANSPORTATION, AND STORAGE

Samples in the trailer are taken directly into pre-labeled bottles which are labeled with the experiment number, sample point in the trailer, an identifier for the set of conditions, and the date. The identifier and date may both be related to a daily run sheet on which conditions at the time of sampling are recorded by the plant operator taking the sample. The sample bottle already contains sulfite quench solution if the sample is to be stored for analysis for TOC or TTHMFP. Samples to be stored are placed in the refrigerator until transport to the UTD laboratory, generally not more than one week and only once longer than ten days. Up to this point, samples have been transported by UTD laboratory personnel in private vehicles, with the samples packed in ice. Upon arrival from the three hour trip, the samples are placed in the cold room for storage at 4°C until analysis on the next full working day. In the future, some samples will be packed in ice and sent by bus from the pilot plant in Longview, Texas to Dallas, where they will be picked up the same day by UTD laboratory personnel.

A study of the effect of storage time is currently being carried out to determine the suitability of the preservation, storage, and transportation procedures. These results will be reported as they become available.

MEASUREMENT METHODS AND TEST PROCEDURES

GROUP 1 - Laboratory Measurements at UTD

1. TRIHALOMETHANES

Trihalomethanes are analyzed by the LLE method using 25 mL screw-capped septum vials. Extraction is into pentane and samples are always analyzed the same day as extraction. Because of interferences with more common internal standards by compounds formed upon chlorination of Sabine River water, tetrachloroethylene is routinely used as the internal standard. Internal standard peak areas are compared between blanks, standards, and samples to insure the absence of TCE in the samples, and check samples are extracted with pentane containing a different internal standard as a further precaution. Samples are prepared in triplicate and the first two samples analyzed. If the two samples differ by more than 4%, the third sample is analyzed. Results are averaged and the standard deviation (defined below) calculated. THM concentrations are calculated automatically by the HP 5840 gas chromatograph, and are checked periodically by hand for correctness. The instrument is calibrated against a mid-range standard.

2. TRIHALOMETHANE FORMATION POTENTIAL (TTHMFP)

Samples are prepared in triplicate, buffered (phosphate) to pH 7, and chlorinated with sodium hypochlorite solution at an applied chlorine dose of 30 mg/L (as chlorine) in excess of any ozone quench which was previously added. Samples are stored in the dark in a laboratory cabinet for seven days, then quenched with sulfite and analyzed by LLE as in Method 1, above. An unquenched sample is used to verify the presence of a chlorine residual at the end of seven days, and an unchlorinated sample is used to determine any instantaneous THMs present at the time of chlorination.

3. CHLORINE RESIDUAL

Aqueous chlorine is measured in two instances:

a) To determine the concentration of the stock solution of sodium hypochlorite used for chlorination in Method 2, above, and

b) To confirm the presence of a chlorine residual after the seven-day chlorination in Method 2, above.

In both cases, chlorine is analyzed by the colorimetric determination of iodine liberated from boric acid buffered potassium iodide solution by the chlorine. See TOTAL OXIDANTS BKI method below for calibration.

4. TOTAL ORGANIC CARBON (TOC)

Total Organic Carbon is measured using a Dohrmann DC-54 low-level TOC analyzer. The instrument is standardized against potassium hydrogen phthalate solution which is made up as a primary standard by weighing oven dried KHP. An instrument blank is run and taken into account in the calibration of the instrument (see QA/QC procedures, below).

5. OXIDANTS IN AQUEOUS SOLUTION

The individual methods are described below. General comments follow:

A. Ozone - HBI Method.

Ozone is measured by the indigo method of Hoigne and Bader (4) using the disulfonate potassium salt. The method was calibrated for accuracy against both the BKI method (below) and the UV absorbance method, using the extinction coefficient of ozone given by Hart, et al. (3). Comparison and testing of the method was described in Quarterly Reports from budget period - 01 of this project and in reference 4. Since the method works by bleaching the color of the reagent, the (colored) reagent blank is always run in triplicate. Reagent is dispensed into volumetric flasks using a dedicated automatic dispenser which has been calibrated for delivery by weighing the aliquots delivered. Sample is added to the mark, mixed well, and absorbance measured at 610 nm. Precision is usually a few percent above 1 mg/L and 10-15% in the 0.1 - 1 mg/L range, with an occasional poor value for no known reason. Determination of replicate samples generally makes identification of those erroneous values obvious.

B. Hydrogen Peroxide - Ti(IV) Method

Hydrogen peroxide is determined colorimetrically by formation of the peroxo-titanium complex (5). Since ozone creates a negative interference, it must be sparged from solution before reagent is added (6). The method was calibrated against the BKI/M method below. Testing of the method and comparison to the BKI/M method are described in the quarterly reports of budget period -01 of this project.

C. Total Oxidants - BKI/M Method

Total oxidants are determined by the liberation of iodine from boric acid buffered potassium iodide solution, by a modification of the method of Flamm (7). The addition of 9 mg/L of ammonium molybdate catalyses the otherwise slow reaction of hydrogen peroxide with iodide to the point that reaction is complete in less than one minute. Reaction with atmospheric oxygen is still slow enough that it is negligible if the absorbance is measured one minute after mixing sample and reagents. The method was calibrated to check stoichiometry by the liberation of iodine from the reaction of iodide and iodate, and calibrated for accuracy against the UV absorbance method, using the extinction coefficient of Hart, et al. (4).

D. General Comments on the Oxidant Methods

All methods were calibrated against the BKI/M method, which was in turn calibrated against iodide/iodate and UV absorbance for ozone. When highly purified water was used it was shown that in ozone/H_2O_2 mixtures, the sum of the HBI (for ozone) and Ti(IV) (for H_2O_2) methods gave the same result as the BKI/M (for total oxidants) method, to within a few percent. This is not, however, true when organic matter is present, the result of the BKI/method giving, in general, higher than the sum of the HBI and Ti(IV) methods. These studies as well as the applicability of the methods is discussed in detail in the quarterly reports from budget period -01 of this project.

6. pH

The pH of samples is measured using a pH meter and combination electrode which have been standardized against commercial buffers at two different pH values.

GROUP 2 - Parametric Measurements Inside the Trailer

1. WATER FLOW

Water flow is measured directly by timing the filling of a bucket to the 2-gallon mark. Precision of this method has been seen in practice to be approximately ±3% in the flow range of interest (1-6 gpm). Accuracy will be checked by weighing the filled bucket or by comparison with volumetric laboratory glassware.

2. GAS FLOW

In the first budget period gas flow was checked using a mass flow meter. Several different test meters of other types were tried and found to not be in agreement. During the current budget period the mass flow meter is not available and flow will have to be measured routinely with rotameters. Since in the actual system these rotameters do not discharge to atmospheric pressure, they will have to be calibrated for accuracy under operating conditions against rotameters at the exit of the system, that is, discharging to atmospheric pressure or by direct volumetric measurement of a timed flow of gas. Precision of this reading varies from ±5% at low flow (L/min) to about ±2% at higher flow (0 SCFH).

3. OZONE CONCENTRATION

Ozone concentration is measured by a PCI ozone monitor, calibrated at the factory. This calibration was checked iodimetrically and will be checked again during this budget period. Precision as reflected by repetitive measurements at 1% ozone is about 0.02%, which is considerably smaller than that of the rotameter readings.

4. WATER TEMPERATURE

Water temperature will be measured with a thermometer installed in-line. Although this thermometer has not yet been received, readability is given as ±0.5°C. The thermometer will be checked against more accurate laboratory thermometers for accuracy.

GROUP 3 - Parameters Measured by Sabine River Water Treatment Plant Laboratory Personnel

Conductivity, pH, alkalinity, and iron will be measured on a daily basis by SRWTP laboratory personnel. Conductivity and iron are performed with the Hach equipment designed for water plant use, alkalinity is done by titration, and pH is measured with a pH meter. Precision and accuracy of the methods by plant personnel on a day-to-day basis is extremely difficult to assess. These parameters are to be used as indicators of water quality but are not considered as important to the goals of the project as are the Group 1 and Group 2 parameters. If accurate values of these parameters are required, they will be checked at the UTD laboratory using standard methods.

QA/QC PROCEDURES

1. TRIHALOMETHANES

The liquid-liquid extraction method for trihalomethanes has been in use in this laboratory for several years. For calibration of the instrument a fresh standard concentrate is prepared every three to four weeks by weighing the pure compounds into methanol. This concentrate is volumetrically diluted into methanol to make a spiking solution which is spiked into water in a 25 ml vial to prepare the standard. Standards are prepared in triplicate as are the blanks, and the solvent (pentane, distilled from sodium) with internal standard (tetrachloroethylene) is chromatographed daily to check for contamination. Water for the standards is prepared by distillation followed by treatment in a Millipore system, which is then followed by distillation from alkaline potassium permanganate. Comparison of chromatographic resolution as well as compound response is followed from day to day to detect analytic problems. All samples are made up in triplicate whenever sample volume allows. If the anlyses of the first two samples agree with less than 4% difference those two determinations are averaged. If not, a third sample is analyzed and the three values averaged. The EPA Quality Assurance Performance Evaluation for trihalomethanes is run quarterly to insure ongoing analytical accuracy. Past results have always been within a few percent of the correct answer.

2. TRIHALOMETHANE FORMATION POTENTIAL

Quality Assurance in the determination of trihalomethane formation potential is more difficult to assess than in many cases such as THMs. The best indicators of consistent quality in the analysis are probably the precision within a determination on a single sample, and day-to-day reproducibility. The smoothness of a plot of TTHMFP in pilot plant feedwater from day to day can be taken as a measure of reproducibility of the TTHMF determination. Periodic (bimonthly) checks of day to day reproducibility on a single sample will be run to more closely check this factor. Assuming that this reproducibility is found, it will also help to confirm the independence of results upon storage time before chlorination.

The precision of the TTHMFP determination on samples analyzed to date is indicated by the standard deviation of replicate determinations on those samples. The standard deviations for fifty-five samples run in duplicate, triplicate, or quadriplicate were averaged. It was found that the average precision of these determinations was 2.8 ± 1.9%, or about 8 g/L out of 300.

3. CHLORINE RESIDUAL

Since water samples are chlorinated in the process of TTHMFP determination, the stock solution used for chlorination is checked for chlorine content each time before it is used. Since the analytical procedure involves only color development and the reading of absorbance, no additional QA is required beyond that normally used in the iodimetric oxidant determination.

4. TOTAL ORGANIC CARBON

The Dohrmann DC-54 TOC analyzer is calibrated against a standard potassium acid phthalate solution each time it is used. This standard is kept refrigerated and is made up fresh at least weekly from a concentrate which is made up by weight monthly. Instrument blanks are run and accounted for in the calibration. The various transfer lines of the instrument are cleaned when the blank reaches an unacceptable value (approaching 100 g/L). Highly purified water (described earlier) is used in the preparation of blanks and standards.

5. OXIDANTS

A. HBI method for Ozone

The method was calibrated against both BKI and UV absorbance. The extinction coefficient thus calculated is used for subsequent determinations. As recommended by Hoigne (4) the reagent is prepared fresh when the absorbance falls to 80%

of its original value, typically three months. The blank is run in triplicate as are the samples if sample volume allows. As with any oxidant method, sample is withdrawn directly from the experiment into the reagent, which quenches further reaction. Calibration is checked quarterly against the BKI method.

B. Ti(IV) Method for Hydrogen Peroxide

This method has been calibrated against the BKI/M method and calibration is rechecked quarterly. Reagent has been found to be extremely stable.

C. BKI/M Method for Total Oxidants

This method was originally calibrated against UV absorbance and calibration has been rechecked. Calibration was confirmed by liberation of iodine by iodide/iodate.

6. pH

No QA/QC for pH determination is employed other than calibration versus standard commercial buffers at two different pH values each time the pH meter/glass electrode is used.

7. WATER FLOW IN TRAILER

This parameter is measured directly each time using only a calibrated bucket and watch with a second hand. No further QA/QC is necessary beyond that described earlier in Section 3.

8. GAS FLOW IN TRAILER

This parameter is measured by the use of rotameters which need occasional checking and cleaning. The rotameter installation is about to be reconfigured and the flow rates will be checked under operating conditions by direct water displacement and/or a standardized rotameter at the outlet of each vessel, discharging to atmospheric pressure.

9. OZONE CONCENTRATION IN GAS STREAM

Ozone concentration is measured by a factory-calibrated ozone monitor which has been checked once. It will be checked again during this budget period using iodimetry and water displacement to measure the quantity of gas passed.

10. WATER TEMPERATURE

The thermometer used will be calibrated against a standard more accurate thermometer in the laboratory. Further QA is not deemed necessary, as the water temperature is likely to change by an amount greater than the accuracy of the thermometer as the water flows through the pilot plant.

11. PARAMETERS MEASURED BY SRWTP PERSONNEL

Because of their interest in this project, the City of Longview is making available, at no cost to the project, operator time for daily maintenance and sampling in the trailer, and some laboratory technican time for the daily performance of routine analyses. These analyses are carried out in the usual simplified manner that is used in water plants, and the data will not be used for important calculations requiring quantitative reliability, but rather as indicators of day-to-day water quality changes in the plant, as measured by plant personnel. Therefore, no external QA/QC program will be imposed upon the plant personnel.

DATA REDUCTION AND REPORTING PROCEDURES

Data from samples analyzed for THMs are reported by the calibrated gas chromatograph in units of concentration. The reported concentrations for the four chlorine/bromine THMs are summed to give TTHMs or TTHMFP. These sums are then averaged over the replicate values and standard deviation calculated on the basis of N-1 degrees of freedom termed "standard deviation estimate" in the EPA QC manual (8). Although the number of replicates used does not allow a strict statistical interpretation of the standard deviation, it nonetheless gives a measure of the comparative precision of the data points for later comparison. The 4 rule (9) is used to decide whether an outlying data point may be disregarded. In cases where a linear correlation is sought, a linear regression is performed on the averages, again with use of the 4PO rule for outlying data points. In plotting data, outliers are also plotted, even if they were not used in the linear regression. Data are reported by the analyst to the project manager on a form provided for that purpose, and the original chromatograms as well as copies of the completed forms are filed.

Other analyses which yield replicate answers are treated by the same procedures, i.e. N-1 standard deviation, 4 rule for outliers, etc. These other analyses include TOC and those of the oxidants, as well as direct measurements of water flow rate in the trailer.

REFERENCES FOR APPENDIX C

1. Symons, J.M.; A.A. Stevens, R.M. Clark, E.E. Geldreich, O.T. Love, Jr., and J. DeMarco, "Treatment Techniques for Controlling Trihalomethanes in Drinking Water", DWRD, MERL, ORD, USEPA, Cincinnati, OH, 1981, p.24.

2. By our judgement, and concurred with by J. Hoigne in a casual personal communication. This is the value determined by Hart et. al. reference 3. Literature values for 254 range from about 2900 to 3300 $M^{-1}cm^{-1}$.

3. Hart, E.J., K. Sehested, and J. Holcman, Anal. Chem. 55 (1983) 46.

4. Bader, H., and J. Hoigne, Water Res. 15 (1981) 449.

5. Parker, G.A., in "Colorimetric Determination of Nonmetals", D.F. Boltz and J.A. Howell, eds, Wiley, 1978, p. 301.

6. Glaze, W.H. and G.R. Peyton, Quarterly Report covering 6/1/81 - 8/31/81 of this project.

7. Flamm, D.L., Environ. Sci. Technol., 11 (1977) 978.

8. "Handbook for Analytical Quality Control in Water and Wastewater Laboratories", USEPA, Cincinnati, OH, EPA-600/4-79-019, 1979, p. 7-5.

9. Skoog, D.A., and D.M. West, "Fundamentals of Analytical Chemistry", Holt, Rinehart & Winston, New York, 1963, p.57.